

https://dspace.org/

The effect of novel compounds on the growth of Plasmodium falciparum and haemozoin formation

Chen, Chien-Teng

2015

http://hdl.handle.net/10539/18663

Downloaded from a DSpace repository. https://dspace.org/

The effect of novel compounds on the growth of *Plasmodium falciparum* and haemozoin formation



Chien-Teng Chen

A dissertation submitted to the Faculty of Health Sciences, University of the Witwatersrand, Johannesburg, in fulfilment of the requirements for the degree of Master of Science in Medicine.

Johannesburg, South Africa, 2015.

Declaration

I, Chien-Teng Chen, declare that this dissertation is my own work. It is being submitted for the degree of Master of Science in Medicine at the University of the Witwatersrand, Johannesburg, South Africa. It has not been submitted before for any degree or examination at this or any other University.

……

Chien-Teng Chen

……day of……., 2015

Abstract

With the social economic hardships plaguing the malaria-affected areas, new drug targets and treatment strategies are being sought to combat the emergence of resistance to the mainstay antimalarial combination therapies. The process of haemozoin formation is the ideal target for many reasons: it is not encoded nor expressed in the parasite genome, and the process cannot be mutated, lending itself as an ideal target for novel drug designs. The high-throughput β-haematin inhibitory activity (BHIA) assay was optimised to screen a series of novel synthetic compounds and compare this activity to the effects on the whole asexual parasite (tritiated hypoxanthine assay) taking into account cytotoxicity (using the tetrazolium cell viability assay).

All five corrin derivatives were found to inhibit the *in vitro* β-haematin formation process, with aquocobalamin 43 times more effective than chloroquine and adenosylcobalamin the most promising antimalarial (IC_{50} = 2.65 ± 0.50μM). Adenosylcobalamin interacted in an additive manner with chloroquine and quinine against the parasites (∑FIC = 0.974 and 1.004, respectively); while there was a synergistic interaction with chloroquine (∑FIC = 0.522) in the BHIA assay. Only one of the six porphyrin thiosemicarbazide derivatives was active against β-haematin formation and the lack of activity against the *in vitro* malarial parasite was probably due to the large size of the macromolecules, limiting their uptake into the intra-erythrocytic parasite food vacuole.

The 8- and 4-hydroxyquinoline derivatives with their basic quinoline ring, were theorised to possess activities against β-haematin formation. However, none of the fifteen 8-hydroxyquinoline derivatives possessed any inhibitory activities against β-haematin formation. In contrast, 5-amino-8-hydroxyquinoline (IC_{50} = 0.12 ± 0.01 μM) possessed promising antimalarial activity similar to that of chloroquine (IC_{50} = 0.103 ± 0.004 μM). 5-Amino-8-hydroxyquinoline possessed iron chelating properties, which could have contributed to its antimalarial and cytotoxic activities. The thirty-three 4-hydroxquinolines possessed variable activity against both *in vitro* malaria parasites and β-haematin formation inhibition depending on its chemical structure. PN8S was the most promising with an IC_{50} of 2.92 ± 1.56 μM and safety index of 136.5; which warrants further investigation.

Only M-5 of the chalcone derivatives possessed activity against β-haematin formation that was 2.4 fold less active than chloroquine. All the other chalcones (seventeen) and thiosemicarbazide (twenty-two) derivatives possessed limited activity against β-haematin formation, with the bromoacetophenones being more effective than their acetophenone counterparts - but not as effective as chloroquine. Additive interactions were observed between CA-9 and M-9 of the chalcones with quinine (∑FIC = 0.920 and 0.985, respectively) and 6B (∑FIC = 0.971 and 0.908, respectively) and 7B (∑FIC = 1.129 and 1.057, respectively) of the thiosemicarbazides with chloroquine and quinine, respectively. The bulkier groups at 1-*N* of the thiocarboxamide appeared to enhance the antimalarial activity of the thiosemicarbazones, where their mechanism of action could possibly have been due to metal chelation, inhibition of cysteine protease falcipain-2 or induction of apoptosis.

Overall, the corrins and porphyrin derivatives warrant further investigation due to their efficacy in inhibiting β-haematin formation. But their uptake into the malaria parasite needs optimising, which could be facilitated by linking them to a β-glucoside to facilitate the transport of the macromolecules via the hexose transporter system into the parasite. Alternatively, they could be encapsulated into peptide-based nanostructures for optimal delivery to the target site within the malaria parasites.

Acknowledgements

I would like to thank my supervisor Professor Robyn van Zyl for her immense patience with me. Her constant guidance and support helped me and pushed me to conclude this work.

The following people require special acknowledgement, without their expert contributions, my laboratory work would never have been completed:

- Professor Azam Amir for the porphyrin thiosemicarbazide derivatives.
- Dr Susan Chemaly for her expertise on the corrin derivative chemistry.
- Dr Arina Lourens for her assistance with the FTIR work.
- Prof Sandra van Dyk for the 4-hydroxyquinoline derivatives.
- Mr Christiaan van der Merwe at the Laboratory for Microscopy and Microanalysis unit at the University of Pretoria for his assistance with the scanning electron microscopy work.

Special thanks:

- To my family and my pets, I cannot thank you all enough.
- To my friends, all of you are special.
- To my work colleagues, there are just too many of you to list, but you know who you are.

Financial support

Belgium Technical Corporation (BTC), Wits Faculty of Health Sciences Research Office and the Wits University Staff Bursary fund.

List of Publications from this Dissertation

Full papers

1. Chemaly SM, Chen C-T, van Zyl RL. Naturally occurring cobalamins have antimalarial activity. *Journal of Inorganic Biochemistry* (2007) 101:64–773.

   Contribution made in the publication:

   Established the β-haematin inhibition assay in the Division, conducted all the experiments for the antimalarial, cytotoxicity and β-haematin formation inhibition assays; data analysis and interpretation, wrote methods for paper and contributed to the discussion; proof read the final paper.

2. Bhat AR, Athar F, Van Zyl RL, Chen C-T, Azam A. Synthesis and biological evaluation of novel 4-substituted 1-{[4-(10,15,20-triphenylporphyrin-5-yl)phenyl]methylidene} thiosemicarbazides as new class of potential antiprotozoal agents. *Chemistry & Biodiversity* (2008); 5(5):764-776.

   Contribution made in the publication:

   Conducted all the experimental work for the antimalarial, cytotoxicity and β-haematin formation inhibition assays; data analysis and interpretation, wrote methods for paper and contributed to the discussion; proof read the final paper.

Published congress abstracts

- C-T Chen, R van Zyl. *In vitro* antiplasmodial activity of 8-hydroxyquinoline derivatives. *Basic & Clinical Pharmacology & Toxicology* (2010), 107 (Suppl. 1), 227.

List of Congresses Attended

- C-T Chen, R van Zyl. *In vitro* antiplasmodial activity of 8-hydroxyquinoline derivatives. The University of the Witwatersrand Faculty of Health Sciences Research Day, 22 September 2010. [Poster presentation]
- C-T Chen, R van Zyl. *In vitro* antiplasmodial activity of 8-hydroxyquinoline derivatives. The 16th World Congress on Basic and Clinical Pharmacology, Copenhagen, Denmark, July 17-23, 2010. [Poster presentation]
- CT Chen, RL van Zyl, SM Chemaly. Combined effect of cyanocobalamins with standard antimalarial agents. The SA Society for Basic & Clinical Pharmacology and The Southern African Neuroscience society Congress, Grahamstown, 5-8 October 2008. [Poster presentation]
- CT Chen, RL van Zyl, A Azam, S van Dyk, JC Breytenbach. Structure-Activity Relationships of Novel Antimalarial Agents. Faculty Research Day, University of the Witwatersrand, Johannesburg, South Africa, 20 August 2008. [Poster presentation]
- CT Chen, RL van Zyl, A Azam, S van Dyk, JC Breytenbach. Structure-Activity Relationships of Novel Antimalarial Agents. Pharmacology and Toxicology Conference, Buffelspoort, North West Province, 2-5 October 2007. [Poster presentation]
- C-T Chen, RL van Zyl, SM Chemaly. *In vitro* antiplasmodial activity of corrinoid derivatives. 15th World Congress of Pharmacology, Beijing, China, July 2-7, 2006. [Poster presentation]
- C-T Chen, RL van Zyl, SM Chemaly. *In vitro* antiplasmodial activity of corrinoid derivatives. Faculty Research Day, University of the Witwatersrand, South Africa, 23 August 2006. [Poster presentation]
- Chen C-T, van Zyl RL, Chemaly SM. *In vitro* antiplasmodial activity of corrinoid derivatives. 14th International Congress of Pharmacology and Pharmaceutical Sciences, Vanderbijlpark, South Africa, 20-23rd September 2006 [Poster presentation]
- C-T Chen, RL van Zyl, SM Chemaly. *In vitro* antiplasmodial activity of cyanocobalamin. 34th Annual South African Parasitology Society Congress, Magoebaskloof, Limpopo Province, 25 – 28 September 2005. [Poster presentation]

- RL van Zyl, C-T Chen, NC Jansen van Vuuren. The Metal Chelating and Chemotherapeutic Properties of 8-Hydroxyquinoline derivatives. Gordon Research Conference on Metals in Medicine held June 2012 Andover, NH, USA. [Poster presentation]
- RL Van Zyl, C-T Chen, A Hibbins. The chemotherapeutic, toxicological and anti-oxidant properties of 8-hydroxyquinoline derivatives. The 44th South African Society of Basic and Clinical Pharmacology and 7th Toxicological Society of South Africa Joint Congress, Cape Town, South Africa, 3-6 October 2010. [Podium presentation]
- RL van Zyl, A Azam, M Abid, AA Ramjeeth, C-T Chen. Antimalarial Activity Of New 1-*N*-Substituted Cyclized Pyrazoline Analogues Of Thiosemicarbazones. Research Forum Day of School of Therapeutic Sciences, Parktown, 10-11 August 2005 [Podium presentation]
- RL Van Zyl, A Azam, M Abid, AA Ramjeeth, C-T Chen. Antimalarial activity of new 1-N-substituted cyclized pyrazoline analogues of thiosemicarbazones. 34th Annual South African Parasitology Society Congress, Magoebaskloof, Limpopo Province, 25 – 28 September 2005. [Podium presentation]
- SM Chemaly, C-TChen, N Ashraf-Moosa, RL van Zyl. Inhibition of β-haematin formation by cobalamins. Gordon Research Conference on: Vitamin B_{12} and Corphins, Queen's College, Oxford, 18-23 September 2005. [Poster presentation]

Table of Content

Declaration ii
Abstract iii
Acknowledgements v
List of Publications vi
List of Congresses Attended vii
Table of Contents ix
List of Figures xiv
List of Tables xvii
List of Equations xviii
List of Abbreviations xix

Chapter 1 Introduction 1

1.1 Malaria etiology 1
1.2 *Plasmodium* species 3
1.3 Life cycle 3
1.4 Pathogenesis: clinical features of malaria 4
1.5 Standard antimalarial agents, mechanism of action and resistance 5
1.5.1 Guidelines for the treatment of malaria in South Africa 10
1.6 Nutrient acquisition 10
1.7 Haemoglobin degradation and haemozoin formation 10
1.7.1 Haemoglobin degradation 10
1.7.2 Haemozoin formation 12
1.7.3 Haemozoin structure 15
1.7.4 The detoxification of the reactive oxygen intermediates 17
1.7.5 Haemozoin as a drug target 19
1.8 Aims and objectives 19

Chapter 2 Methodology 21

2.1 Compounds and reagents 21
2.2 β-Haematin inhibition assay 21
2.2.1 Synthesis of β-haematin crystals 21
2.2.2 Characterisation of the β-haematin crystals via Fourier transformed infrared spectroscopy 22
2.2.3 Scanning electron microscopy 24
2.2.4 Isolation of haemozoin from infected red blood cells 24
2.3 Assay of β-haematin formation inhibition 25
2.4 β-Haematin inhibitory activity assay 27
2.4.1 Haemin concentration calibration curve 27

2.4.2	β-Haematin: time versus formation	28
2.4.3	High-throughput screening: β-haematin inhibitory activity assay	30
2.5	Combination assay	31
2.6	Malaria culture maintenance	33
2.6.1	Maintenance of *P. falciparum* (FCR-3) culture	34
2.6.2	Preparation of incomplete culture medium	34
2.6.3	Preparation of complete culture medium	35
2.6.4	Preparation of heat-inactivated human plasma	35
2.6.5	Preparation of red blood cells	35
2.6.6	Giemsa stain	36
2.6.7	Synchronisation of the malaria parasite culture	37
2.6.8	Cryopreservation and initiation of cultures	37
2.6.8.1	Cryopreservation of malaria parasites	37
2.6.8.2	Initiation of malaria culture from frozen stock	37
2.7	Tritiated hypoxanthine incorporation assay	38
2.7.1	Preparation of the uninfected red blood cells and parasites	39
2.7.2	Preparation of the classical antimalarial agents	39
2.7.3	Preparation of the novel test compounds	39
2.7.4	Preparation of the microtiter plates	39
2.7.5	Incubation of experimental plates	40
2.7.6	Preparation of the isotope	40
2.7.7	Harvesting and beta counting of the radiolabelled parasitic DNA	40
2.7.8	Combination assays and isobolograms	41
2.8	Red blood cell lysis assay	42
2.8.1	Preparation of the red blood cell suspension	42
2.8.2	Haemolytic assay	42
2.8.3	Data analysis	44
2.9	Cellular viability assay	44
2.9.1	Culture maintenance	45
2.9.2	Preparation of incomplete culture medium	45
2.9.3	Preparation of complete culture and experimental medium	46
2.9.4	Preparation of foetal calf serum	46
2.9.5	Cryopreservation and initiation of cultures	46
2.9.6	MTT cellular viability assay	46
2.9.7	Safety index	48
2.10	Anti-oxidant assays	49
2.10.1	Free radical scavenging assay	49
2.10.2	Free radical scavenging assay procedure	49
2.11	Iron chelation assay	50
2.11.1	Iron chelation assay procedure	51
2.12	Data and statistical analysis	51

Chapter 3 Porphyrins and Corrins 53

3.1 Introduction 53
3.1.1 Porphyrins 53
3.1.2 Corrins 54
3.1.2.1 Vitamin B_{12} 55
3.2 Objectives 56
3.3 Methodology 57
3.3.1 Porphryin thiosemicarbazides 57
3.3.2 Corrins 58
3.4 Results 59
3.4.1 Porphyrin thiosemicarbazides 59
3.4.2 Corrins 59
3.5 Discussion 62
3.5.1. Porphyrin thiosemicarbazides 63
3.5.1.1 Uptake and accumulation of porphyrin thiosemicarbazides 63
3.5.1.2: Mechanism of action: inhibition of β-haematin formation 64
3.5.2 Corrins 65
3.5.2.1 Uptake of corrins 65
3.5.2.2 Accumulation of corrins and antimalarial activity 67
3.5.2.3 Mechanism of action: inhibition of β-haematin formation 67
3.5.2.4 Mechanism of action: methionine synthase co-factor 70
3.5.2.5 Combination interactions 72
3.6 Conclusions 72

Chapter 4 8- and 4-Hydroxyquinolines 73

4.1 Introduction 73
4.2 Hydroxyquinolines 74
4.2.1 8-Hydroxquinoline derivatives 74
4.2.1.1 Antimicrobial properties 74
4.2.1.2 Metal chelating properties 74
4.2.2 4-Hydroxquinolines 75
4.3 Objectives 76
4.4 Methodology 76
4.4.1 8-Hydroxquinoline derivatives 76
4.4.2 4-Hydroxquinoline derivatives 78
4.5. Results 78
4.5.1 Pharmacological properties of 8-hydroxyquinolines 78
4.5.1.1 Inhibition of β-haematin formation 78
4.5.1.2 Antimalarial and β-haematin formation inhibitory activities 80
4.5.1.3 Ferrous ion chelation activities 80

4.5.1.4	Free radical scavenging activities	80
4.5.1.5	Haemolytic activity	80
4.5.1.6	Cytotoxic activities	82
4.5.2	4-Hydroxyquinoline derivatives	82
4.6	Discussion	82
4.6.1	8-Hydroxyquinoline derivatives	82
4.6.1.1	Inhibit of β-haematin formation	82
4.6.1.2	Antimalarial activity related to structure	82
4.6.1.3	Mechanism of action: metal chelation	86
4.6.1.4	Mechanism of action: pro- or anti-oxidant	88
4.6.1.5	Cytotoxic effect	89
4.6.2	4-Hydroxyquinoline	92
4.6.2.1	β-Haematin inhibitory activity of the 6-, 7- and 8-dialkylamino 4-hydroxyquinolines	92
4.6.2.2	Antimalarial and cytotoxicity activities of the 6-, 7- and 8-dialkylamino 4-hydroxyquinolines	92
4.6.2.3	Dehydrogenase inhibition by 4-hydroxyquinoline derivatives	94
4.6.2.4	Anti-oxidant activities	95
4.6.2.5	5-Lipoxygenase inhibition by 4-hydroxyquinolines	96
4.6.2.6	Cytotoxic and anticancer properties	96
4.7	Summary	97
4.7.1	8-Hydroxyquinolines	97
4.7.2	4-Hydroxyquinolines	98

Chapter 5 Chalcones and Thiosemicarbazones 99

5.1	Introduction	99
5.1.1	Chalcones	99
5.1.2	Thiosemicarbazones	101
5.2	Aims	101
5.2.1	Objectives	102
5.3	Methodology	103
5.3.1	Chalcone derivatives	103
5.3.2	Thiosemicarbazone derivatives	103
5.3.3	Pharmacological assays and analysis	103
5.4	Results	106
5.4.1	Chalcone derivatives	106
5.4.1.1	Antimalarial, cytotoxic and β-haematin formation inhibitory properties	106
5.4.1.2	Combination studies	108
5.4.2	Thiosemicarbazone derivatives	108
5.4.2.1	Antimalarial, cytotoxic and β-haematin formation inhibitory properties	108

5.4.2.2 Combination studies 110
5.5 Discussion 111
5.5.1 Chalcone derivatives 111
5.5.2 Thiosemicarbazone derivatives 114

Chapter 5 Conclusion 118

References 122

Appendices 143

Appendix A: Biosafety ethics clearance: protocol number: 20090503 143
Appendix B: Human Ethics clearance to use and purchase human plasma and blood: waiver certificate number: W-CJ-131030-1 146
Appendix C: Human ethics clearance to obtain drug-free human whole from healthy volunteers: clearance certificate number: M140669 147
Appendix D: Human ethics clearance certificate for use of human cell lines: reference number: W-CJ-150330-1 148

List of Figures

Figure 1.1	The world map illustrating the malaria endemic and non-malaria endemic countries in the western and eastern hemispheres.	2
Figure 1.2	The life cycle of the malaria parasite in the mosquito and the human host.	5
Figure 1.3	A schematic presentation of haemoglobin degradation/digestion and the formation of haemozoin from the toxic Fe(III)PPIX in a process that has been proposed to have started in the digestive vacuole and ended in the lipid body	12
Figure 1.4	The different chemical structures of haemozoin crystals.	14
Figure 1.5	A schematic depicting the proposed formation of haemozoin in lipid bodies.	17
Figure 1.6	The detoxification of the H_2O_2 and the superoxide anion (O_2^-) after the autoxidation of Fe(II)PPIX to Fe(III)PPIX.	18
Figure 2.1	The IR spectra of the synthetic β-haematin crystals at 0 (green), 30 (blue) and 60 (red) minutes at 60^{o}C.	23
Figure 2.2	SEM of β-haematin.	24
Figure 2.3	The haematin standard curve in β-haematin formation inhibition assay.	26
Figure 2.4	A standard curve of haemin in DMSO measured at 405 nm.	28
Figure 2.5	Kinetics of β-haematin formation.	29
Figure 2.6	The dose-dependent effect of the positive control, chloroquine in the high-throughput assay.	31
Figure 2.7	Possible pharmacological interactions between compounds **X** and **Y** were visualised using an isobologram.	33
Figure 2.8	A summarised flow chart of the [^{3}H]-hypoxanthine incorporation assay.	38
Figure 2.9	A representative layout of the 96-well microtiter plate used for a [^{3}H]-hypoxanthine incorporation assay.	40
Figure 2.10	Representative layout for the red blood cell lysis assay.	43
Figure 2.11	The 96-well microtiter plate format used for a haemolytic assay with colour control wells.	44
Figure 2.12	Layout for the MTT cell viability assay taking the colour of the test compounds into account.	47
Figure 2.13	The interaction between DPPH free radical and an anti-oxidant (AH/A^-).	49
Figure 3.1	The chemical structures of porphyrin ring and corrin ring.	53

Figure 3.2	The uptake of cobalamin is initiated by the extraction of vitamin B_{12} from the food source in the acidic environment in the stomach.	55
Figure 3.3	The effects of the porphyrin thiosemicarbazide compounds against malaria parasite growth and β-haematin formation	60
Figure 3.4	Inhibitory activities of corrin derivatives.	60
Figure 3.5	β-Haematin inhibition assays showing the effects of chloroquine (left) and adenosylcobalamin (right) on the *in vitro* formation of β-haematin formation.	61
Figure 3.6	Isobolograms depicting the combination effect of adenosylcobalamin with antimalarial agents against malaria *in vitro* as well as against the formation of β-haematin.	62
Figure 3.7	The uptake and ingestion of the host haemoglobin by the parasite.	66
Figure 3.8	The effect of chloroquine (CQ) on haem (FPIX) detoxification in the lysosome of a chloroquine-resistant malaria parasite.	68
Figure 3.9	Equilibria of base-on, base-off and protonated base-off forms of cobalamins.	70
Figure 3.10	The folate scavenging pathway in the malaria parasite.	71
Figure 4.1	The antimalarial activity comparisons of chloro- and bromo-substitution on the acridone base structure.	84
Figure 4.2	8-Hydroxyquinoline and its metal complex.	87
Figure 4.3	Structure of 8-hydroxyquinoline-2-carboxaldehyde thiosemicarbazone	91
Figure 5.1	The chemical structure of chalcone (1,3-diphenyl-2-propen-1-one) (Nowakowska, 2007).	99
Figure 5.2	General structure of semicarbazones (X = O) and thiosemicarbazones (X = S).	101
Figure 5.3	Correlation between the antimalarial activity of the uncomplexed derivatives compared to the Pd^{2+}-complexed derivatives.	107
Figure 5.4	The isobologram of quinine in combination with CA-9 and M-9.	108
Figure 5.5	Correlation between the inhibitory effects of the thiosemicarbazones on β-haematin formation and antimalarial activity.	110
Figure 5.6	The isobolograms of chloroquine and quinine with 6B and 7B of the thiosemicarbazone derivatives.	111
Figure 5.7	Comparative structures of the Guantai (8b) and Hayat chloroquine-chalcone derivatives (Compound 17).	112
Figure 5.8	Amido-iminol tautomerism of thiosemicarbazone.	115
Figure 5.9	The O, N, S-tri-coordination of the thiosemicarbazones.	115

Figure 5.10 The C,N,S-tricoodination, N,S-coordination forming a five member chelating ring and N,S donor formed by a four-member chelating ring. 116

List of Tables

Table 1.1	The description of the four human malaria parasites.	4
Table 1.2	Clinical features of malaria infection and the possible mechanisms of disease.	7
Table 1.3	Standard antimalarial agents, their mechanism of action and their mechanism of resistance.	8-9
Table 1.4	Drugs possessing the possible ability to inhibit β-haematin formation.	19
Table 2.1	Haematin recovered from the β-haematin formation reaction.	30
Table 2.2	Combined concentration ratios of compounds X and Y .	32
Table 3.1	The structure and side groups of the synthesized porphyrin thiosemicarbazide molecules - 5-(4-phenyl-N^4-substituted thiosemicarbazone)-10, 15, 20-(trisphenyl) porphyrins	57
Table 3.2	The structure of the corrin derivatives with the blue corrin ring structure.	58
Table 3.3	pK_a values, accumulation ratios and accumulation ratios relative to chloroquine of corrin derivatives.	68
Table 4.1	Pharmacological activities of quinoline-based derivatives.	73
Table 4.2	The chemical names, chemical structures and the abbreviations of the tested 8-hydroxyquinoline derivatives.	77
Table 4.3	The β-haematin inhibitory and antimalarial activities of the 4-hydroxyquinoline derivatives, with their respective cytotoxicity.	79
Table 4.4	The inhibitory properties of 8-hydroxyquinolines.	81
Table 4.5	Metal affinity constants for selected ligands.	86
Table 5.1	Antimalarial activities of chalcones.	100
Table 5.2	Antimalarial activities of thiosemicarbazones.	102
Table 5.3	The chalcone derivatives with their R-side groups and their chemical descriptions.	104
Table 5.4	The 1-N-substituted thiocarbamoyl-3-phenyl-2-pyrazolines base structure with the various R-side groups and chemical descriptions.	105
Table 5.5	The pharmacological activities of the 1-N-substituted thiocarbamoyl-3,5-diphenyl-2-pyrazolines derivatives and their palladium (II) complexes.	106
Table 5.6	The antimalarial activities and β-haematin formation inhibition activities of thiosemicarbazone derivatives.	109

List of Equations

Equation 2.1	Percentage β-haematin formation.	26
Equation 2.2	Percentage inhibition of β-haematin formation.	30
Equation 2.3	Relative ratios of X:Y.	32
Equation 2.4	The ΣFIC value calculated using the $BHIA_{50}$ values of the combined and individual $BHIA_{50}$ values of **X** and **Y**.	33
Equation 2.5	The equation used to calculate the percentage parasitaemia from a stained thin blood smear	36
Equation 2.6	Percentage [^{3}H]-hypoxanthine incorporation or parasite growth.	41
Equation 2.7	The percentage haemolysis of the red blood cells.	43
Equation 2.8	An equation used to calculate the percentage haemolysis of the red blood cells with compounds that possessed a colour.	43
Equation 2.9	The equation used to calculate the percentage cell viability taking both the test and the reference wavelengths into account.	48
Equation 2.10	Selectivity index for *P. falciparum* compared to human cancer cell lines**.**	49
Equation 2.11	The equation used to calculate the percentage decolourization of the $DPPH^{\bullet}$ by the test compound.	50
Equation 2.12	Percentage iron chelation as calculated by the decrease in colour intensity of the ferrous-ferrozine complex.	51

List of Abbreviations

AA	Amino acid
Abs	Absorbance
ACD-B	Acid citrate dextrose solution b
BHIA	B-haematin inhibition activity
$BHIA_{50}$	Concentration required to inhibit 50% of β-haematin formation
Ci	Curie
cm	Centimeter
CPM	Counts per minute
CQ	Chloroquine
CQ	Chloroquine
dbzm	5,6-diemethylbenzimidazole base
DDT	Dichlorodiphenyl-trichloroethane
DHFR	Dihydrofolate reductase
DHPS	Dihydropteroate synthase
DMEM	Dulbecco's modified eagle's medium
DMSO	Dimethyl sulphoxide
DPAP	Dipeptidyl aminopeptidase
$DPPH^{\bullet}$	2,2-diphenyl-1-picrylhydrazyl
DV	Digestive vacuole
ECAFS	Extended X-ray absorption fine structure
EDTA	Ethylenediaminetetraacetic acid
EMC	European medicines council
FCR-3	Falciparum chloroquine resistant subculture 3
FCS	Foetal calf serum
Fe(II)PPIX	Haem
Fe(III)PPIX	Ferriprotoporphyrin IX
FIC	Fractional inhibitory concentra
∑FIC	Sum fractional inhibitory concentration
FPIX	Ferriprotoporphyrin IX
FTIR	Fourier transformed infrared spectroscopy

g	Gravitational constant
GIT	Gastrointestinal tract
GLC-MS	Gas-liquid chromatography-mass spectrometry
GSH	Glutathione (reduced)
GSSG	Glutathione disulfide
H_2O_2	Hydrogen peroxide
HAP	Histoaspartic protease
Hb	Haemoglobin
HEK293	Human epithelial kidney cells
HEPES	N-2-hydroxyethylpiperazine-N'-2-ethane-sulfonic acid
HF	Halofantrine
HF	Halofantrine
HPLC	High performance liquid chromatography
HRPII	Histidine-rich protein II
IC_{50}	Concentration required to inhibit 50% of parasite/cell growth
IR	Infrared
LB	Lipid body
MDR	Multidrug resistance
MDR	Multidrug resistant
µl	Microlitre
µM	Micromolar
mg	Milligram
mM	Millimolar
MMG	Monomyristoylglycerol
MMV	Medicines for Malaria Venture
MMV	Medicines for Malaria Venture
MPa	Megapascals
MQ	Mefloquine
MTT	3-(4,5-Dimethylthiazol-2-yl)-2,5-diphenyltetrazolium bromide
NADH	Nicotinamide adenine dinucleotide (reduced form)
NADP	Nicotinamide adenine dinucleotide phosphate

NADPH	Nicotinamide adenine dinucleotide phosphate hydrogen
nm	Nanometer
O_2^-	Superoxide anion
PBS	Phosphate buffered saline
PfCRT	Plasmodium falciparum chloroquine-resistant transport
PfHT	*P. falciparum* hexose transporter
PfLAP	*P. falciparum* m17 leucyl aminopeptidase
Pgh	P-glycoprotein
Pgh1	P-glycoprotein homologue 1
PPM	Parasite plasma membrane
PVM	Parasitophorous vacuolar membrane
PVS	Parasitophorous vacuolar space
PYM	Pyrimethamine
PYM	Pyrimethamine
QN	Quinine
QN	Quinine
RBC	Red blood cells
rpm	Revolutions per minute
RPMI-1640	Roswell Park Memorial Institute medium formula number 1640
s.d.	Standard deviation
SA DOH	South African Department of Heath
SEM	Scanning electron microscopy
SI	Safety index
TEM	Transmission electron microscopy
TH_4	N^5,N^{10}-methylene-tetrahydrofolate
TLC	Layer chromatography
UV-VIS	Ultra-violet/Visible
% v/v	Percentage volume/volume
% w/v	Percentage mass/volume
% w/w	Percentage mass/mass
WHO	World Health Organisation

Chapter 1

Introduction

1.1 Malaria etiology

Malaria cases has been recorded as far north as 64^{o}N latitude (in the former USSR) and as far south as 32^{o}S latitude (Argentina). It has also been recorded in the vicinity of the Dead Sea at 400 m below sea level and at 2800 m above sea level in Bolivia. There are large populations living in malaria-free regions, with the highest prevalence being reported in Africa, South East Asia and Eastern Mediterranean (Snow and Gilles, 2002; Sachs and Malaney, 2002; WHO, 2014). According to the World Health Organisation (WHO), there are several malaria endemic countries worldwide (Figure 1.1), including South Africa with malaria endemic areas in the Limpopo, Mpumalanga and northern Kwa-Zulu-Natal (WHO World Malaria report, 2014; www.cdc.gov/malaria/map).

Since the discovery of the synthetic insecticidal compound, dichlorodiphenyl-trichloroethane, commonly known as DDT at the beginning of the Second World War, and the discoveries of synthetic antimalarial agents (i.e. pamaquine in 1924, mepacrine in 1930, chloroquine in 1934, proguanil in 1944, amodiaquine in 1946, primaquine in 1950 and pyrimethamine in 1952) malaria eradication programmmes in the 1950s and 1960s were regarded as successful (Gilles, 2002; Greenwood and Mutabingwa, 2002). However, the resurgence of malaria around the world re-initiated such programmes to control malaria transmission and mortality rates (WHO World Malaria report, 2014).

The outcome of these programmes was shown in the recent World Malaria Report of 2014, where an estimated 198 million positive cases of malaria infection were reported in 2013 with an estimated 584,000 deaths, which is a 30% decline between the years of 2000 and 2013. Africa was the most endemic continent where it accounted for 90% of all reported malaria deaths, even though there had been a 34% decline over the past 13 years (WHO World Malaria Report, 2014).

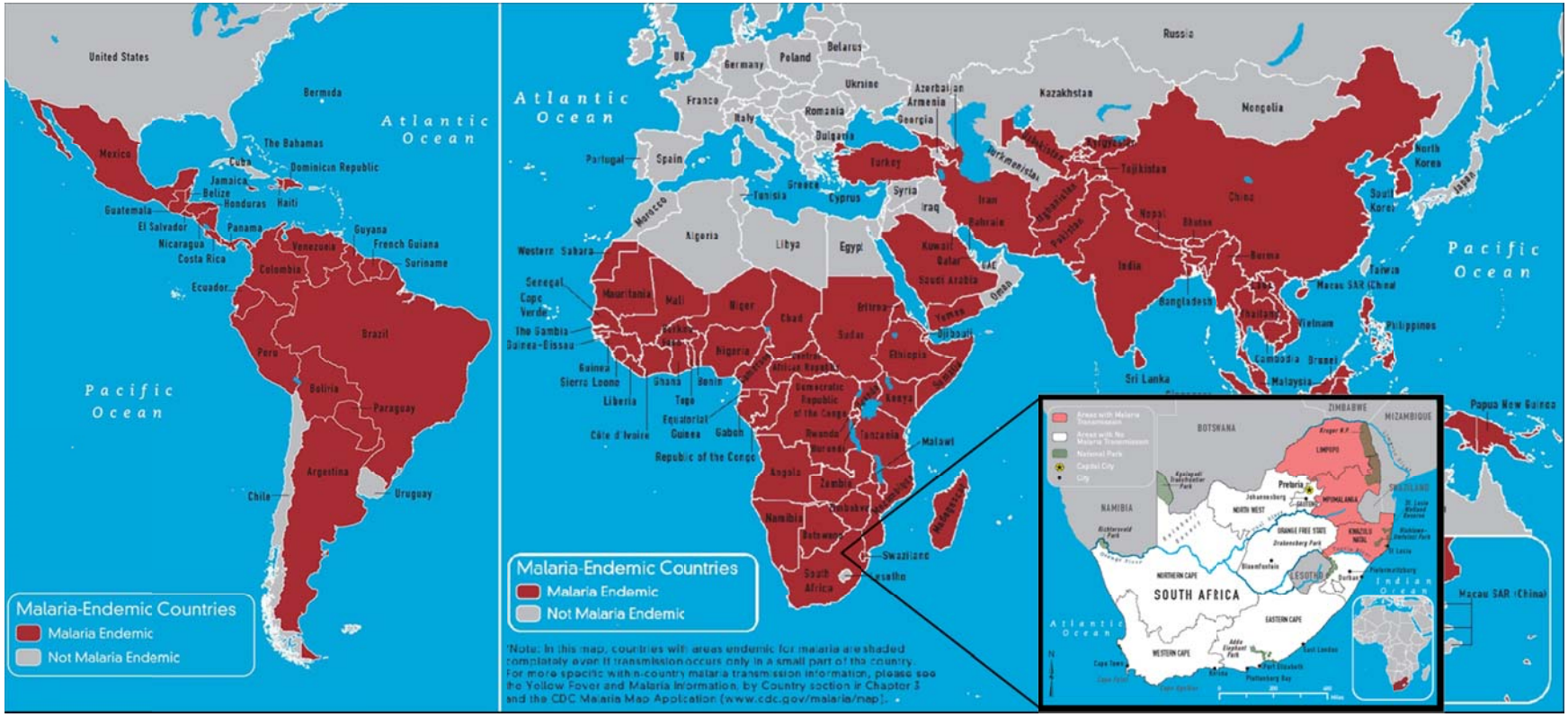


Figure 1.1 The world map illustrating the malaria endemic and non-malaria endemic countries in the western and eastern hemispheres. The map of South Africa has been inserted to illustrate malaria endemic areas in the Limpopo, Mpumalanga and northern Kwa-Zulu Natal provinces (WHO World Malaria report 2014; www.cdc.gov/malaria/map).

1.2 *Plasmodium* species

The malaria disease is caused by the protozoa of the genus *Plasmodium*, family Plasmodiidae, suborder Haemosporidiidae, order Coccidia. There are about 120 or so species of *Plasmodium* that are found in the blood of mammals, birds and reptiles. These are taxonomically categorised by the two types of asexual division: schizogony, in the vertebrate host; and sporogony, in the insect vector. Within the vertebrate host, schizogony is found within erythrocytes (erythrocytic schizogony) and in other tissues (exo-erythrocytic schizogony) (Sinden and Gilles, 2002; WHO World Malaria Report, 2014).

The majority of the malaria parasites are transmitted by mosquitoes, and in humans, the parasites is transmitted exclusively by the bite of infected female mosquitoes of the genus *Anopheles* (Fujioka and Aikawa, 1999; Miller *et al.*, 2002; WHO World Malaria Report, 2014).

The human *Plasmodium* parasites are sub-divided into two subgenera, *Laverania* and *Plasmodium*. The *Laverania* subgenus includes *P. falciparum*, the most pathogenic form of malaria, while the *Plasmodium* subgenus includes *P. vivax, P. malariae* and *P. ovale* (Table 1.1). *P. falciparum, P. vivax* and *P. ovale* are found exclusively in humans and *P. malariae* is found in both humans and African apes (Miller *et al.*, 2002; Sinden and Gilles, 2002; WHO World Malaria Report, 2014).

1.3 Life cycle

The duration of the asexual erythrocytic schizogony stage cycle differs between the species of human *Plasmodium* parasites. *P. falciparum*, *P. ovale* and *P. vivax* are 48 to 50 hour cycles, which are termed tertian periodicity, while *P. malariae* is termed quartan (72-hour) periodicity (Sinden and Gilles, 2002).

Malaria parasite requires the *Anopheles* mosquito and human as its two hosts to complete its life cycle. The haploid parasite has developed three different strategies, but distinct phases in its complex life cycle. The first strategy is to replicate extensively (schizogony). This is achieved by the three vegetative stages: the sporogony stage – the oocyst stage in the mosquito; the tissue schizogony (exo-erythrocytic schizogony) in the liver of the human hosts (30,000 merozoites); and erythrocytic schizogony (16-32 merozoites). The second strategy is the ability of the parasite to disperse and invade the host cells. This is the extracellular strategy where the merozoite, sporozoite and ookinete invade its host cells.

Table 1.1 The description of the four human malaria parasites (WHO World Malaria Report, 2014).

***Plasmodium* species**			
P. falciparum	*P. vivax*	*P. ovale*	*P. malariae*
Pathogens			
Malignant tertian	Benign tertian	Benign tertian	Benign quartan
Clinical features			
Cerebral	Milder, relapse	Milder, relapse	Mild, relapse
Geography			
Tropics/subtropics	Most wide spread	Tropics	Rare-subtropics
Africa	Tropics/subtropics	W. Africa/ Asia/ S. America	Spotty in location
P. falciparum & *P. vivax* account for more than 95% of infections			

The third strategy is the formation of gametocytes in the peripheral circulation of the human host, with the formation of the fused ookinete in the mosquito gastro-intestinal tract following its blood meal (Fujioka and Aikawa, 1999; Sinden and Gilles, 2002).

The complex parasite life cycle involves the malaria parasites undergoing three distinct asexual replicative stages (exo-erythrocytic schizogony, blood stage schizogony, and sporogony) resulting in the production of invasive forms (merozoites and sporozoites) (Figure 1.2). A sexual reproduction occurs with the switch from vertebrate to invertebrate host and leads to the formation of the invasive ookinete. All invasive stages are characterized by the apical organelles typical of apicomplexan species.

1.4 Pathogenesis: clinical features of malaria

The clinical manifestations of malaria vary with geography, epidemiology, immunity and age. In areas where malaria is highly endemic, groups at highest risk include young children (6 to 36 months) who can develop severe illness, and pregnant women, who are at risk for

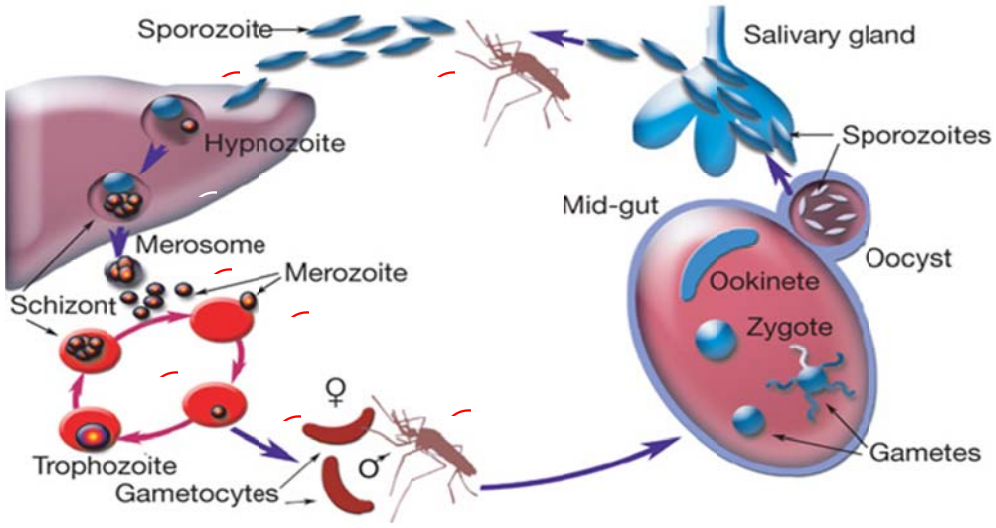


Figure 1.2 The life cycle of the malaria parasite in the mosquito and the human host (Winzeler, 2008). The life cycle of the malaria parasite begins with the ① injection of sporozoites by the bite(s) of female anopheline mosquitoes during its regular blood meals. The sporozoites are immediately phagocytosed, but surviving sporozoites circulating in the blood stream invade hepatocytes within two minutes post inoculation. During the next 5 to 16 days, the sporozoites develop into exo-erythrocytic schizogony ②. Within the hepatocytes, the sporozoites develop and mature into exo-erythrocytic schizonts ③, which upon rupturing release 10,000 to 30,000 merozoites into the sinusoids ④. The invasion of the erythrocytes takes about 30 seconds following the aligned of the ligands on the merozoite surface to the specific receptors on the erythrocyte ⑤. The asexual stage of the life cycle begins with the development of the merozoites within the host erythrocytes through the ring, trophozoite and schizont (erythrocytic schizogony) stages. During this period multiple rounds of nuclear division occurs without cytokinesis. The segmented schizont ruptures in the erythrocyte and the released merozoites (16-32 per schizont) invade additional erythrocytes ⑥. As an alternative to the asexual replicative cycle, a small fraction of these merozoites can differentiate into sexual forms known as macro- or microgametocytes ⑦. After the ingestion of the gametocytes by the mosquito ⑧, the flagellated microgametes fertilize the macrogamete leading to a zygote. The zygote develops into a motile ookinete which penetrates the gut epithelial cells and develops into an oocyst. The oocyst undergoes multiple rounds of asexual replication resulting in the production of sporozoites. Rupture of the mature oocyst releases the sporozoites into the hemocoel (i.e., body cavity) of the mosquito. The sporozoites migrate to and invade the salivary glands ready for injection into the next human host, thus completing the life cycle.

delivering low birth weight newborns. In areas where malaria is transmitted throughout the year, older children and adults develop partial immunity after repeated infections and are at relatively low risk for severe disease (WHO World Malaria Report, 2014).

Following the bite of an infected female *Anopheles* mosquito, the inoculated sporozoites invade the liver within 1 to 2 hours. Individuals are asymptomatic for 12 to 35 days (depending on parasite species), until the erythrocytic stage of the parasite life cycle. Release of merozoites from infected red blood cells (RBCs) results in clinical symptoms such as fever, in an infected patient (Table 1.2). The relapsing species, *P. vivax* and *P. ovale* present as a new infection weeks or months after the initial illness due to activation of residual hypnozoites in the liver (WHO World Malaria Report, 2014).

The incubation period for a *P. falciparum* infection is approximately 12 to 14 days. Longer incubation periods are more likely in semi-immune individuals and individuals taking ineffective malaria prophylaxis. The incubation period for *P. vivax* and *P. ovale* is also about two weeks; most relapses due to these species occur within three months. In contrast, *P. falciparum* and *P. malariae* have no dormant (hypnozoite) phase.

1.5 Standard antimalarial agents, mechanism of action and resistance

Antimalarial agents are classified according to their mechanism of action against different stages of the parasites' life cycle. Certain antimalarial agents are more effective in the treatment of an acute attack of malaria. The WHO has strongly recommended that more than one agent should be used simultaneously to avoid resistance. Some antimalarial agents are used as prophylactic agents in order to kill the parasite as soon as it enters the host (WHO World Malaria Report, 2014).

The objectives of any chemotherapeutic intervention against malaria are to prevent mortality and reduce morbidity; prevent disease progression and development of severe malaria in terms of *P. falciparum* infection; eliminate parasitaemia and minimise transmission; and to limit the emergence and spread of drug resistance (SA DOH, 2011).

The South African Department of Health recommend the use of specific drugs in the prevention and treatment of malaria where the agents have complementary mechanisms of action when used in combination and to reduce the development of resistance (Table 1.3).

Table 1.2 Clinical features of malaria infection and the possible mechanisms of disease (Mackintosh *et al*., 2004).

Syndromes	Clinical features	Disease mechanisms
Severe anaemia	Shock; impaired consciousness; respiratory distress	Reduced RBC production (reduced erythropoietin activity, pro-inflammatory cytokines); increased RBC destruction (parasite-mediated, erythrophagocytosis, antibody and complement-mediated lysis)
Cerebral complications (cerebral malaria)	Impaired consciousness; convulsions; long-term neurological deficit	Microvascular obstruction (parasites, platelets, rosettes, microparticles); pro-inflammatory cytokines; parasite toxins (e.g. glycosylphos-phatidylinositol)
Metabolic acidosis	Respiratory distress, hypoxia, tachypnea; acidaemia; reduced central venous pressure	Reduced tissue perfusion (hypovolaemia, reduced cardiac output, anaemia); parasite products; parasite products; pro-inflammatory cytokines; pulmonary pathology (airway obstruction, reduced diffusion)
Other	Hypoglycaemia; disseminated intravascular coagulation	Parasite products and/or toxins; pro-inflammatory cytokines; cyto-adherence
Malaria in pregnancy	Placental infection; low birth weight and fetal loss; maternal anaemia	Premature delivery and fetal growth restriction; placental mononuclear cell infiltrates and inflammation; pro-inflammatory cytokines

Table 1.3 Standard antimalarial agents, their mechanism of action and their mechanism of resistance.

Drug	Mechanism of Action	Mechanism of Resistance	Resistance marker	Pf ID	Allele associated with resistance or decreased drug sensitivity
Chloroquine (CQ)	Parasite haem metabolism inhibition; haemozoin formation inhibition[2]	Decreased intra-parasite accumulation of CQ. Probably predominantly mediated by mutations in PfCRT, a transmembrane protein in the parasite phagolysosome, resulting in increased efflux of CQ from the lysosome. Mutations in multidrug resistance (MDR) P-glycoprotein pumps (Pgh) encoded by *Pfmdr1* and *Pfmdr2* may also contribute[1]	CQ resistance transporter pfcrt[1]	MAL7P1.27	K76T[1]
			Multidrug resistance protein MDR1[4]	PFE1150w	H191Y and S437A[3]
Mefloquine (MQ), halofantrine (HF), Quinine (QN)	Proposed to inhibit haem metabolism in the parasite and to inhibit parasite haemozoin formation[11]	MQ and HF resistance may be related to amplification of *Pfmdr1*[5,6], increased expression of Pgh 1[7,8], mutation in *pfcrt*, and increased efflux of drug . QN resistance is not fully understood, however QN and MQ resistance are often correlated[9].	**MQ:** ABC transporter, (CT family) pfmrp[10]	PFE1150w	Copy number > 1[5]
			QN: Na^+/H^+ antiport[12]	PF13_0019	Number of motifs : DNNND > 2 or NHNDNHNNDDD < 3[13]
			QN: ABC transporter, (CT family) pfmrp[10]	PFA0590w PFL1410c	H191Y and S437A[14]
Artemisinin derivatives	Damage of intraparasitic organelles and alkylation of parasite proteins via intraparasite haem-catalyzed production of carbon-centered free radicals[15]	ART resistance has been linked to mutations in the propeller domain of the *K13* gene. K13-propeller mutations contribute to ART resistance by reprogramming the intra-erythrocytic developmental cycle and upregulating the UPR, which mitigates protein damage caused by ART.[28]	*K13* gene - kelch superfamily of proteins[28]	PFA0310c	S769N[14]

Table 1.3 cont. Standard antimalarial agents**,** their mechanism of action and their mechanism of resistance**.**

Drug	Mechanism of Action	Mechanism of Resistance	Resistance marker	PfID	Allel associated with resistance or decreased drug sensitivity
Cycloguanil, chlorocyclo-guanil, pyrimethamine (PYM)	Block folate synthesis via inhibition of dihydrofolate reductase (DHFR)[16-20]	Resistance mediated through point mutation in *dhfr* and *dhps* genes.[23] Although more efficient use of available folate may also contribute	**Cycloquanil:** Tetrahydrofolate dehydrogenase[14]	PFD0830w	S108T+A16V S108N+N51I and/or+[14]
			PYM: Tetrahydrofolate dehydrogenase DHFR[14]	PFD0830w	S108N S108N+ N51I+ C59R[14]
			Sulfadoxine-PYM: DHFR/DHPS combination[14]	PFD0830w PF08_0095	S108N+N51I+C59R/A437G+K540E[14]
			Sulfadoxine-PYM: ABC transporter, (CT family) pfmrp[14]	PFA0590w PFL1410c	K1466R[14]
Sulfonamides and sulfones (sulfadoxine, dapsone)	Block folate synthesis via inhibition of dihydropteroate synthase (DHPS)[21,22]		**Sulfadoxine:** Dihydropteroate synthetase DHPS[14]	PF08_0095	A437G A437G+K540E[14]
Atovaquone	Inhibition of mitochondrial electron transport in cytochrome bcl complex, resulting in collapse of mitochondrial membrane potential[25-27]	Point mutations in mitochondrial- encoded cytochrome b gene[24]	ubiquinol-cytochrome c reductase[14]	PF14_0248	Y268N or Y268S[14]
			ubiquinol-cytochrome c reductase	PF14_0373	
			ubiquinol-cytochrome c reductase	PF10_0120	

[1]Fidock *et al.,* (2000) [2]Slater (1993);[3]Pirahmadi *et al.,* (2013);[4]Sidhu *et al*., (2006);[5]Price *et al*., (2004);[6]Wilson *et al*., (1993);[7]Cowman *et al*., (1994);[8]Reed *et al*., (2000);[9]Warhurst (2000);[10]Briolant *et al*. (2010);[11]Mungthin *et al.,* (1998);[12]Nakashima and Garlid (1982);[13]Andriantsoanirina *et al*., (2010);[14]Eboumbou Moukoko *et al*., (2009);[15]Meshnick (2002);[16]Hyde (1990);[17]Canfield *et al*., (1993);[18]Milhous *et al*., (1985);[19]Winstanley *et al.*, (1995);[20]Mookherjee *et al*., (1999);[21]Brooks *et al*., (1994);[22]Triglia and Cowman (1994);[23]Ndiaye *et al*., (2005);[24]Srivastava *et al.,* (1999);[25]Fry and Pudney (1992);[26]Vaidya *et al*., (1993);[27]Baggish and Hill (2002). [28]Nunes-Alves (2015)

1.5.1 Guidelines for the treatment of malaria in South Africa

Artemether-lumefantrine (Coartem®) or quinine plus either doxycycline or clindamycin are used for uncomplicated *P. falciparum* malaria infections. For mixed infections of *P. falciparum* plus *P. ovale* or *P. vivax*, artemether-lumefantrine is used followed by a two-week regimen with primaquine (SA DOH, 2011).

Artemether-lumefantrine plus primaquine or chloroquine plus primaquine are recommended for uncomplicated non-*P. falciparum* malarial infections (*P. ovale* or *P. vivax*).

For severe malaria, intravenous quinine or intravenous artesunate is used for emergency treatment, and when able the patient will be initiated on oral treatment with artemether-lumefantrine or quinine (plus doxycycline or clindamycin).

1.6 Nutrient acquisition

In order to acquire essential nutrients, *Plasmodium* has to compete with both the vertebrate and insect hosts and therefore has developed a highly efficient mechanism of regulating uptake in accordance with nutrient availability (Landfear, 2011). *Plasmodium*, along with many other endoparasitic parasites, has numerous channels in their parasitophorous vacuole membrane rendering it permeable to organic solutes to allow the uptake of necessary nutrients (Kirk and Lehane, 2014). The *P. falciparum* hexose transporter (PfHT) is such a transporter, which is critical for the uptake of glucose and fructose and therefore survival of the parasite (Slavic *et al*., 2010). These organic molecules have to cross a sequence of three membranes; namely, the plasma erythrocytic membrane, the *Plasmodium* plasma membrane and the parasitophorous food vacuole membrane facilitated by transporters/channels to provide the essential nutrients and minerals for the optimal growth of the parasite (Leirião *et al.,* 2004)

One main pathway of amino acid acquisition is the breakdown of the haemoglobin by the malaria parasite during the intra-erythrocytic stage of their life cycle.

1.7 Haemoglobin degradation and haemozoin formation

1.7.1 Haemoglobin degradation

The malaria parasite requires amino acids for the synthesis of proteins and nucleotides for replication and there are three sources of amino acids: *de novo* synthesis, import from the host plasma or digestion of host haemoglobin. Haemoglobin is an

extremely abundant source of protein in the erythrocyte cytoplasm and therefore it serves as a major source of amino acids for the parasite. The parasite digests between 60% and 80% of the haemoglobin in the RBC into amino acids; however the majority of these amino acids are effluxed from the infected RBCs and only about 16% of these amino acids are incorporated into parasite proteins (Krugliak *et al.* 2002). During the early ring stage, the parasite takes up the host cell stroma by pinocytosis resulting in double membrane vesicles (Figure 1.3). The inner membrane (which corresponds to the parasitophorous vacuolar membrane [PVM]) rapidly disappears and the digestion of haemoglobin takes place within these small vesicles during the early trophozoite stage. As the parasite matures, it develops a special organelle called the cytostome, for the uptake of host cytoplasm and the small pigment-containing vesicles fuse to form a large digestive vacuole. Double membrane vesicles "pinch-off" from the base of the cytostome and fuse with the digestive vacuole (Olliaro and Goldberg, 1995). The inner membrane (originally the PVM) is lysed and the haemoglobin in released into the digestive vacuole. The digestive vacuole is a specialised acidic organelle (pH 5.2-5.8) within the parasite (also known as the food vacuole) that resembles the organelle lysosome (Olliaro and Goldberg, 1995; Kirk, 2001; Bennet *et al*., 2004).

Three of the four major classes of proteases have been identified in the digestive vacuole, namely the plasmepsins (the aspartic acid class), the falcipains (the cysteine [thiol] class) and falcilysin (the metallo class). The digestion of haemoglobin occurs by a semi-ordered process involving the sequential action of different proteases (Goldberg, 2005). Working in conjunction, plasmepsin-I and plasmepsin-II result in cleaving the undenatured haemoglobin into globin fragments while plasmepsins I, II and IV, histoaspartic protease (HAP) and falcipains 2 and 3 (also possibly capable of cleaving undenatured haemoglobin) reduce the globin fragments into peptides; while falcilysin reduces the peptides into smaller peptides (Banerjee *et al.*, 2002; Rosenthal *et al.*, 2002; Eggleson *et al.,* 1999). A dipeptidyl aminopeptidase (DPAP) found in the digestive vacuole converts the smaller peptides into dipeptides along with dipeptidyl peptidase and aminopeptidase which cleave the dipeptides into amino acids (Klemba, 2004; Dalal and Klemba, 2007). In the parasite cytoplasm, *P. falciparum* M17 leucyl aminopeptidase (PfLAP) has been proposed to cleave the peptides into amino acids (Stack *et al.* 2006).

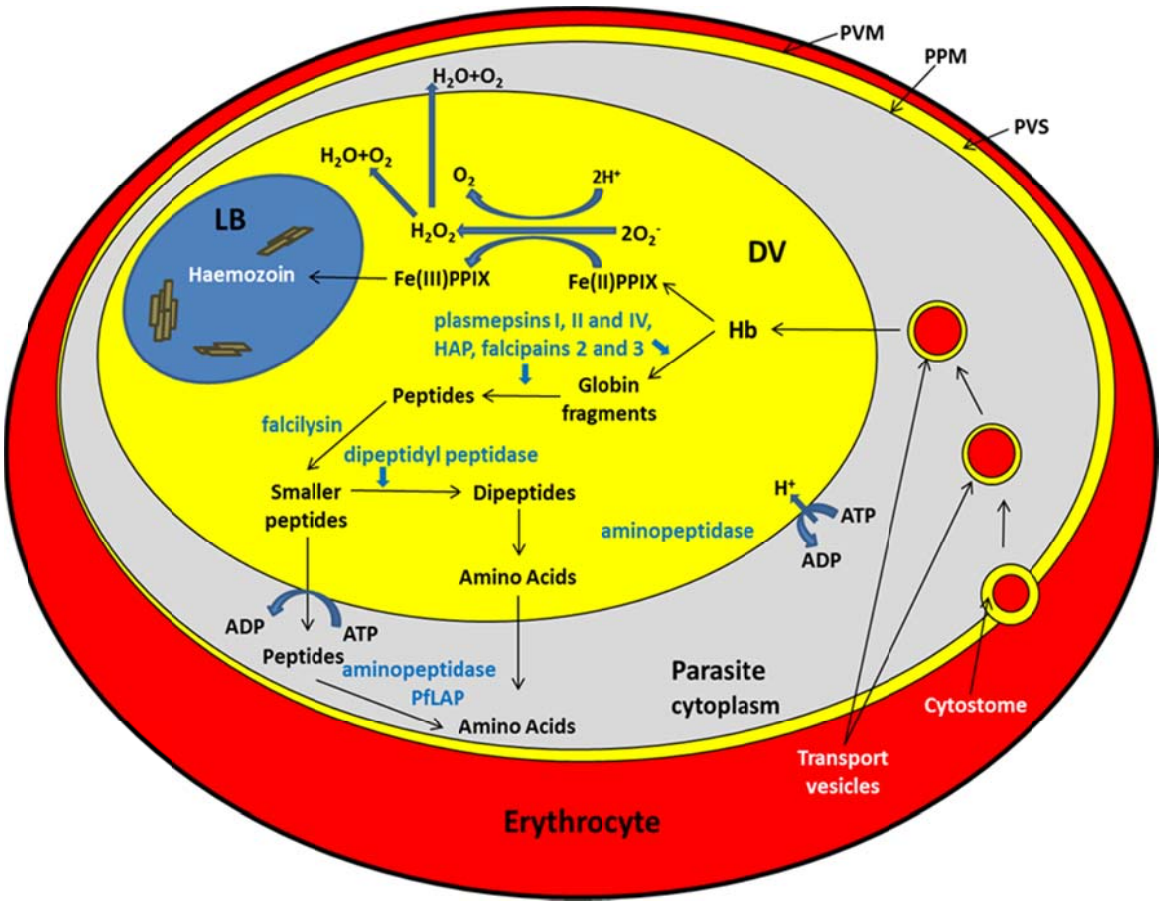


Figure 1.3 A schematic presentation of haemoglobin (Hb) degradation/digestion and the formation of haemozoin from the toxic Fe(III)PPIX in a process that has been proposed to have started in the digestive vacuole (DV) and ended in the lipid body (LB) (Adapted from Atamna and Ginsburg, 1997). PVM = parasitophorous vacuolar membrane, PVS = parasitophorous vacuolar space, PPM = parasite plasma membrane, HAP = histoaspartic protease, PfLAP = *P. falciparum* M17 leucyl aminopeptidase.

1.7.2 Haemozoin formation

Haemozoin formation is a haem detoxification process in which the hydrolysis of globin by erythrocytic parasites liberates large amounts of haem. Free haem is toxic to the parasite and induces lysis of the parasites (Orjih *et al.*, 1981). The malaria parasite has not been shown to degrade haem enzymatically, they apparently incorporate haem molecules into particulate haemozoin as a detoxification mechanism (Egan *et al.*, 2002).

Haemozoin formation is not exclusive to malaria parasites, but has been found in other haematophagous organisms such as the bird-infecting protozoan, *Haemoproteus*

columbae (Chen *et al.,* 2001), blood feeding helminths, *Schistosoma mansoni* (Chen *et al.,* 2001 and Oliveira *et al.,* 2000), *Echinostoma trivolvis* (Pisciotta *et al.,* 2005) and the blood-sucking triatomine insect, *Rhodnius prolixus* (Oliveira *et al.,* 1999).

Using Mössbauer spectra and electron spectroscopic imaging, Egan *et al.* (2002) demonstrated that at least 95% of the haem was sequestered in haemozoin. This finding was supported by Solomonov *et al.* (2007) using spinning disc confocal microscopy that measured the volume of haemozoin formed by the end of the trophozoite parasite stage (1.5 fmol per cell) which accounts for 88% of the total iron content of a RBC. These two findings disputed the finding of Zhang *et al.* (1999) that reported that only 20 to 30% of the haem released from the haemoglobin is sequestered into haemozoin.

In 1987, Fitch and Kanjananggulpan established that haemozoin can be purified and consisted of ferriprotoporphyrin IX (Fe(III)PPIX) which had previously been thought to be a haemoprotein. In the same study they suggested that haemozoin is probably identical to β-haematin, a synthetic Fe(III)PPIX. The structure of haemozoin was confirmed by elemental analysis to consist solely of Fe(III)PPIX, whilst X-ray diffraction showed that haemozoin is chemically and structurally identical to β-haematin (Slater *et al.,* 1991). Using infrared spectroscopy and extended X-ray absorption fine structure (ECAFS), it was demonstrated that the Fe(III)PPIX molecules are linked through co-ordination of the haem propionate group of one molecule to the Fe(III) centre of its neighbour (Slater *et al.,* 1991). From the study, it was proposed that the structure of haemozoin and/or β-haematin consisted of long chains of linked Fe(III)PPIX (Figure 1.4a). Using synchrotron X-ray powder diffraction, Bohle *et al.* (1997) confirmed that the haemozoin crystal *in situ* in the malaria parasite to be identical to β-haematin. The structure was proposed to consist of antiparallel polymer chains (Figure 1.4b). Further structure elucidation revealed that haemozoin/β-haematin to be a cyclic dimer of Fe(III)PPIX in which the propionate group of each Fe(III)PPIX molecule co-ordinates to the Fe(III) centre of its partner, while the dimers are linked through hydrogen bonding of the propionic acid groups (Figure 1.4c) (Pagola *et al*., 2000).

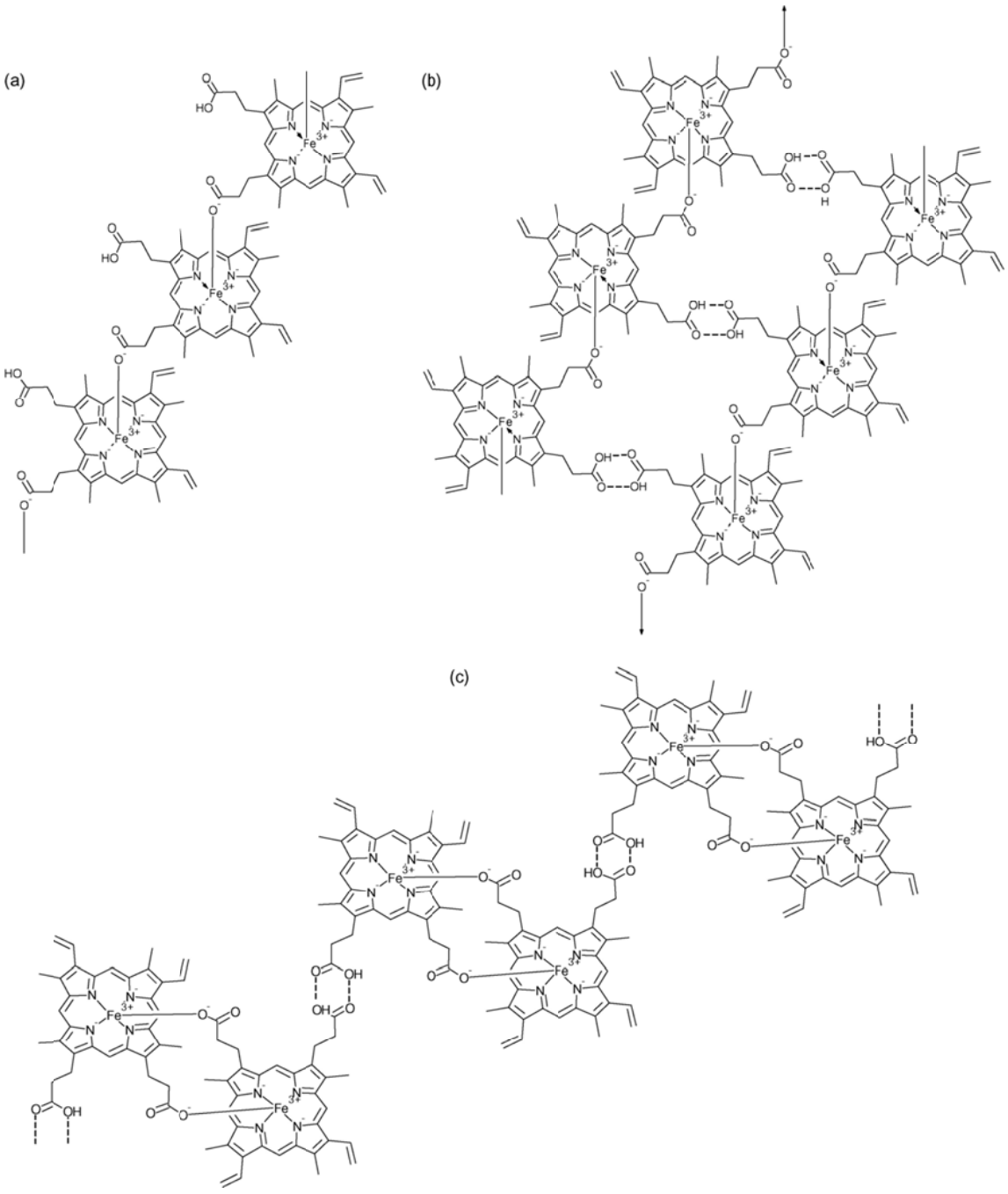


Figure 1.4: The different chemical structures of haemozoin crystals (Egan, 2008).

(a) Fe(III)PPIX molecules are linked via Fe(III)–propionate coordination bonds forming long chains of crystals. (b) the haemozoin (and β-haematin) structure involves a centrosymmetric unit cell in an antiparallel polymer chains linked by hydrogen bonds between the non-ionised propionic acid groups. (c) haemozoin crystals are centrosymmetric dimers linked by hydrogen bonds between the propionic acid groups.

1.7.3 Haemozoin structure

Several researchers have proposed that in addition to the polymerized haem units, lipids may be associated with the haemozoin structure. The understanding of how lipids or lipid bodies form part of the haemozoin formation process was shown to occur within the lipid bodies (dubbed lipid nanospheres) found in the parasite digestive vacuole (Pisciotta *et al.* 2007). Using electron microscopy, the lipids bodies were examined by fixing the whole parasites with Malachite Green before the haemozoin and lipids were separated by sucrose cushion centrifugation. The subsequent analysis using gel electrophoresis staining with Coomassie Brilliant Blue and with Western blotting failed to detect any presence of proteins and histidine-rich protein II (HRPII). Sullivan *et al.* (1996) had proposed that HRPII, an abundant protein in *P. falciparum*, catalysed or initiated haemozoin formation. However, using immunofluorescence labelling, Papalexis *et al*. (2001) demonstrated that HRPII is mainly localised in the RBC cytoplasm and only a sub-population is located in the digestive vacuole. It was also discovered that 97% of HRPII is exported from the parasite to the RBC with only 3% found in the digestive vacuole where the haemozoin formation occurs (Akompong *et al.,* 2002).

It was Bendrat *et al.* (1995) and Dorn *et al.* (1995) that discovered that haemozoin and β-haematin were contaminated with lipids which may play a part in the autocatalytic reaction of haemozoin formation and that the parasite factor responsible for promoting β-haematin formation was not deactivated by boiling or protease (or polymerase activities as suggested by Slater and Cerami (1992)). Dorn *et al.* (1995) also demonstrated that haemozoin and preformed β-haematin supported β-haematin formation suggesting the process is autocatalytic and non-enzymatic. Fitch *et al*. (1999) studied the lysate of *P. falciparum* and found that uninfected RBC lysate possessed no β-haematin formation activity, while the uninfected RBC lysate possessed 50% of the β-haematin formation activity compared to the infected RBC lysate. This work further supported that of Dorn *et al.* (1998) who demonstrated that the non-lipid components of the RBC membranes were incapable of promoting β-haematin formation, while the infected RBCs showed that lipids were essential in haemozoin formation. Fe(III)PPIX co-precipitated with a series of lipids, fatty acids and detergents and incubated at a pH range from 4-6 at 37 ^{o}C or 70^{o}C resulted in a rapid rate of β-haematin formation with an optimal pH found to be around 5. Jackson *et al.* (2004) used a combination of fluorescence microscopy using Nile red dye and transmission electron microscopy to discover lipid particles closely

associated with the digestive vacuole of the parasite. These lipids were found to be predominantly mono-, di- and tri-acylglycerols which promoted β-haematin formation. Coppens and Vielemeyer (2005) subsequently published an electron micrograph image showing haemozoin in the digestive vacuole of *P. falciparum* completely encapsulated within neutral lipid body.

Using thin layer chromatography, Pisciotta *et al*. (2007) found a predominance of mono-acylglycerols with a significant quantity of phosphatidyl ethanolamine from the isolated haemozoin and lipids. The lipid bodies consisted mainly of monopalmitoyl- and monostearoyl-glycerol. The phosphatidyl ethanolamine (an amphipathic phospholipid) played a role in stabilising the lipid nanospheres since such lipid bodies are usually surrounded by a monolayer of phospholipids, glycolipids or sterol (Coppens and Vielemeyer, 2005). These lipids may have originated from the inner membrane of the endocytotic transport vesicles (PPM in Figure 1.3) which transport the haemoglobin to the digestive vacuole. It has been proposed that the acylglycerols were assembled from the by-products of the digested lipids of the PPM by phospholipidases when the transport vesicles fused with the digestive vacuoles (Jackson *et al*., 2004). Egan *et al.* (2006) studied the lipid-water interface and demonstrated the immediate formation of β-haematin within 30 minutes at 37^{o}C at an environmental pH of 4.8 in a simulated lipid environment. Again demonstrating that lipids or lipid bodies are required for the formation of β-haematin.

In the conditions mimicking those of the digestive vacuole, it has been assumed that the dimerization of the Fe(III)PPIX were in the form of the μ-oxo dimer (James, 1978); however de Villiers *et al.* (2007) demonstrated that H_2O-Fe(III)PPIX and HO-Fe(III)PPIX spontaneously formed π-π complexes in aqueous solution (Figure 1.5). Under conditions prevailing in the digestive vacuoles, only one propionic acid group on each porphyrin is ionised in the neutral $(H_2O\text{-Fe(III)PPIX})_2$ species ; however it was postulated that at a higher pH, both propionic acid groups on each porphyrin are ionised. Haemozoin crystals are formed when the haemozoin precursors in the forms of H_2O-Fe(III)PPIX or HO-Fe(III)PPIX are transported/delivered to or fused with lipid bodies, are orientated for the negatively charged propionate group of one Fe(III)PPIX to interact with the positively charged Fe(III) centre of the other and vice versa (Figure 1.4c). The concomitant formation of the Fe(III)-propionate bond and the displacement of the axial H_2O and/or OH^- molecules then formed a haemozoin dimer.

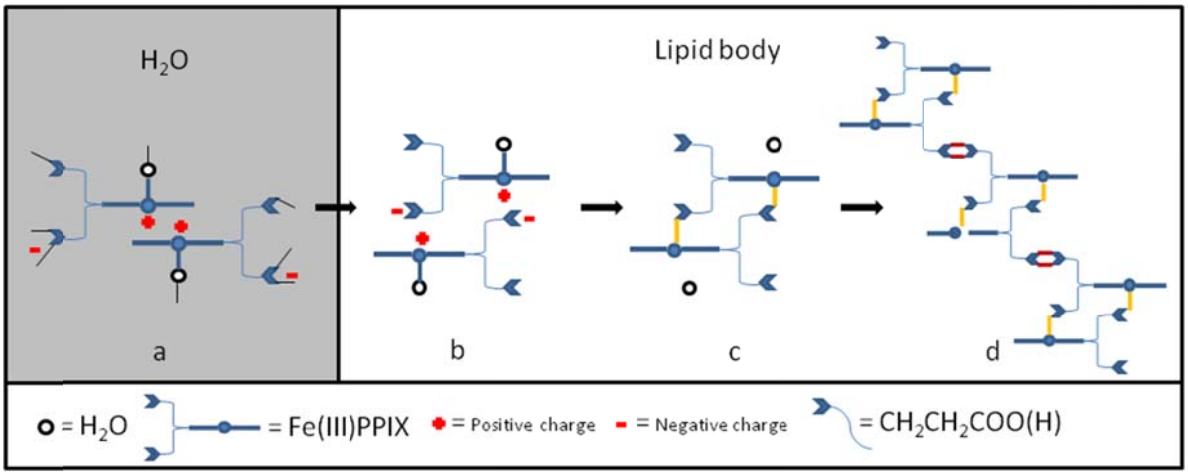


Figure 1.5 A schematic depicting the proposed formation of haemozoin in lipid bodies. The H_2O-Fe(III)PPIX formed the π-π dimers in the aqueous solution when haemoglobin was degraded forming (b) haemozoin precursor dimers with H_2O axial ligands in the lipid bodies; (c) haemozoin dimers are formed and ultimately (d) haemozoin crystals. The Fe(III)PPIX-propionate bonds are shown in yellow, while the hydrogen bonds between the propionate acid groups are shown in red (de Villiers *et al.*, 2008).

1.7.4 The detoxification of the reactive oxygen intermediates

Haem [Fe(II)PPIX] is released in the digestive vacuole at the same time when the globin subunits are cleaved into peptides and finally into amino acids. Fe(II) is autoxidised to Fe(III) by a mechanism that is poorly understood, it is however presumed that O_2 is the oxidant. Atamna and Ginsburg (1993) established that the process in which oxyhaemoglobin is rapidly oxidised to methaemoglobin at a low pH generated a vast amount of superoxide anion (O_2^-) and under the acidic conditions of the digestive vacuoles, O_2^- dismutes to O_2 and H_2O_2 (Figure 1.6). The formation of the reactive oxygen intermediates (superoxide anions radicals and hydrogen peroxide) can cause extensive cellular damage. But superoxide dismutase and catalase function to prevent oxidative stress by detoxifying these reactive oxygen intermediates in the digestive vacuole. It is speculated that the host erythrocyte cytoplasm may provide these enzymes to the parasite's digestive vacuole during the ingestion of the haemoglobin. Atamna and Ginsburg (1997) discovered that there is a low ratio of reduced glutathione (GSH) and glutathione disulfide (GSSG) in the trophozoite-infected erythrocytes as compared with normal erythrocytes; which is indicative of high oxidative burden. Atamna and Ginsburg (1997) also discovered that the rate at which the GSSG is being extruded from the

parasite to host cytoplasm and out of the erythrocyte indicated that the growing intra-erythrocytic parasite induces permeability pathways.

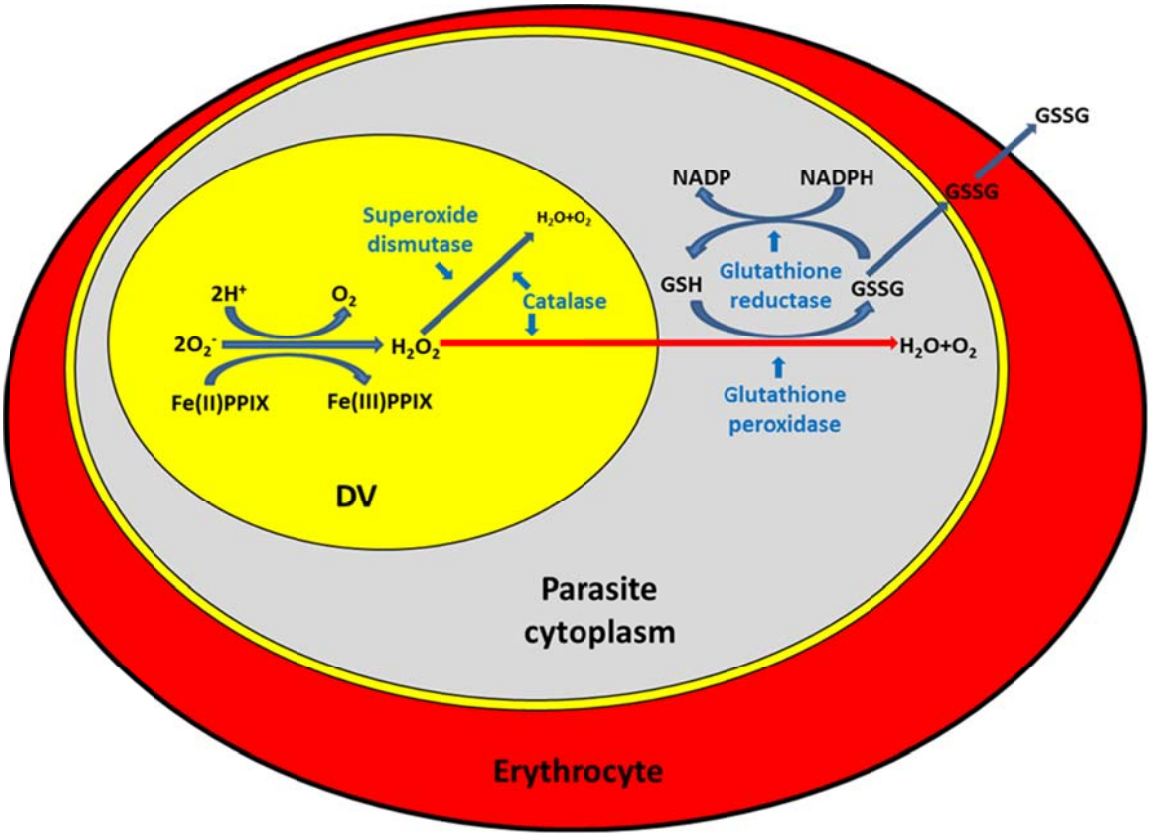


Figure 1.6 The detoxification of the H_2O_2 and the superoxide anion (O_2^-) after the autoxidation of Fe(II)PPIX to Fe(III)PPIX. H_2O_2 is disproportionate into H_2O and O_2 in the digestive vacuole via superoxide dismutase and catalase. The parasite uses glutathione peroxidase from its *de novo* glutathione synthesis and recycling, oxidising GSH (reduced glutathione) to GSSG (glutathione disulfide). Normally the parasite would reduce GSSG back to GSH via the enzyme glutathione reductase with NADPH as a cofactor while the NADP is reduced back to NADPH via the hexose monophosphate shunt. The rate and quantity of GSSG being produced by the parasite mean that in order to maintain its GSH/GSSG homeostasis, the growing parasite increases the permeability of the host-cell membrane exponentially increasing various solutes that translocate along their concentration gradient (Adapted from Atamna and Ginsburg, 1997).

1.7.5 Haemozoin as a drug target

Haem is not a parasite encoded molecule and biomineralisation or biocrystallisation is therefore a non-mutatable target, therefore the process of haemozoin formation is a pathway for targeting by novel drugs. Hänscheid *et al*. (2007) summerised the drugs that possess β-haematin formation inhibition (Table 1.4). As can be seen this is a susceptible target still being investigated by numerous agencies such as the Medicines for Malaria Venture (MMV) and warrants further investigation to determine if there are additional compounds that can inhibit this pathway and interact in an additive/synergistic manner with classical antimalarials.

Table 1.4 Drugs possessing the possiblity to inhibit β-haematin formation (Hänscheid *et al*., 2007).

Drugs	Reported β-haematin formation inhibition
Quinacrine	Hawley *et al.* (1998)
Chloroquine	Slater and Cerami (1992)
Amodiaquine	Slater and Cerami (1992)
Quinine / Quinidine	Slater and Cerami (1992)
Mefloquine	Hawley *et al.* (1998)
Halofantrine	Hawley *et al.* (1998)
Lumefantrine (benflumetol)	Olliaro and Milhous (2001)
Piperaquine	Warhurst *et al.* (2007)
Tafenoquine	Vennerstrom *et al.* (1999)
Pyronaridine	Hawley *et al.* (1998)
Isoquine	Not published
Ferroquine	Biot *et al.* (2005)
AQ-13	Hänscheid *et al*. (2007)
Methylene blue	Atamna *et al.* (1996)

1.8 Aims and objectives

Due to the wide spread of resistance by the malaria parasite to chemotherapeutic agents, the WHO has recommended combination therapies for first-line treatment against the complicated and uncomplicated forms of the disease. Since the haemozoin

formation pathway is not encoded and expressed in the parasite genome, it is therefore a viable and a non-mutatable target for novel drug designs (Hänscheid *et al*., 2007).

Thus the aim of this study was to establish a high-throughput ß-haematin formation inhibition assay on which to evaluate the properties of 7 known and 95 novel compounds and to correlate this activity with the biological activity of these compounds.

To achieve the latter, the objectives of the study are:

- Synthesise and characterise β-haematin crystals in order to establish and replicate the screening methods of β-haematin formation inhibition assay using acid acetate solutions.
- Establish and replicate high-throughput screening method of β-haematin formation inhibition in microtiter plates
- Elucidate the β-haematin formation inhibition properties of corrins, porphyrins and novel derivatives of 8-hydroxyquinolones, 4-hydroxyquinolines, chalcones and thiosemicarbazones.
- Elucidate the *in vitro* antimalarial properties of these compounds against a chloroquine-resistant strain of *P. falciparum*.
- Determine the interaction between the active compounds and standard antimalarial agents on β-haematin formation and antimalarial activity.
- Elucidate the cytotoxic properties of the novel derivatives against human RBCs and human epithelial kidney (HEK293) cells.
- Pro- and anti-oxidant effects of the compounds will be investigated by examining iron chelation and free radical scavenging properties.

Chapter 2

Methodology

2.1 Compounds and reagents

The highest quality reagents and compounds were purchased from reputable commercial companies and the new experimental compounds were synthesized and characterized as indicated in the following chapters.

2.2 β-Haematin inhibition assay

2.2.1 Synthesis of β-haematin crystals

The first step the project was to synthesise and characterise the β-haematin crystals in the laboratory according to the existing published methodology as described by Egan *et al*. (1994). Briefly, haematin solution was prepared by dissolving 15 mg haemin (Sigma-Aldrich®) in 3 ml of 0.1 M NaOH (Merck). The solution was constantly stirred in an Erlenmeyer flask. To this, 300 µl of 1.0 M hydrochloric acid (Rochelle Chemicals) was added, followed by the addition of 1.74 ml of 12.9 M sodium acetate buffer (pH 5) and heated to 60^{o}C.

The sodium acetate buffer was prepared with 105.82 g anhydrous sodium acetate (Sigma-Aldrich®) dissolved in Milli-Q® (double distilled deionised) water with constant stirring with a magnetic stirrer bar. The buffer solution was adjusted to pH 5 with HCl and made up to volume of 100 ml with Milli-Q® water. The buffer solution was preheated to 60^{o}C to dissolve the precipitated sodium acetate crystals before use.

Reaction samples were collected into 2.0 ml microcentrifuge tubes and quenched on ice for 5 minutes to stop the reaction at 0, 10, 30 and 60 minutes intervals. The solutions were filtered through 8 micron cellulose acetate/nitrate filter (Whatman®) with the aid of a vacuum pump and the crystals were washed with copious amount of Milli-Q® water. The crystals were dried over silica gel and phosphorous pentoxide at 37^{o}C for 48 hours and were stored at room temperature (25^{o}C) in a closed glass vial in an airtight container before being characterized (Section 2 2.2).

2.2.2 Characterisation of the β-haematin crystals via Fourier transformed infrared spectroscopy

The Fourier transformed infrared spectroscopy (FTIR) was used to obtain the infrared spectrum of absorption, emission, photoconductivity or Raman scattering of the synthesised β-haematin crystals. The FTIR analysis was primary used in identifying types of chemical bonds (function groups) which possess characteristic wavelengths of light that they could absorb.

Briefly, following the departmental protocol used in the Department of Pharmacy and Pharmacology, University of the Witwatersrand:

i. The samples from Section 2.2.1 were dried again in a 60^{o}C oven for 2 hours to remove any excess moisture that might have accumulated in the sample during storage.

ii. Using a mortar and pestle, the β-haematin crystals and anhydrous potassium bromide were mixed thoroughly at a 1% (w/w) ratio of sample to KBr.

iii. Approximately 200 mg of the sample was loaded into the stainless steel die, sandwiched between the two polished metal pellets inside an evacuable tube with the plunger resting lightly on the top of the metal pellet.

iv. The die assembly was mounted in a press and then connected to the vacuum pump and evacuation was performed for 10 minutes. The press lever was depressed until 8 tons or 8 MPa of pressure was achieved. The pump was switched off and the pressure was released slowly via a pressure release valve.

v. The base of the die was removed and the two polished metal pellets along with the pressed disk were gently pushed out using the plunger.

vi. The brown coloured transparent disk was placed in a disk holder, which was inserted in the Nicolet IMPACT FTIR system. Using the OMNIC™ software, a broad scanning spectra was selected with wavenumbers from 4000 to 300 cm^{-1}. The intensity or the percent transmission was dependent on the quality and transparency of the sample disk prepared. The IR spectrogram (Figure 2.1) was generated and the wavenumber scale adjusted to display the definitive bands between 1800 and 1000 cm^{-1}.

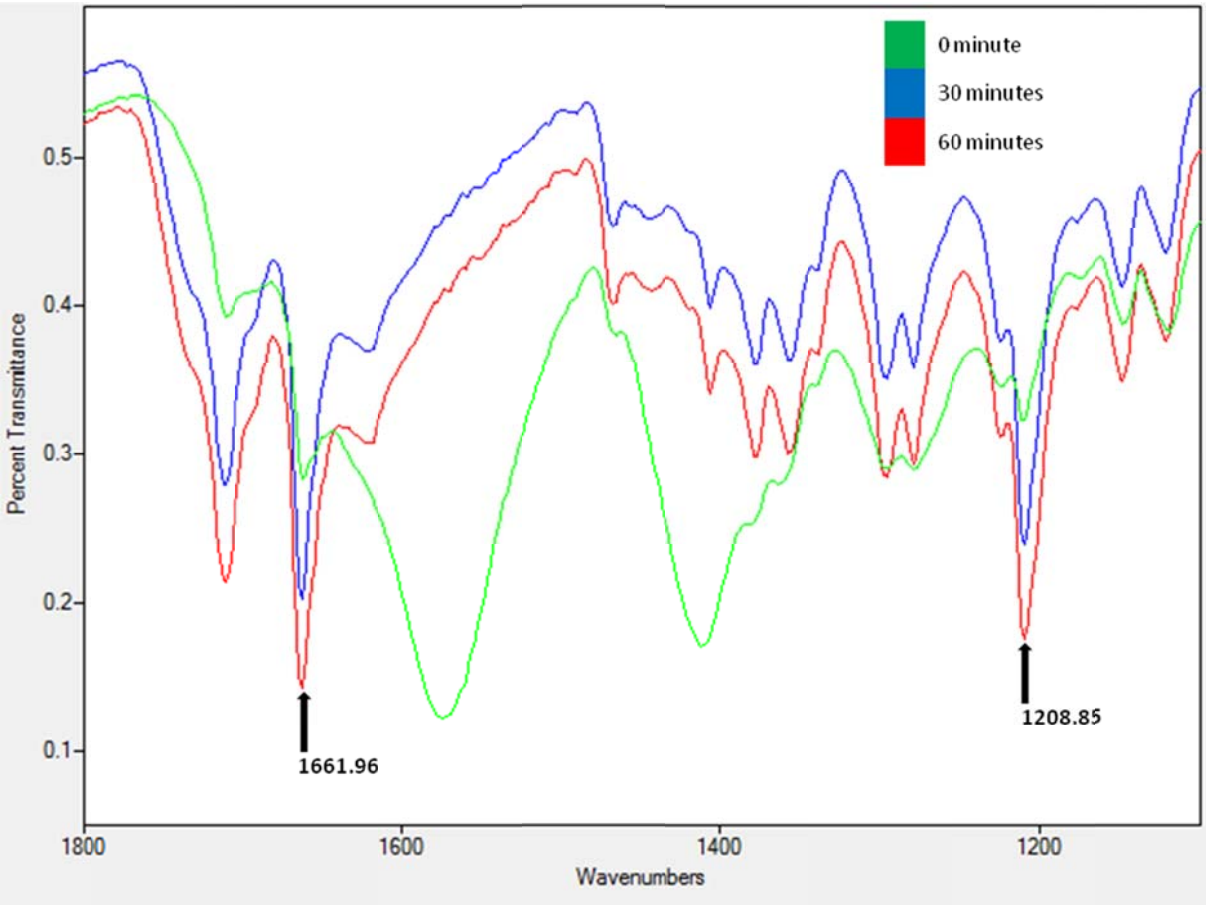


Figure 2.1: The IR spectra of the synthetic β-haematin crystals at 0 (green), 30 (blue) and 60 (red) minutes at 60°C. The infrared spectra of 1661.96 and 1208.85 cm^{-1} were marked with arrows.

Two definitive sharp bands (1661.96 and 1208.85 cm^{-1}) from the infrared spectra of the synthesised β-haematin crystals were used to determine the complete formation of the β-haematin crystals (Figure 2.1). These were comparable to those obtained by Egan *et al*. (1994), 1660 and 1207 cm^{-1}, Basilico *et al*. (1997), 1662 and 1209 cm^{-1}, and Slater *et al*. (1991), 1664 and 1211 cm^{-1}. The absorption between the 1700 to 1600 cm^{-1} of the IR spectrum denoted the presence of an unidenate carboxylate coordination onto the iron in the β-haematin crystals or the haemozoin pigment. The second distinctive IR absorbance of haemozoin between the regions of 1270 and 1080 cm^{-1}, denoted an axial carboxylate ligand where the C-O stretching frequencies from the O-methyl groups linked to various metalloporphyrins. From Figure 2.1, it could be concluded that the β-haematin crystals were synthesised as described in literature and the methodology was reproducible.

2.2.3 Scanning electron microscopy

The scanning electron microscopy (SEM) was also performed to verify the structures of the synthesised β-haematin crystals (Section 2.2.1), in comparison to isolated haemozoin pigments from infected RBCs (Sections 2.2.4), and the starting product, haemin chloride crystals (Sigma-Aldrich®).

The SEM imaging was performed along with Mr Christiaan van der Merwe at the University of Pretoria following the Laboratory for Microscopy and Microanalysis unit's procedural protocol. Using the cryo method, briefly, the three samples were prepared for imaging by mounting them on stubs with carbon tape and critically point dried with liquid nitrogen to remove any moisture from the samples before the samples were coated with ruthenium tetroxide. The images were examined using the JEOL 6000F SEM at -180^{o}C (Pretorius *et al*., 2006).

Following the analysis of the three samples (Figure 2.2) the crystals shape and size were found to be comparable to that described by Egan *et al*. (2001) and Sullivan (2002).

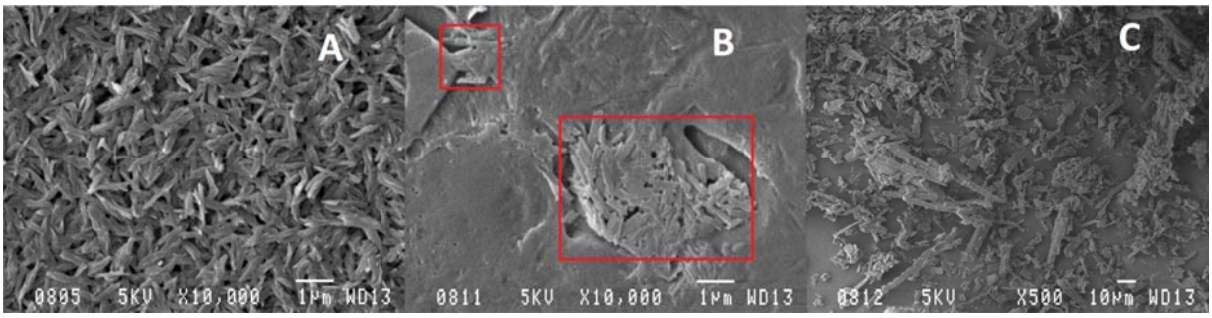


Figure 2.2: SEM of β-haematin (A), haemozoin isolated from infected RBCs (B) and haemin crystals (C). The haemin crystals were included for size comparison to β-haematin and haemozoin crystals. The haemozoin sample required further washing steps to remove the contaminant RBC membranes and improve upon the definition of the SEM; however, haemozoin crystals were observed (B, red squares).

2.2.4 Isolation of haemozoin from infected red blood cells

The malaria-infected blood in the mid to late trophozoite stages (Figure 1.2) of the life cycle were harvested and stored at -20^{O}C until needed. Using the departmental protocol and Orjih (1994), the frozen malaria-infected blood was thawed to room temperature (25^{o}C) before being centrifuged at 400*g* for 5 minutes. The supernatant was aspirated before the

addition of 4 volumes of 0.1% (w/v) saponin (Sigma-Aldrich®) in 10% (v/v) PBS. The saponin-washing process was repeated thrice before washing with PBS (8.0 g NaCl, 0.3 g KCl, 0.73 g $Na_2HPO_4 \bullet 2H_2O$ and 0.2 g KH_2PO_4 in 1 liter Milli-Q® water, pH 7.4). Following three PBS washes, the haemozoin was washed thrice with Milli-Q® water (double distilled deionised water filtered at 18 megaohms). The isolated haemozoin crystals were placed on a glass petri-dish and allowed to dry in an incubator at 37°C for 72 hours and stored until used in Section 2.2.3.

2.3 Assay of β-haematin formation inhibition

Once the β-haematin was synthesised and characterised, the ability for standard antimalarial agents to inhibit the formation of the β-haematin was investigated. β-Haematin formation was observed from temperatures 37°C to 70°C under acidic conditions (Slater *et al.* 1991; Egan *et al*. 1994), therefore the reaction temperature was lowered from 60°C to 37°C in order to observe the inhibitory effect at the optimal temperature for growing the malaria parasite and the temperature at which the radioactive drug sensitivity assay (Section 2.7.5) was conducted. The incubation period was extended from 60 minutes (at 60°C to 24 hours at 37°C) to ensure optimal crystal formation and to mimic body temperature (data not shown).

The determination of inhibition of β-haematin formation was adopted from a modified method of Auparakkitanon *et al.* (2003). Preliminary studies indicated that to ensure optimal crystal formation, the order in which the reagents were added was essential (data not shown). As such the following sequential order was employed, a 100 µl of freshly prepared haemin (6.5 mM dissolved in 0.1 M NaOH); 50 µl drug or solvent (water or dimethyl sulphoxide (DMSO) as the control); 200 µl 3 M sodium acetate; 50 µl 17.485 M glacial acetic acid were aliquot into microcentrifuge tubes. After 24 hours of incubation at 37°C, the microcentrifuge tubes were spun in a high speed centrifuge (Jouan MR1812) at 9000*g* for 15 minutes and the supernatants removed. The pellets were resuspended in 400 µl DMSO to remove unreacted or uncomplexed haematin from the β-haematin crystals, which were insoluble in DMSO. This DMSO-washing process was repeated three times before the final pellets were dissolved in 1400 µl of 0.2 M NaOH. The suspensions were aliquot into a 96-well microtiter plate in triplicate, diluted in a 1 in 4 ratio with 0.2 M NaOH for spectroscopic quantification at 405 nm.

A standard curve of haematin (Sigma-Aldrich®) dissolved in 0.2 M NaOH was constructed in each experiment to determine the amount of haematin present. A linear-regression standard curve was generated and the straight-line equation was used to determine the amount of haematin in the sample. The percentage of β-haematin formed was calculated using Equation 2.1.

$$\% \text{ β-haematin formed} = \frac{\text{moles of haematin in sample}}{\text{moles of haematin in control}} \times 100$$

Equation 2.1: Percentage β-haematin formation.

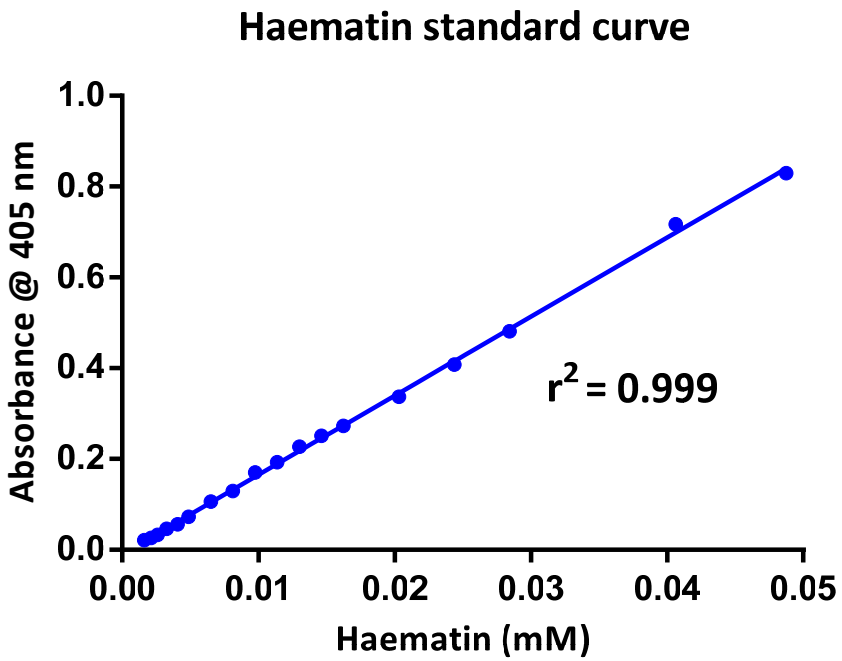


Figure 2.3: The haematin standard curve in β-haematin formation inhibition assay. The plotted points are the mean and standard deviations of 3 separate experiments.

The results were presented as the inhibitory concentration at which 50% of β-haematin crystals (IC_{50} value) were formed. Auparakkitanon *et al*. (2003) reported an IC_{50} value for chloroquine as 0.125 mM, while in this project, an IC_{50} value for chloroquine of 0.134 ± 0.004 mM was observed.

2.4 β-Haematin inhibitory activity assay

High-throughput testing is critical in drug screening and as such the previous method (Section 2.3) was too laborious and too time consuming. As such an improved and modified method was established using the quantitative β-haematin inhibitory activity (BHIA) assay as described by Parapini *et al*. (2000) and Deharo *et al*. (2002).

2.4.1 Haemin concentration calibration curve

In order to determine the optimal concentration of haemin to be used in the high-throughput assay, a standard curve was generated. A 2 mg/ml stock solution of haemin in DMSO was prepared and 50 µl of the stock solution was serially (1:2) diluted in triplicate in a non-sterile 96-well microtiter plate along with 50 µl of Milli-Q® water, before the assay was initiated with the addition of 100 µl 0.5 M acetate buffer (pH 4.4). The 0.5 M acetate buffer (pH 4.4) was prepared according to Deutscher (1990) where 30.5 ml of 0.5 M acetic acid was added to 19.5 ml of 0.5 M sodium acetate and made up to volume with 50 ml Milli-Q® water to a final pH of 4.4. Preliminary studies indicated that the maximum final concentration of DMSO present in the reaction should be no more than 25%, where percentages greater than this interfered with the formation of the crystals (data not shown; Ncokazi and Egan, 2005).

After incubation at 37^{o}C for 24 hours, the microtiter plate was centrifuged at 1600*g* for 20 minutes, 100 µl of the supernatant was discarded. The pellets were resuspended in 100 µl DMSO and centrifuged as before. Two further DMSO washing steps were performed. The plate was washed once with Milli-Q® water and 150 µl supernatant was removed. The pellets were dissolved in 150 µl of freshly prepared NaOH to a final NaOH concentration of 0.2 M. The plate was placed in an orbital shaker (MRC Thermo-Shaker MB100-4P) and shaken for 2 minutes at 1200 rpm to ensure the pellets were completely dissolved. Dissolved β-haematin/NaOH suspension (50 µl) was aliquoted into a new 96-well microtiter plate, and diluted 1:4 with 150 µl of 0.2 M NaOH for spectroscopic quantification at 405 nm using the iEMS Reader MF (Labsystems) and Ascent™ software version 2.6. A standard curve was constructed and the haemin concentration to be used in the subsequent high-throughput BHIA assays was determined to be 0.5 mg/ml, which gave an absorbance of 1.0 at 405 nm (Figure 2.4).

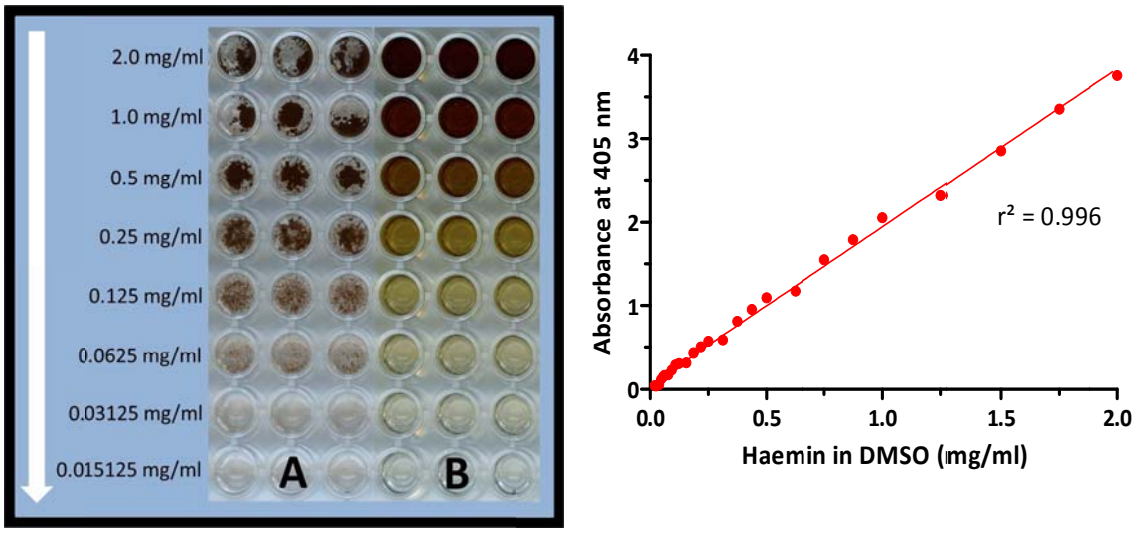


Figure 2.4: A standard curve of haemin prepared in DMSO measured at 405 nm. The haemin was converted into β-haematin after 24 hours at 37°C with the crystals clearly visible (A) and when the β-haematin crystals were dissolved in NaOH, a yellow-brown colour was observed (B). The plotted points include the standard deviation of 3 separate experiments.

The amount of crystals formed was directly proportional to the amount of starting haemin. From the standard curve, it was decided to use a concentration of 0.5 mg/ml haemin for the high-throughput assays at which the maximum absorbance value was 1.0.

2.4.2 β-Haematin: time versus formation

The kinetics of 0.5 mg/ml haemin used in the high-throughput assay of β-haematin was determined. The experiment was set up as follows; in microcentrifuge tubes, haemin, Milli-Q® water and the acetate buffer were added in the same ratio and order as in Section 2.4.1 and the samples were collected at hourly intervals for 24 hours. As in Section 2.2.1, the reactions were stopped by quenching the microcentrifuge tubes on ice and the tubes stored in -20°C until the washing steps. The microcentrifuge tubes were centrifuged at 1600*g* for 20 minutes and the supernatant collected, i.e. Fraction I which consisted of the soluble fraction of unprecipitated material, Fraction II consisted of the unreacted, uncomplexed haemin that was collected after the pellets were resuspended in DMSO and centrifuged. After two more DMSO wash-steps, and a Milli-Q® water wash-step, the pellets were dissolved in 0.2 M NaOH. The NaOH soluble Fraction III along with the other two fractions

was aliquoted into 96-well microtiter plates and measured spectrophotometrically at 405 nm. The amount of haematin (M) recovered in each fraction at each collection period was calculated from the haematin standard curve (Figure 2.3). A time versus haematin concentration was plotted (Figure 2.5), depicting the amount of haematin recovered in each fraction.

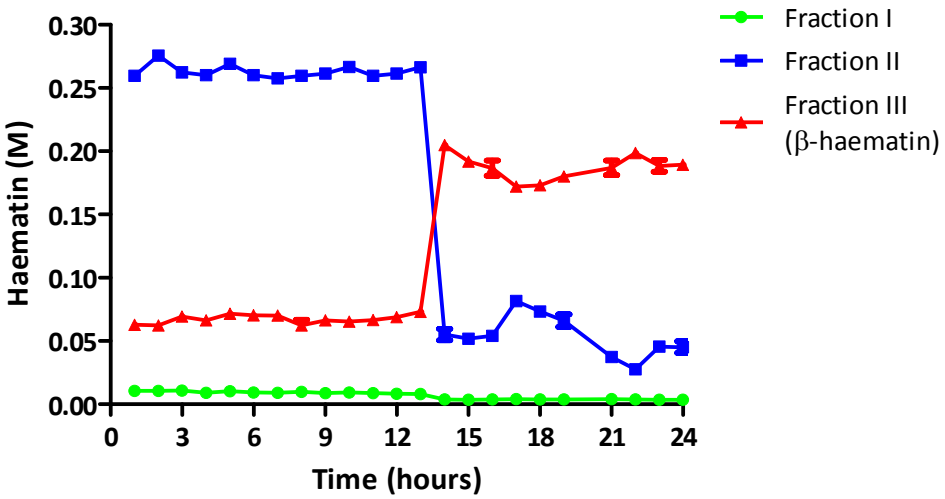


Figure 2.5 Kinetics of β-haematin formation. Data expressed as the amount of haematin recovered from β-haematin formation from each fraction. Data points included standard deviation of 3 separate experiments.

The reaction of β-haematin formation reached the plateau after 15 hours and stayed constant until 24 hours. The amount of haematin recovered was also calculated (Table 2.1). The percentage recover for Fraction III was 76.3%, which was lower than the averaged 85% recovery that was reported by Parapini *et al*. (2000) across a range of acidic pH (2.7 - 5.1) (Table 2.1). This could be contributed to the fact that Parapini *et al*. (2000) used more starting haemin, as well as an 8 M acetate buffer that was 16 times more concentrated than the concentration used in this reaction. Only 54% of haematin was recovered from this methodology, which was slightly better than the 52% haematin recovered by Basilico *et al*. (1998) and 50% by Dorn *et al.* (1998), even though the experimental parameters were not entirely the same.

Table 2.1 Haematin recovered from the β-haematin formation reaction. Haematin recovered in Fractions I, II and III following incubation of 0.5 mg/ml haemin (0.7669 mM) in an acidic acetate buffer (pH 4.4) at 37^{o}C for 24 hours.

Fraction	Haematin recovery (M)	% Recovery
I	0.004 ± 0.0002	1.58
II	0.054 ± 0.017	22.12
III	0.185 ± 0.001	76.30
Total	0.243 ± 0.027	100

2.4.3 High-throughput screening: β-haematin inhibitory activity assay

The high-throughput assay allowed for numerous compounds (up to 28 compounds) tested at one concentration in triplicate wells to be tested at one time along with standard antimalarial agents known to inhibit haemozoin formation, such as chloroquine and quinine. In this method the 50% inhibitory concentration for β-haematin formation inhibition ($BHIA_{50}$) could also be determined for the compound under testing conditions as determined in Section 2.4.2. A total of 50 µL of a 0.7669 mM (0.5 mg/ml) solution of haemin was dissolved in DMSO and distributed into 96-well flat-bottom microplates (38.3 nmol/well) along with 50 µL of water soluble compounds in 5:1; 1:1; 0.1:1 molar equivalents to haemin, into triplicate test wells. In the control wells, 50 µL of water was added.

Whilst for the water insoluble compounds, the final concentration of DMSO per well was kept constant at 25%, as it was found that a higher percentage DMSO interfered with crystal formation (data not shown).

β-Haematin formation was initiated by the addition of 100 µL of 0.5 M acetate buffer to a final reaction pH between 5.0-5.2. The plates were then incubated at 37^{o}C for 24 hours. Following centrifugation as in Section 2.4.2, the diluted 1:4 Fraction III (Section 2.4.2) was spectroscopic quantified at 405 nm using the iEMS Reader MF (Labsystems) Ascent™ software version 2.6. The data was expressed as the percentage inhibition of β-haematin formation calculated by using Equation 2.2.

$$\%\ \beta\text{-}Haematin\ formation\ inhibition\ = \frac{(O.D.Control - O.D.Drug)}{(O.D.Control)} \times 100$$

Equation 2.2: Percentage inhibition of β-haematin formation.

Where possible the $BHIA_{50}$ value was obtained for each compound and controls from the log sigmoid dose response curve (Figure 2.6) generated from the computer software Enzfitter® (Biosoft, UK) and GraphPad Prism® (GraphPad Software, Inc., U.S.A). At least three separate experiments were performed for each compound/control tested. The $BHIA_{50}$ value for each experiment was calculated and the average and standard deviation (s.d.) determined for each of the compound tested. The $BHIA_{50}$ values were used to compare those of the test compound to that of chloroquine (expressed as % β-haematin formation inhibitory activity compared to chloroquine).

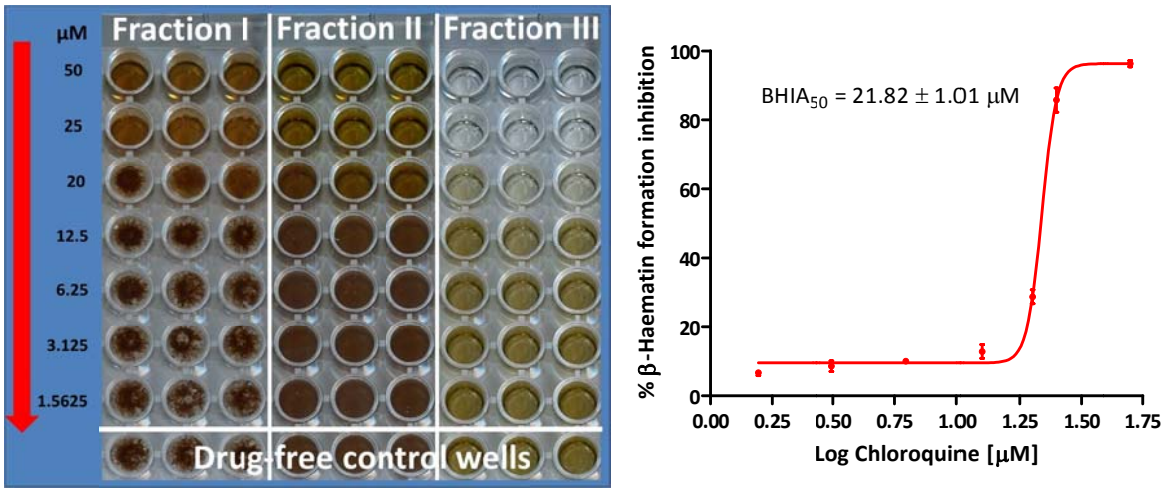


Figure 2.6: The dose-dependent effect of the positive control, chloroquine in the high-throughput assay. The crystals in the control and lower chloroquine concentrations wells can be observed.

2.5 Combination assay

In accordance with the WHO guidelines, treatment of malaria should consist of two or more drugs to decrease the risk of drug resistance developing (WHO World Malaria Report, 2014), as has been widely used in the treatment of diseases such as cancer, AIDS and tuberculosis. The use of multiple drugs may target multiple targets, multiple subpopulations, or multiple diseases simultaneously. The use of several drugs with different mechanisms of action may also direct the effect against a single target and treat it more effectively. Outcomes of therapeutic synergism include:

- Increased efficacy of the therapeutic effect,

- Decreased dosage, but with increased or equivalent efficacy to avoid toxicity, and
- Minimal or reduced development of drug resistance (Chou, 2010).

Quinine has been shown to display synergistic interactions when combined with artemisinin and artemether (Gupta *et al.,* 2002) and antagonism with atovaquone (Canfield *et al.*, 1995). As such, the most effective novel test compounds in this study were combined with standard antimalarial agents to determine the combined effects against the parasite.

Combination studies were carried out using the tritiated hypoxanthine incorporation assay as described in Section 2.7.8, but was modified to accommodate the addition of the combined drugs (van Zyl *et al*., 2010). Based on the initial $BHIA_{50}$ values obtained for the individual compounds, various drug concentration ratios were prepared taking a 20 times dilution factor into account. This was due to the 10 times dilution factor for the tritiated hypoxanthine incorporation assay (Section 2.7), as well as a dilution factor of 2 for the 1:1 combination of compound **X** and compound **Y** (Table 2.2).

Table 2.2: Combined concentration ratios of compounds **X** and **Y**. Where **X** and **Y** were mixed in a 1:1 volume ratio.

X	100%	90%	85%	75%	50%	45%	35%	15%	0
Y	0	10%	15%	25%	50%	55%	65%	85%	100%

The $BHIA_{50}$ values for the eight drug combinations were determined (Section 2.4.3) and to determine the interaction between the two compounds, an isobologram (Figure 2.7) was constructed by plotting X- and Y-axis points generated using Equation 2.3:

$$(X{:}Y) = \frac{BHIA_{50}\ of\ X\ in\ combination}{BHIA_{50}\ of\ X\ alone} ; \frac{BHIA_{50}\ of\ Y\ in\ combination}{BHIA_{50}\ of\ Y\ alone}$$

Equation 2.3: Relative ratios of **X**:**Y**. Ratios were calculated using the $BHIA_{50}$ values of combined ratio of X and Y over the individual IC_{50} values of **X** and **Y**, respectively.

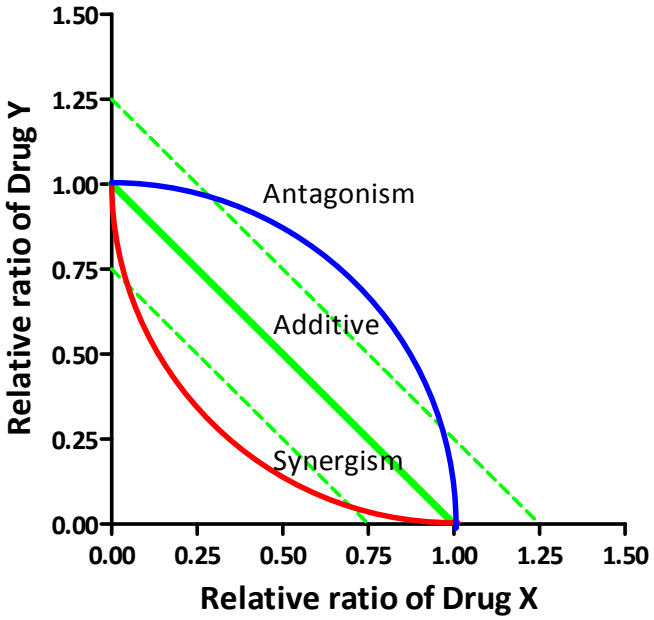


Figure 2.7: Possible pharmacological interactions between compounds **X** and **Y** were visualised using an isobologram.

The fractional inhibition concentration (FIC) was used to calculate the strength of the interactions. Whilst, the sum of the FIC values (∑FIC) depicted the combined interactions of the compounds **X** and **Y** (Equation 2.4). According to a sum of a 1 is an additive interaction, <1 a synergistic interaction and >1 an antagonistic interaction. In this study, a modified calculation and interpretation of the FIC value was adopted; where an additive interaction had an FIC value between 0.75-1.25, <0.75 a synergistic interaction while >1.25 was interpreted to have antagonistic interaction (Berenbaum, 1978; van Zyl *et al*., 2010).

$$\sum FIC = \frac{BHIA_{50} \text{ of } X \text{ in combination}}{BHIA_{50} \text{ of } X \text{ alone}} + \frac{BHIA_{50} \text{ of } Y \text{ in combination}}{BHIA_{50} \text{ of } Y \text{ alone}}$$

Equation 2.4: The ΣFIC value calculated using the $BHIA_{50}$ values of the combined and individual $BHIA_{50}$ values of **X** and **Y**.

2.6 Malaria culture maintenance

The chloroquine-resistant strain of *Plasmodium falciparum* (FCR-3) was obtained from Dr Janet Freese of the Research Institute for Diseases in the Tropical Environment, Durban,

South Africa. *P. falciparum* was cultured *in vitro* according to modified methods of Freese *et al.* (1988) and Trager and Jensen (1976). Biosafety ethics clearance (protocol number: 20090503) was obtained from the institutional Biosafety Committee of the University of the Witwatersrand (Appendix A) which allowed for the *in vitro* culturing and experimentation of the malaria parasite, as well as the handling of human plasma and human RBCs. All procedures were conducted in Class II sterile biosafety cabinets with 70% ethanol used to prevent contamination.

2.6.1 Maintenance of *P. falciparum* (FCR-3) culture

The FCR-3 strain of *P. falciparum* was maintained in 75 cm^2 tissue culture flasks (Corning®, Sigma-Aldrich®) at 5% haematocrit and between 5~10% parasitaemia. Complete culture medium was aspirated and replaced every 24 hours. The percentage parasitaemia and morphology of the parasite were determined daily from Giemsa-stained thin blood smears (Section 2.6.6). If the parasitaemia was >10% (mainly in the trophozoite and/or schizont stages), approximately half the culture was discarded such as to not unduly stress the culture by being exposed to excessive waste metabolites and competition for nutrients. If the latter did occur, it resulted in the asynchrony of the culture and parasite death. The discarded culture was aspirated following centrifugation at 400*g* for 5 minutes and replaced with freshly, washed RBCs (Section 2.6.5) and all resuspended in 20 ml of complete culture medium (Section 2.6.3). The culture was then re-incubated at 37^{o}C in a 5% CO_2, 3% O_2 and 92% N_2 atmosphere (Jensen and Trager, 1977). If the parasite was in the early to mid-ring stage regardless of parasitaemia, the culture was synchronised (Section 2.6.7) to ensure the continuation of a synchronised culture for experiments and optimal growth.

2.6.2 Preparation of incomplete culture medium

The incomplete culture medium consisted of 10.4 g/l Roswell Park Memorial Institution (RPMI)-1640 (Sigma-Aldrich®), 5.9 g/l N-2-hydroxyethylpiperazine-N'-2-ethane-sulfonic acid (HEPES) buffer (Sigma-Aldrich®), 4 g/l *D*-glucose monohydrate (Merck), 44 mg/l hypoxanthine (Sigma-Aldrich®) and 50 mg/l gentamicin (Sigma-Aldrich®) dissolved in Milli-Q® water. The incomplete medium was sterilised through a Sterivex™-GS 0.22 µm filter (Millipore®) and stored at 4^{o}C until required. The incomplete experimental medium was prepared as above with the omission of hypoxanthine and gentamicin.

2.6.3 Preparation of complete culture medium

For the culturing of the *P. falciparum* FCR-3 strain, complete culture medium (pH 7.2~7.4) was prepared under sterile condition by supplementing incomplete culture medium (Section 2.2.3.1) with 10% (v/v) heat-inactivated human plasma (Section 2.6.4) and 4.2 ml $NaHCO_3$ (Merck). The 5% (w/v) $NaHCO_3$ was prepared in Milli-Q® water and sterilised through 0.22 µm filter and stored at 4°C. Similarly, the incomplete experimental medium was supplement with 10% (v/v) heat-inactivated human plasma and 5% (w/v) $NaHCO_3$ to prepare the complete experimental medium.

2.6.4 Preparation of heat-inactivated human plasma

Frozen plasma was purchased from the South African National Blood Services with the following exclusion criteria:

- Patients should not have visited a malaria area one month prior to donating blood.
- Patients should not have been on the following medication for at least 3 weeks before donating blood: any antibacterial agents, antimalarial, antifungal, antiviral, aspirin, heparin, and warfarin.

Three bags of plasma, thawed at 4°C, were pooled before being heat-inactivated at 56°C for 2 hours then centrifuged at 1750*g* for 10 minutes at room temperature. The supernatant was decanted and stored at -20°C until required. Human ethics clearance was obtained from the University of the Witwatersrand Human Ethics committee to use and purchase human plasma and blood (waiver certificate number: W-CJ-131030-1, Appendix B).

2.6.5 Preparation of red blood cells

Drug-free human whole blood was obtained from healthy volunteers (clearance certificate number: M140669, Appendix C1 and C2) using the same exclusion criteria as above for the collection of plasma (Section 2.6.4). The whole blood was collected in 6 ml blood tubes containing 1 ml of ACD-B (Acid Citrate Dextrose Solution B) anticoagulant (Lasec). The whole blood was centrifuged at 400*g* for 5 minutes before aspirating the plasma and buffy coat. The remaining RBCs were washed in equal volume of PBS (pH 7.2) by centrifuging the resuspended RBCs at 400 *g* for 5 minutes. PBS (pH 7.2) was prepared by dissolving 8 g NaCl (Merck), 0.3 g KCl (Sigma-Aldrich®), 0.73 g $Na_2HPO_4{\cdot}2H_2O$ (Riedel-de Haën®) and 0.2 g KH_2PO_4 (Fluka) in one litre of Milli-Q® water (pH 7.2). The solution was

autoclaved (121^{o}C at 1.2 kg/cm^{2} for 20 minutes) and stored at 4^{o}C. The blood was washed three times with PBS (pH 7.2), before resuspending the pellet in equal volumes of incomplete experimental medium (50% haematocrit) and stored at 4^{o}C for no longer than a week. The unwashed whole blood was used within 2 weeks of collection. The white blood cells were removed to prevent any interference with the [^{3}H]-hypoxanthine incorporation assay (Section 2.7).

2.6.6 Giemsa stain

Thin blood smears of the malaria culture were prepared daily on ethanol cleaned glass slides and air dried. The smears were fixed with 100% methanol (Sigma-Aldrich®) and air dried before staining with 10% (v/v) Giemsa stain for 20 minutes. The Giemsa stain consisted of: Commercial Giemsa stain solution (Merck) diluted 5-fold with a Giemsa buffer. The latter was prepared by dissolving 3.5 g KH_2PO_4 and 14.5 g $Na_2HPO_4{\cdot}12H_2O$ (Sigma-Aldrich®) in one litre Milli-Q® water (pH 7.2). The buffer was autoclaved and stored at 4^{o}C. The slides were stained for 20 minutes, rinsed with water and dried before viewing.

An alternative and quick staining procedure composed of using three prepared solutions, Rapi-Diff Stain Set (Alere Healthcare) was also used. Solution 1 fixed the slide, solution 2 stained the RBCs and solution 3 stained the parasites. Five dips of 1 second each in sequential order was sufficient to optimally observe the parasite after washing the slide with water and then drying.

The slide was microscopically examined at 1000x magnification under oil immersion. The stage, morphology of the parasite and the percentage parasitaemia (Equation 2.5) were determined after viewing and counting at least 10 fields of the thin blood smear before the appropriate action was taken for the optimal maintenance of *P. falciparum* culture (Section 2.6.1).

$$\%\, Parasitaemia = \frac{Total\ number\ of\ parasitised\ \text{RBCs}}{Total\ number\ of\ uninfected + parasitised\ \text{RBCs}} \times 100$$

Equation 2.5: The equation used to calculate the percentage parasitaemia from a stained thin blood smear.

2.6.7 Synchronisation of the malaria parasite culture

In order to maintain a synchronised malaria parasite culture, the D-sorbitol method as described by Lambros and Vanderberg (1979) was used. Briefly, when the parasites were predominantly in the early ring-infected stage of its life cycle, the culture was centrifuged at 400*g* for 5 minutes. The supernatant was discarded and the pellet resuspended in 20 ml of sterile 5% (w/v) D-sorbitol (Sigma-Aldrich®). The suspension was then incubated at room temperature for 20 minutes. The osmotic action of the D-sorbitol lysed the trophozoites and early schizonts, keeping the culture in synchrony. After 20 minutes, the suspension was centrifuged at 400*g* for 5 minutes, the supernatant discarded and the synchronised culture resuspended in complete culture medium and re-incubated (Section 2.6.3).

2.6.8 Cryopreservation and initiation of cultures

2.6.8.1 Cryopreservation of malaria parasites

In order to ensure the continued preservation of the malaria parasites, the parasites were regularly cryopreserved according to the modified methodology of Freese *et al.* (1988). A culture predominantly in the ring stage was pelleted by centrifugation at 400*g* for 5 minutes at room temperature. The pellet was resuspended in a 1:1 ratio of freezing solution. Aliquots of this suspension were transferred into sterile cryotubes (Corning®, Sigma-Aldrich®). The tubes were left to stand for 5 minutes at room temperature before being stored in liquid nitrogen. The freezing solution consisted of 28% (v/v) glycerol (Merck) in the freezing buffer which contained 7.2 g NaCl, 1.48 g $Na_2HPO_4 \cdot 2H_2O$ and 0.44 g KH_2PO_4 dissolved in 100 ml Milli-Q® water. This solution was sterilised through a 0.2 µm syringe filter (Separations) and stored at -20^{o}C.

2.6.8.2 Initiation of malaria culture from frozen stock

To reinitiate a culture, the frozen liquid nitrogen culture was rapidly thawed at 37^{o}C to which 0.1 volume of 12% (w/v) NaCl was added drop wise with continuous swirling of the cryotube (Freese *et al.,* 1988). The mixture was transferred to 9 volumes of 1.6% (w/v) NaCl, before being left to stand for 5 minutes at room temperature. The suspension was then centrifuged at 200 *g* for 5 minutes, before an additional 9 volumes of a 0.9% (w/v) NaCl and 0.2% (w/v) glucose (Merck) solution was added to the pellet. The suspension was re-centrifuged at 400*g* for 5 minutes and the pellet was resuspended in complete culture

medium (Section 2.6.3) with 20% (v/v) heat-inactivated human plasma and freshly washed RBCs to achieve a 5% haematocrit to optimise parasite growth. The suspension was transferred to a 25 cm^2 tissue culture flask (BD Falcon®, The Scientific Group), gassed and incubated at 37°C. Once the parasites were established in culture (parasitaemia ≈ 5%), the heat-inactivated human plasma was reduced to 10% (v/v) in the complete culture medium and the culture suspension transferred to a 75 cm^2 tissue culture flask and maintained as described in Section 2.6.1.

2.7 Tritiated hypoxanthine incorporation assay

Hypoxanthine is able to cross the parasitic membranes and ultimately be incorporated into both ribonucleic acid and deoxyribonucleic acid. The incorporation of a radiolabelled-isotope of hypoxanthine was used as an index for parasite metabolism. The inhibition of ^{3}H-hypoxanthine incorporation into the parasitic DNA served as the basis of screening possible antimalarial chemotherapeutic agents and to quantify the extent of cross-resistance amongst antimalarial agents. The modified method of Desjardins *et al.* (1979) was used to determine the inhibitory effect of various novel and standard test compounds on the intra-erythrocytic asexual form of the chloroquine-resistant FCR-3 strain of *P. falciparum* (Figure 2.8)

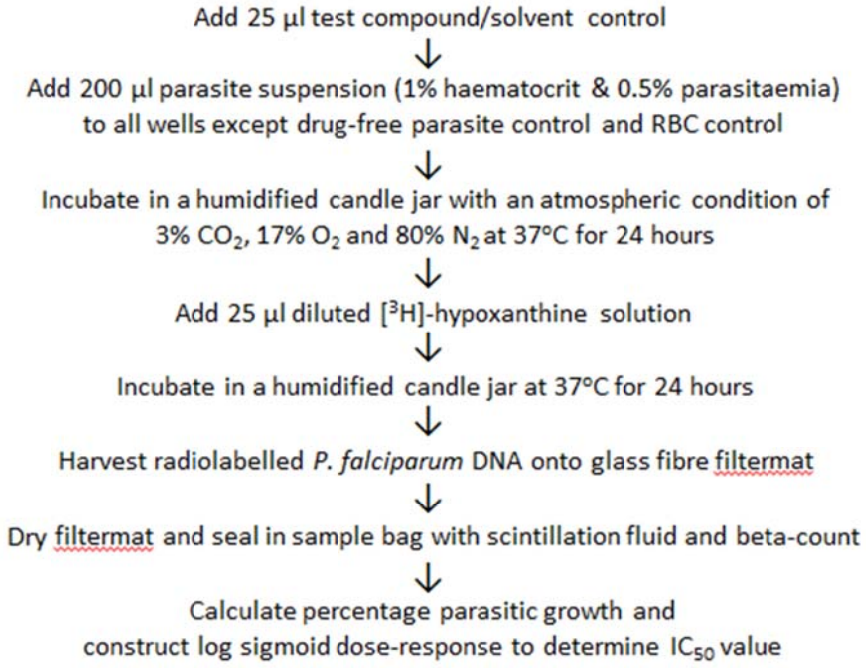


Figure 2.8: A summarised flow chart of the [^{3}H]-hypoxanthine incorporation assay and analysis.

2.7.1 Preparation of the uninfected red blood cells and parasites

The malaria parasite culture was pelleted by centrifugation at 400*g* for 5 minutes and washed three times with PBS (pH 7.2) before a thin blood smear was prepared to determine the percentage parasitaemia (Section 2.6.6). The experimental parasitaemia was adjusted to 0.5% with the addition of washed uninfected RBCs (Section 2.6.5) such that a final 1% haematocrit was prepared in complete experimental medium (Section 2.6.3).

2.7.2 Preparation of the classical antimalarial agents

Chloroquine diphosphate (M_r = 515.86 g/mol) and quinine hydrochloride (M_r = 396.91 g/mol) (Sigma-Aldrich®) both served as reference antimalarial agents. A stock solution of 10 mM of the reference antimalarial agents was prepared in Milli-Q® water and sterilised through a 0.22 µm syringe filter and aliquots stored at -20^{o}C. Incomplete experimental medium (Section 2.6.2) was used in the preparation and dilution of the reference antimalarial agents with a dilution factor of 10 taken into account.

2.7.3 Preparation of the novel test compounds

As in Section 2.7.2, hydrophilic compounds were dissolved in Milli-Q® water and sterilised through a 0.22 µm syringe filter and aliquots stored at -20^{o}C. However, certain test compounds were lipophilic and therefore synthesis grade DMSO (Merck) was used to dissolve and sterilise the compounds, where the maximum final DMSO concentration in the assay did not exceed 1% (v/v). The 1% DMSO concentration had no adverse effect on the permeability of the RBC membranes and was evaluated to have no effect on the parasite growth at this concentration (data not shown).

2.7.4 Preparation of the microtiter plates

The antimalarial activity of the test compounds and standard antimalarial agents were evaluated in a 96-well microtiter plate (Figure 2.9). Briefly, 25 µl of each drug was added in triplicate to wells A1 to G12, whilst 25 µl of solvent (incomplete experimental medium) was added to the 12 wells in row H. The adjusted parasite suspension (200 µl) was added to all the wells, except to wells H1 to H4, to which 200 µl of a 1% haematocrit (parasite-free) RBC suspension was added to serve as the uninfected RBC control. Wells H5 to H12 served as the drug-free parasite control or the 100% parasite growth control.

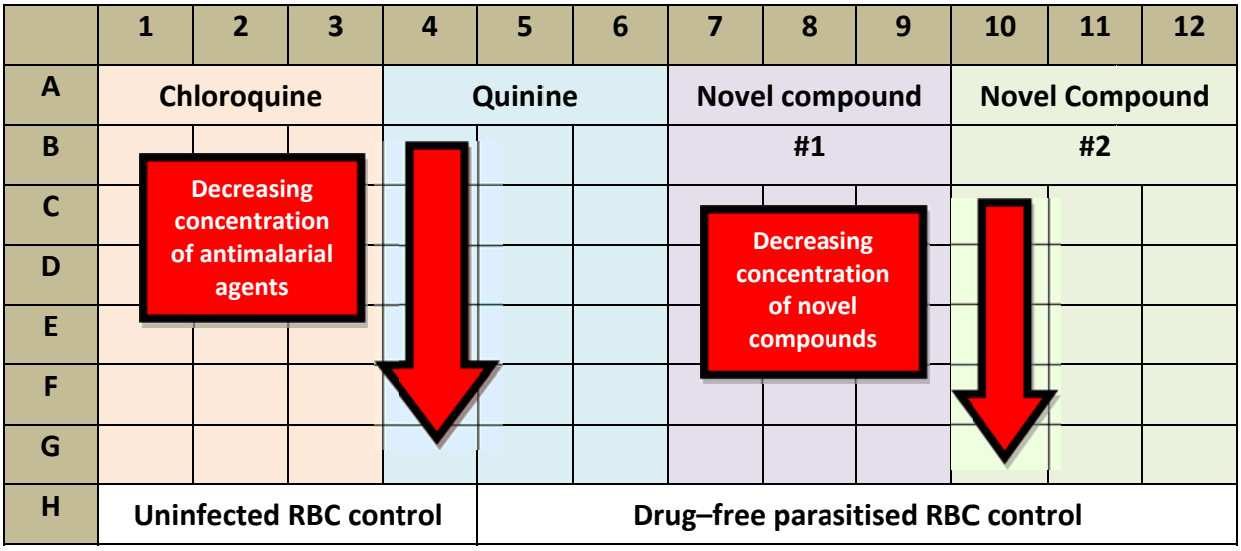


Figure 2.9: A representative layout of the 96-well microtiter plate used for a [^{3}H]-hypoxanthine incorporation assay.

2.7.5 Incubation of experimental plates

Once prepared, the plates were incubated at 37^{o}C for 24 hours in sterile glass candle jars which contained Milli-Q® water to ensure an humidified environment. The approximate micro-anaerobic atmospheric conditions (3% CO_2, 17% O_2 and 80% N_2) were achieved by burning fragrant-free candles in the airtight candle jars (Jensen and Trager, 1977).

2.7.6 Preparation of the isotope

Tritiated labelled hypoxanthine (5 mCi/ml) (Amersham Pharmacia Biotech) was stored in 50% (v/v) ethanol:water at -20^{o}C. From this 10 µl of the [^{3}H]-hypoxanthine was removed per 96-well microtiter plate. Following the evaporation of the ethanol with sterile filtered medical grade CO_2 gas (Afrox), 2.7 ml of incomplete experimental medium (Section 2.6.2) was added to the isotope and mixed well before 25 µl (0.92 µCi) was added to each well. The plate was then returned to the candle jar and incubated under micro-anaerobic-conditions at 37^{o}C for another 24 hours.

2.7.7 Harvesting and beta counting of the radiolabelled parasitic DNA

A semi-automated cell harvester (Titertek®, Flow Laboratory) was used to lyse the RBCs with Milli-Q® water before aspirating the parasite lysate from each well and depositing the negatively-charged radiolabelled parasitic DNA onto the positively charged glass fibre (GFB)

1205-401 Printed Filtermat A (Filtermat for use with 1205 Betaplate™, PerkinElmer®). The filtermat was air dried before being sealed in a 1205-411 Sample Bag (Sample Bag for Betaplate™, PerkinElmer®) along with 10 ml of scintillation fluid (1205-440 Betaplate™ Scint, PerkinElmer®). The bagged filtermat was placed in a Wallac 1205 Betaplate® liquid scintillation counter and each sample well beta counted for one minute. The results from the scintillation counter were expressed in counts per minutes (CPM). The percentage [^{3}H]-hypoxanthine incorporated into the parasite DNA (the percentage survival of the malaria parasite) was determined according to Equation 2.6 (Desjardin *et al*., 1979).

% [^{3}H]-Hypoxanthine incorporation =

$$\frac{CPM\ (drug) - CPM\ (mean\ uninfected\ RBC\ control)}{CPM\ (mean\ parasitised\ RBC\ control) - CPM\ (mean\ uninfected\ RBC\ control)} \text{x}100$$

Equation 2.6: Percentage [^{3}H]-hypoxanthine incorporation or parasite growth.

The concentration of compound that inhibited 50% [^{3}H]-hypoxanthine incorporation or parasite growth (IC_{50} value) was obtained from the log sigmoid dose response curve generated from the computer software Enzfitter® (Biosoft, UK) and GraphPad Prism® (GraphPad Software, Inc., U.S.A). At least three separate experiments were performed for each compound tested. The IC_{50} value for each experiment was calculated and the average and s.d. determined for each of the compound tested.

2.7.8 Combination assays and isobolograms

The most active antimalarial agents as determined from the [^{3}H]-hypoxanthine incorporation assay (Section 2.7), where combined with standard antimalarials such as chloroquine, quinine, mefloquine, primaquine and pyrimethamine to observe the interaction. The concentration ratios were determined based on the IC_{50} obtained and prepared as described in Section 2.5 and the *in vitro* drug sensitivity assay conducted as described in Section 2.7. The IC_{50} values were further analysed as described in Section 2.7.7.

2.8 Red blood cell lysis assay

In the antimalarial drug sensitivity assay (Section 2.7), the test compounds may have lysed the RBCs before directly affecting the malaria parasite, thereby giving a false positive result as indicated by the low CPM and percentage parasite growth values (Section 2.7.7). Thus to ensure this was not the case, the compounds were incubated along with healthy uninfected RBCs to ensure no haemolysis occurred. The release of haemoglobin into the experimental medium was used as an indicator of membrane instability and RBC lysis, with the haemoglobin being spectrophotometrically detected at 540 nm. The protocol used in the Pharmacology Division was adapted from using micro-centrifuge tubes to a high-throughput assay using a 96-well plate. Parallel assays were initially run to validate the new protocol (data not shown).

2.8.1 Preparation of the red blood cell suspension

Freshly drawn RBCs were washed three times in PBS (pH 7.2) (Section 2.6.5). A 1% (v/v) haematocrit suspension in complete experimental medium (Section 2.6.3) was prepared. The experimental conditions and volumes used were as in the [^{3}H]-hypoxanthine incorporation assay (Section 2.7.5).

2.8.2 Haemolytic assay

Test compounds (25 µl) diluted in incomplete experimental medium (Section 2.6.2) or a maximum of 1% DMSO were plated in triplicate (A1-G12); whilst 25 µl incomplete experimental medium was added to the drug-free controls (H1-H6). The positive control (H7-H17) to indicate 100% haemolysis was achieved with 0.2% (v/v) Triton® X-100 (25 µl; Sigma-Aldrich®) prepared in incomplete hypoxanthine-free medium (Figure 2.10).

Following the addition of 225 µl of the 1% (v/v) RBC suspension to all the wells and the plate was incubated in a humidified environment at 37^{o}C for 48 hours. After which, the plate was gently shaken with an orbital shaker (MRC Thermo-Shaker MB100-4P) at 1040 rpm for 2 minutes, before being centrifuged at 400*g* for 10 minutes. The supernatant (50 µl) of each well was plated into a new non-sterile microtiter plate and diluted with 150 µl Milli-

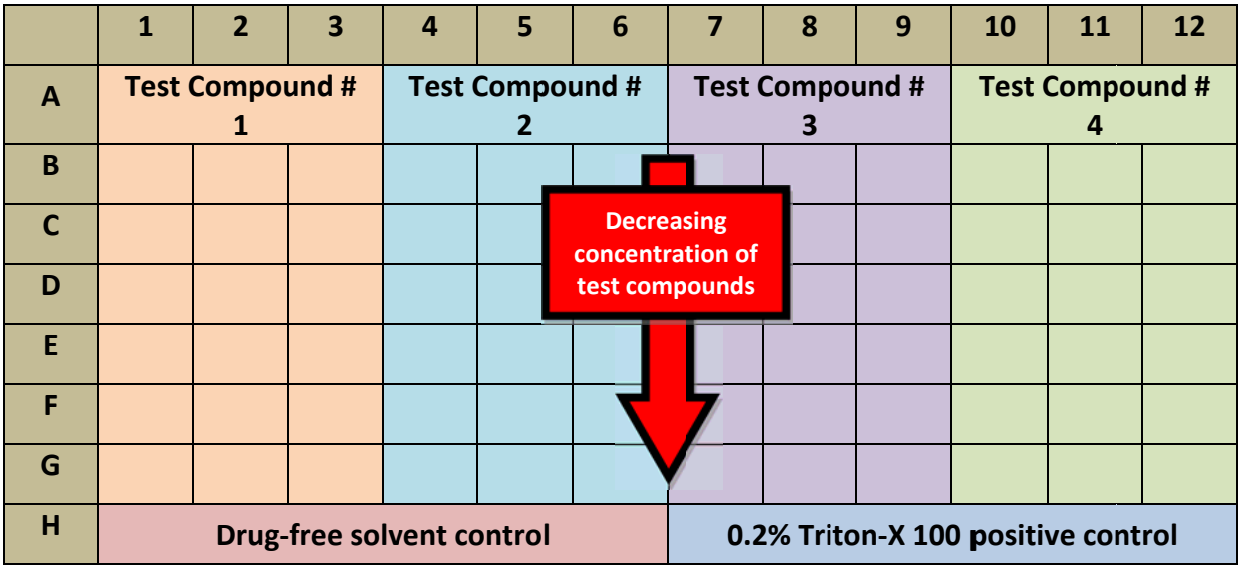


Figure 2.10: Representative layout for the RBC lysis assay.

Q® water, before the absorbance was measured at a wavelength of 540 nm (Labsystems iEMS Reader MF). With a dilution factor of 4 taken into account, the results were expressed as percentage haemolysis using Equation 2.7.

$$\%Haemolysis = \frac{Abs\ (drug) - Abs\ (mean\ drug\ free\ control)}{Abs\ (mean\ positive\ control) - Abs\ (mean\ drug\ free\ control)} \times 100$$

Equation 2.7: The percentage haemolysis of the RBCs.

A colour control was included to compensate for those coloured test compounds which could interfere with spectrophotometric determination in the assay. The colour control of the test compounds consisted of adding 25 µl of the compounds to the wells in columns 1A-1G, 5A-5G and 9A-9G (Figure 2.11). Instead of adding 225 µl of the RBC suspension, 225 µl of complete experimental medium was added. The percentage haemolysis taking the colour control into account was calculated using Equation 2.8.

$$\%\ Haemolysis = \frac{Abs\ (drug) - Abs\ (drug\ colour\ control)}{Abs\ (mean\ positive\ control) - Abs\ (mean\ drug\ free\ control)} \times 100$$

Equation 2.8: The equation used to calculate the percentage haemolysis of the RBCs when tested using compounds that possessed colour.

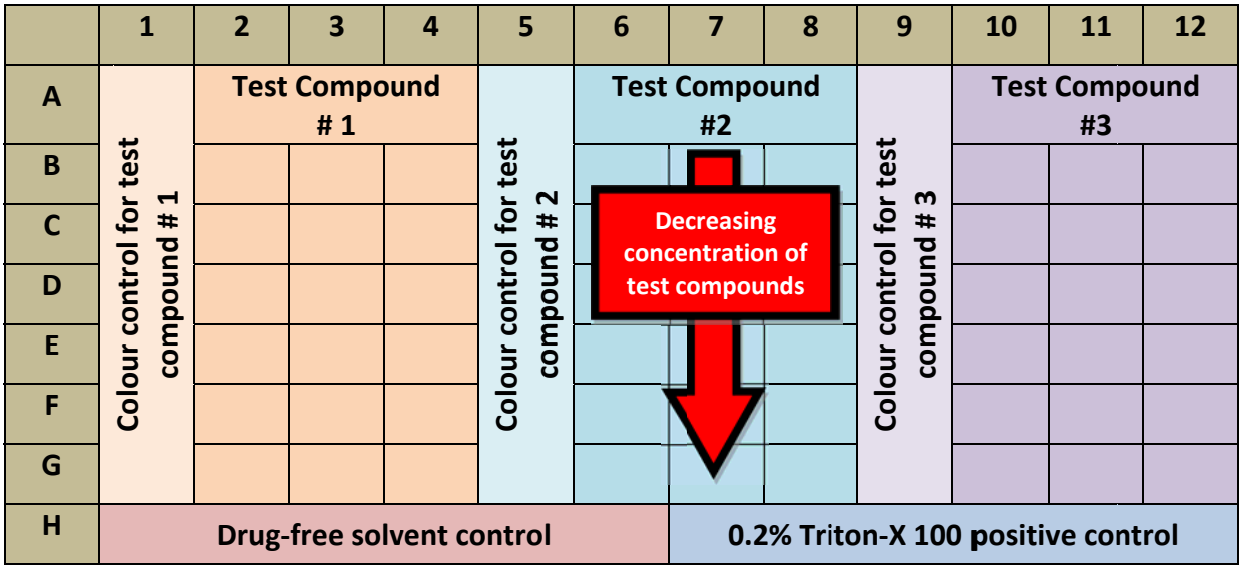


Figure 2.11: The 96-well microtiter plate format used for a haemolytic assay with colour control wells.

2.8.3 Data analysis

For those compounds which did not induce significant haemolysis, the mean percentage haemolysis ± s.d. at the highest tested concentration was reported. Whilst, for those compounds that induced haemolysis, the concentration at which 50% of the RBCs lysed (IC_{50} value) was calculated from the log sigmoid dose response curve using the computer software Enzfitter® (Biosoft, UK) and GraphPad Prism® (GraphPad Software, Inc., U.S.A). The mean IC_{50} value ± s.d. was determined from three or more experiments.

The *in vitro* antimalarial activity of the test compounds was classified as follows highly active, IC_{50} value ≤1 µM; promising activity, IC_{50} value 1-10 µM; moderate activity, IC_{50} values 11-50 µM; low activity, IC_{50} values 51-100 µM; inactive, IC_{50} values > 100 µM (Clarkson *et al.*, 2004; Gathirwa *et al.*, 2008).

2.9 Cellular viability assay

To determine if the compounds were cytotoxic to mammalian cells, the cellular viability or cytotoxic assay with 3-(4,5-dimethylthiazol-2-yl)-2,5-diphenyltetrazolium bromide (MTT) as the substrate, was used. As described by Mossman (1983), the basis of the assay involved the cleavage of the MTT by succinate dehydrogenase found in the mitochondria of living cells. When the tetrazolium ring was cleaved, the yellow water soluble dye changed to a

violet water-insoluble formazan crystal. The assay is favoured as no radioisotope is required, there were no washing steps and the amount of formazan formed is directly proportional to the cell density. Importantly this cellular viability assay was both reproducible and sensitive (Mossman, 1983). A clearance certificate (reference number: W-CJ-150330-1) was obtained from the Human Research Ethics Committee (Medical) of the University of the Witwatersrand (Appendix D), permitting the use of commercial human kidney epithelial (Graham, HEK293) cell line for *in vitro* experimental purposes.

2.9.1 Culture maintenance

Transformed human kidney epithelial (Graham) cells, designated 293 (HEK-293), were continuously maintained in culture at 37^{o}C in a humidified 5% CO_2 (Afrox) incubator (Forma Scientific Water-Jacketed Incubator) according to departmental protocol. The cells were maintained in complete Dulbecco's Modified Eagle's Medium (DMEM) culture medium (Section 2.9.2) which was replaced at least twice a week. The cells were trypsinised at least once a week to subculture the confluent cells or to use the cells experimentally. The cell growth or degree of cell confluency was determined microscopically at 40x magnification. When the cells were 90% confluent, the spent medium was aspirated and the cells washed with PBS (pH 7.2) (Section 2.6.5) before 5 ml of 0.25% trypsin-0.1% Versene-ethylenediaminetetraacetic acid (Versene-EDTA; Sigma-Aldrich®) was added to cover the cells. After 5-10 minutes at 37^{o}C, the cells detached from the surface of the flask. The flask was gently agitated to ensure all the cells detached and 5 ml of complete culture medium (Section 2.9.3) was added such that the foetal calf serum (FCS) could inactivate the trypsin. A single cell suspension was prepared and 10% of the suspension seeded back into the flask along with 25 ml of complete culture medium before being incubated at 37^{o}C in 5% CO_2 for the cells to re-adhere and propagate. The remainder of the cell suspension was either discarded, cryopreserved (Section 2.9.5) or used in an experiment (Section 2.9.6).

2.9.2 Preparation of incomplete culture medium

The incomplete culture medium consisted of 13.5 g/l of high glucose DMEM (Sigma-Aldrich®) supplemented with 3.7 g/l $NaHCO_3$ (Merck) prepared in Milli-Q® water and sterilised through a 0.22 µm Sterivex™-GS filter (Millipore) and stored at 4^{o}C until required.

2.9.3 Preparation of complete culture and experimental medium

The complete culture medium consisted of 10% (v/v) FCS (Sigma-Aldrich®), 1 ml of 200 mM L-glutamine (Sigma-Aldrich®), 1 ml penicillin-streptomycin solution (10,000 units penicillin and 10 mg streptomycin per ml) (Sigma-Aldrich®) and 1 ml 10 mM sodium pyruvate (Sigma-Aldrich®) in 100 ml of DMEM culture medium. The complete experimental medium consisted of 10% (v/v) FCS in 100 ml of DMEM culture medium (Section 2.9.2) supplemented with L-glutamine and sodium pyruvate only (ensuring no antibiotics were added).

2.9.4 Preparation of foetal calf serum

The FCS (Sigma-Aldrich®) was thawed at 4^{o}C and brought up to room temperature before being heat-inactivated at 56^{o}C for 45 minutes, then aliquoted out and stored at -20^{o}C until required.

2.9.5 Cryopreservation and initiation of cultures

As described in Section 2.5.2, the excess cell suspension was cryopreserved. This was done by centrifuging the excess cell suspension at 200*g* for 5 minutes before adding three volumes of cryopreservation solution to one volume of cell pellet. The cryopreservation solution consisted of 60% (v/v) FCS, 30% (v/v) DMEM and 10% (v/v) DMSO, which was stored at -20^{o}C. The cell-cryopreservation suspension was aliquoted into sterile cryotubes and stored at -70^{o}C for short-term storage (2-3 months) and in liquid nitrogen for long term storage. When cultures were re-initiated the cryopreserved cell suspension was thawed out at 37^{o}C, added to 25 ml complete culture medium (Section 2.9.3) supplemented with 20% (v/v) FCS to stimulate cell growth. Once the cells had adhered and were optimally propagating, the percentage FCS in the complete culture medium was decreased to 10%.

2.9.6 MTT cellular viability assay

The toxicity profile of the test compounds was investigated using the MTT cell viability assay using transformed human kidney epithelial (Graham) cells according to the modified methodology of Mossman (1983). Briefly, the trypsinised cell suspension (Section 2.9.1) was centrifuged at 200*g* for 5 minutes. To determine the cell number per ml in the suspension, the cells were stained in a 1:1 ratio with sterile 0.2% (w/v) trypan blue (Sigma-Aldrich®) in

PBS (pH 7.2) and the number of viable clear/transparent cells were counted using a haematocytometer at 100x magnification. The suspension was adjusted to 0.25 million cells per ml with complete experimental medium (Section 2.9.3). To determine the percentage cell viability for the assay, total cell numbers were counted. Viable cells were not stained blue as they possessed good membrane integrity to prevent the uptake of trypan blue; while unhealthy or dead cells stained blue, as the stain traversed the cell membrane of the compromised membrane. Cell viability of 95% (minimum) was required for the assay.

The compounds were diluted in incomplete experimental DMEM medium and 20 µl of each were plated in quadruplet (A1-G12) along with 180 µl of the adjusted cell suspension. Columns 1, 5 and 9 (from rows A-G) only contained complete 180 µl of experimental medium and 20 µl compound such as to serve as the colour control for the test compounds (Figure 2.12). To the drug-free controls (H2-H12), 20 µl of incomplete experimental DMEM medium was added along with 180 µl of the adjusted cell suspension. Whilst 200 µl complete experimental medium was used as the cell-free and colour control (H1). Camptothecin and quinine (Sigma-Aldrich®) were used as the positive controls.

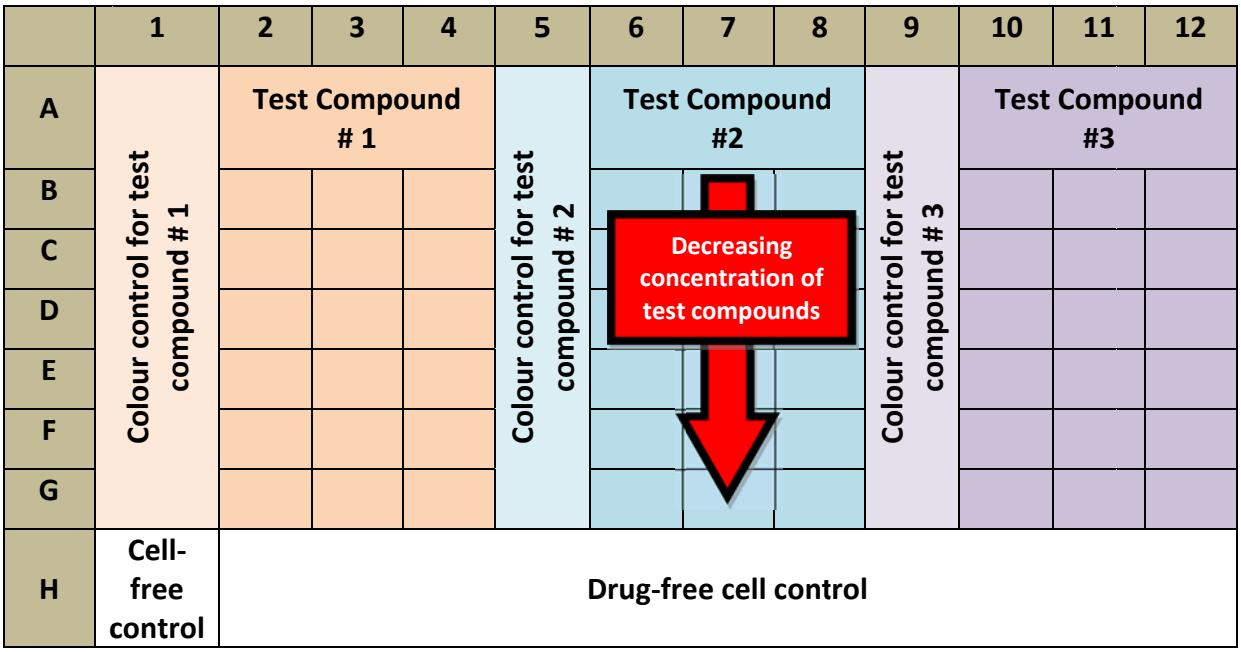


Figure 2.12: Layout for the MTT cell viability assay taking the colour of the test compounds into account.

The plate was incubated for 44 hours at 37^{o}C under humidified conditions in 5% CO_2 before the addition of 20 µl MTT to all the wells. The MTT (USB) 5 mg/ml PBS (pH 7.2) was sterilised through a 0.2 µm syringe filter and stored in the dark at 4^{o}C. The plate was further incubated for 4 hours at 37^{o}C in 5% CO_2 under humidified conditions. Following which, the plate was centrifuged at 200*g* for 10 minutes and 200 µl of the supernatant from each well was discarded and replaced with 150 µl of DMSO to stop the reaction and dissolve the water insoluble formazan crystals. The plate was shaken with an orbital shaker (MRC Thermo-Shaker MB100-4P) at 1040 rpm for 5 minutes to ensure the complete dissolution of the crystals the absorbances were determined in a UV-Vis spectrophotometer (Labsystems iEMS Reader MF) Ascent™ software version 2.6. The absorbances were read at the test wavelength of 540 nm (purple formazan colour) and a reference wavelength of 690 nm (unreacted MTT colour). The percentage cellular viability was calculated using Equation 2.9 after the cell-free colour control absorbance value (H1) or colour control was subtracted from the test and reference wavelength absorbance values, respectively.

$$\%\ Cellular\ viability = \frac{Abs\ drug\ (540nm) - \ Abs\ drug\ (690nm)}{mean\ Abs\ drug\ free\ control\ (540nm) - \ mean\ Abs\ \ drug\ free\ control\ (690nm)} \times 100$$

Equation 2.9: The equation used to calculate the percentage cell viability taking both the test and the reference wavelengths into account.

The IC_{50} values were calculated from log sigmoid dose response curved generated by the computer software Enzfitter® (Biosoft, UK) and GraphPad Prism® (GraphPad Software, Inc., U.S.A). The results are reported as mean ± s.d. of three or more experiments. For those compounds which did not cause significant cell death, the mean percentage cell viability ± s.d. was calculated for the highest concentration tested.

2.9.7 Safety index

The selective activity of the compounds against the *P. falciparum* parasites compared to their cytotoxicity was determined by calculating the safety index (SI; Equation 2.10). All compounds with S.I. values of > 10 were regarded as non-toxic (Pink *et al.*, 2005; Bhat *et al*., 2008).

$$Safety\ index\ (SI) = \frac{Cytotoxicity\ (IC_{50})}{Antimalarial\ activity\ (IC_{50})}$$

Equation 2.10 Selectivity index for *P. falciparum* compared to human cancer cell lines.

2.10 Anti-oxidant assays

2.10.1 Free radical scavenging assay

The 2,2-diphenyl-1-picrylhydrazyl (DPPH) free radical scavenging assay is one of the few stable and commercially available organic nitrogen radicals that has a UV-VIS absorption maximum at 515 nm (Hunsaker and Schenk, 1983). Huang *et al.* (2005) observed that when DPPH$^{\bullet}$ reacted with an anti-oxidant, the colour of the solution faded upon reduction of the DPPH radical and the remaining percentage DPPH$^{\bullet}$ was proportional to the concentration of the anti-oxidant. This DPPH$^{\bullet}$ assay measured the ability of anti-oxidants to scavenge the stable free radical of DPPH, such that the violet colour changes to yellow-clear when the anti-oxidant compound donates an electron to the DPPH radical (Figure 2.13). The degree of decolourisation is stoichiometrically correlates to the number of electrons seized by DPPH$^{\bullet}$ (Huang *et al.*, 2005).

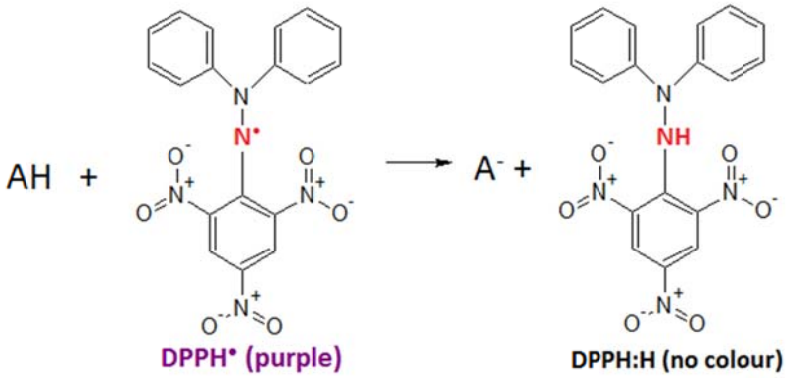


Figure 2.13: The interaction between DPPH free radical and an anti-oxidant (AH/A^{-}).

2.10.2 Free radical scavenging assay procedure

The modified method of Cheng *et al.* (2006) was followed to prepare a 96.2 µM DPPH$^{\bullet}$ (Sigma-Aldrich®) solution in HPLC grade methanol (Rochelle®). The solution was allowed to stand at 4^{o}C in the dark for 24 hours before use. Briefly, 50 µl of test compounds were prepared in DMSO and plated into the wells (A1-G12) of a non-sterile 96-well microtiter plate. DMSO was used in the untreated control wells (H1-H6), while L-ascorbic acid was

used as the positive control. HPLC grade methanol (200 µl) was used instead of $DPPH^{\bullet}$ in the colour control wells when test compounds possessed a colour which could interfere with the quantification of the reaction. $DPPH^{\bullet}$ (200 µl) was added to the test wells, the solutions were gently agitated and incubated at room temperature in the dark for 30 minutes. At which time, the degree of decolourisation was spectrophotometrically determined at 540 nm. The anti-oxidant activity was determined by the percentage of $DPPH^{\bullet}$ decolourisation using Equation 2.11.

$$\% \text{ Free radical scavenging} = \frac{\text{Abs (test compound)} - \text{Abs (colour control)}}{\text{Abs (untreated control)} - \text{Abs (colour control)}} \times 100$$

Equation 2.11: The equation used to calculate the percentage decolourisation of the $DPPH^{\bullet}$ by the test compound.

.

The IC_{50} values were calculated from log sigmoid dose response curved generated by the computer software Enzfitter® (Biosoft, UK) and GraphPad Prism® (GraphPad Software, Inc., U.S.A). Mean percentage free radical scavenging ± s.d. at the highest tested concentration was reported when the compound possessed no anti-oxidant effect. The results are reported as mean ± s.d. of three or more experiments.

2.11 Iron chelation assay

Iron is very important in the metabolic processes of the intra-erythrocytic parasites and if withheld by means of iron chelators would disrupt the metabolism of the parasites; including processes such as DNA synthesis, carbohydrate metabolism, proteolysis of the host haemoglobin, *de novo* synthesis of haem, mitochondrial function and electron transport (Mabeza *et al.,* 1999). Ferrozine (3-[2-pyridyl]-5,6-diphenyl-1,2,4-triazine-4,4'-disulfonic acid sodium salt, Fluka) forms a purple coloured complex with Fe^{2+} (Fe^{2+}-ferrozine) in a quantitative manner with a stoichiometric ratio of 1 Fe^{2+} to 3 ferrozine. Iron chelating agents disrupt the formation of the complex by chelating the ferrous ion before ferrozine, which results in the reduction of the intensity of the purple colour of the complex. To quantify the ability of the test compounds to chelate ferrous iron, the method as described by Dinis *et al*. (1994) was used.

2.11.1 Iron chelation assay procedure

Briefly, 20 µl test compound was plated in triplicate (A1-G12) in the non-sterile 96-well microtiter plates before the addition of 30 µl freshly prepared $FeCl_2$ (Fluka) solution. The 0.48 mM $FeCl_2$ solution was prepared in 5% (w/v) ammonium acetate (Fluka) in Milli-Q® water. To each well, 100 µl ferrozine (1.2 mM, Fluka) solution was added before the plate was allowed to stand in the dark for 30 minutes at room temperature. Thereafter the absorbance was measured at 540 nm. Solvent (DMSO or water; 20 µl) was added to the control wells (H1-H12) as the experimental control. EDTA was used as the positive control, whilst DMSO was added to those wells which served as the control for 100% Fe^{2+}-ferrozine complex formation (H1-H6).

The percentage ferrous ion chelation was calculated using Equation 2.12. The concentration required to chelate 50% of the ferrous ion or inhibit the formation of the ferrous-ferrozine complex was calculated from the log sigmoid dose response curve generated by the computer software Enzfitter® (Biosoft, UK) and GraphPad Prism® (GraphPad Software, Inc., U.S.A). If the test compound possessed no chelating activity, the result was reported as the mean of percentage chelation ± s.d. at the highest concentration tested. At least three separate experiments were performed for each compound tested. The IC_{50} value for each experiment was calculated and the average and s.d. were determined for each of the compound tested.

$$\%\ Ferrous\ ion\ chelation\ = \frac{(Abs\ control\ -\ Abs\ test\ compound)}{(Abs\ control)} \times 100$$

Where: Abs control = mean absorbance for 100% Fe^{2+}-ferrozine complex formation
Abs test compound = absorbance of the test compounds

Equation 2.12: Percentage iron chelation as calculated by the decrease in colour intensity of the ferrous-ferrozine complex.

2.12 Data and statistical analysis

Each compound was tested in triplicate wells per experiment and at least three independent experiments were conducted to determine the final average and standard

deviation (s.d.) for each % activity or IC_{50} value. The Mann-Whitney U-test was performed to determine the statistical differences/similarities between the compounds and the positive controls, where a p value of ≤0.05 was considered significant.

Chapter 3

Porphyrins and Corrins

3.1 Introduction

Due to the high affinity of several of the antimalarial compounds for the haem, the porphyrin structure was identified as a potential target for the development of new drugs. However, the plausibility of using a false substrate to interfere or weaken the haemozoin crystal was investigated in this study. Two such substrates were identified as porphyrins and corrins (Figure 3.1) which are cyclic compounds that contain ligands called macrocycles that bind trace metals in biological systems. The most common examples are the porphyrin and corrin rings with four nitrogen donor atoms.

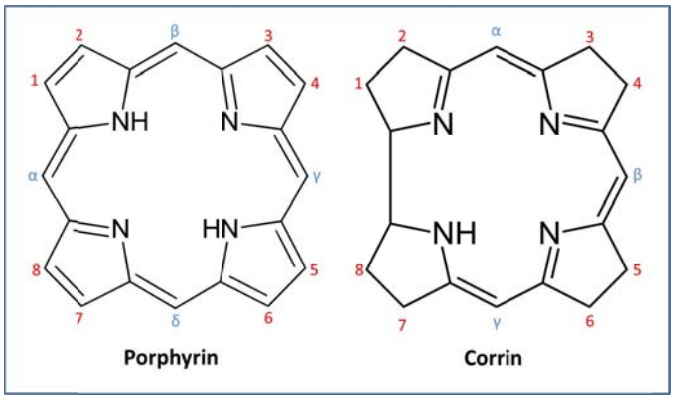


Figure 3.1 The chemical structures of porphyrin and corrin rings. The porphyrin coordinates as a di-anion, whereas the corrin coordinates as a mono-anion. The porphyrin is planar, whereas the corrin tends not to be (Chemaly *et al*., 2007).

3.1.1 Porphyrins

Porphyrins are a large class of natural or synthetic pigments having a substituted aromatic macrocyclic ring consisting of four pyrrole residues linked together by four methine bridging groups. They are deeply coloured (red or purple), fluorescent compounds with an intense and characteristic absorbance band between 390–425 nm (the Soret band or B band) and two to four much weaker bands (Q bands) between 480–700 nm.

The macrocyclic tetrapyrrole structure is ideal for the insertion of metal atoms to form metallo-complexes which are the prosthetic groups in the formation of metalloproteins and metalloenzymes where many essential biochemical processes and bioenergetic reactions of

life take place. They are nature's most important catalysts. Protoporphyrin IX complexes with iron to form the oxygen transport metalloprotein, haemoglobin which uses reversible oxygen coordination to iron (II) for transport of oxygen to organs throughout the body. Myoglobin, found in large amounts in skeletal and cardiac muscles, stores oxygen for use when needed and transports oxygen by diffusion. Other haem containing proteins include the cytochromes, peroxidases, reductases and catalase, which carry out a wide range of important oxidation and reduction reactions vital for all living cells. Sirohaem is the cofactor of sulphite and nitrite reductases. Chlorophylls are magnesium tetrapyrrole complexes which capture and convert absorbed sunlight into usable energy in photosynthesis. Vitamin B12 or cyancobalamin, a cofactor in methyltransferases, is a cobalt tetrapyrrole complex. Factor F430 is involved in methane formation in certain bacteria, and is a nickel tetrapyrrole complex. Uroporphyrinogen III is the common intermediate to all these cellular tetrapyrrole metal complexes. The main physiological significance of porphyrins lies in the pathways of haem and chlorophyll biosynthesis, of which they can be considered as intermediary metabolites or oxidised by-products (Thunell, 2000; Voet and Voet, 2011).

Haemozoin formation in the malarial parasite is a process in which toxic haem subunits, released from the degradation of haemoglobin, is sequestered into inert crystals. It is a potential chemotherapeutic target in which inhibition of the formation of haemozoin can lead to the death of the malaria parasites. It has been previously reported that several metalloporphyrins with cobalt, zinc, iron centres have the ability to interfere with β-haematin formation (Bascilio *et al.*, 1997; Cole *et al.*, 2000) As such inhibition of haemozoin formation remains a sensitive chemotherapeutic target and warrants further investigation using porphyrin-derived compounds.

3.1.2 Corrins

In comparison to the porphyrins, the corrin rings have similar and yet different structures. The corrins have a shorter conjugated system and because of one methylene bridge less, the corrin ring is more buckled than the porphyrin ring. The amide side-chains on the outer periphery of the corrin ring point above and below the plane of the ring whereas some of the side-chains of the porphyrin rings are in the same plane as the ring. Co(III)-corrin rings have six coordinate geometry and in aqueous solution are monomeric, while Fe(III)-porphyrins, as in haematin and β-haematin, have five coordinate geometry and in aqueous solution, the Fe(III)-porphyrins are dimeric (Chemaly *et al.*, 2007). Although never tested

before, the possibility of corrins interfering with haemozoin formation warranted their investigation.

3.1.2.1 Vitamin B_{12}

Neither animals nor plants, except for a few species of bacteria, can synthesize vitamin B_{12}. Humans obtain almost all their vitamin B_{12} directly from their diet, particularly from meat (Figure 3.2).

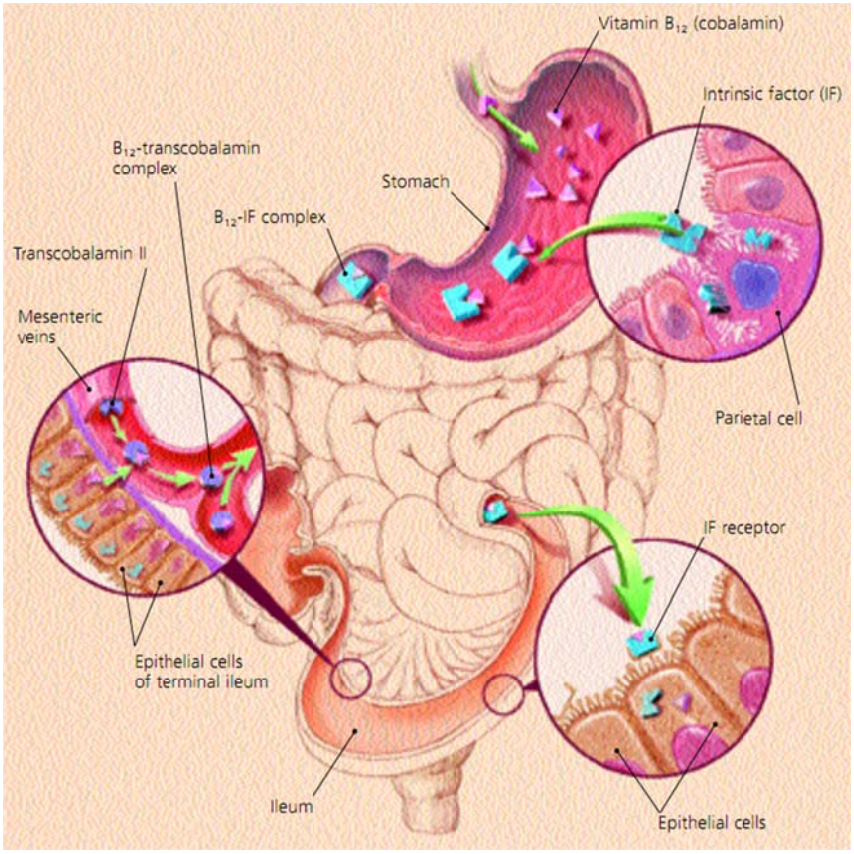


Figure 3.2 The uptake of cobalamin is initiated by the extraction of vitamin B_{12} from the food source in the acidic environment in the stomach. The intrinsic, factor released by the parietal cells in the stomach, binds to the vitamin B_{12} in the duodenum. The uptake occurs in the ileum where the intrinsic-factor bound vitamin B_{12} complex aids in the absorption by binding to a specific receptor in the intestinal mucosa. A second pathway involving in the direct bonding and transport of vitamin B_{12} by transcobalamin II also existed where large doses of oral vitamin B_{12} is absorbed this way. Vitamin B_{12} is bound by transcobalamins to facilitate its uptake by the tissues where about 3 µg is required per day and the liver stores a 3- to 5-year supply (Oh and Brown, 2003; Voet and Voet, 2011).

Vitamin B_{12} or otherwise known as cyanocobalamin occurs naturally in humans in minute amounts and is usually converted to adenosylcobalamin (Coenzyme B_{12}) in the mitochondria in reticulocytes and maturing nucleated erythrocytes, methylcobalamin in the cytoplasm and aquocobalamin (Voet and Voet, 2011).Humans have two enzymes that use vitamin B_{12} derivatives as co-factors, namely methylmalonyl-CoA mutase and methionine synthase (Banerjee and Ragsdale, 2003; Voet and Voet, 2011). Methionine synthase is the only cobalamin-depended enzyme that has been identified in *P. falciparum* (Krungkrai *et al.,* 1989), where it is vital in the synthesis of the DNA precursor N^5,N^{10}-methylene-tetrahydrofolate. Structurally, cyanocobalamin is a tetrapyrrolic cofactor in which the central cobalt (III) atom is coordinated by four equatorial coplanar nitrogen ligands donated by the four pyrroles of the corrin ring. Two co-ordination sites of upper and lower axial positions that lie above and below the plane of the ring exist. In methylcobalamin, a methyl group is bonded to the cobalt in the upper axial position, and the lower axial position is occupied by nitrogen of the dimethylbenzimidazole nucleotide substituent of the corrin ring. In adenosyl-, aquo- and cyanocobalamin, the upper axial position is occupied by an adenosyl, water and cyanide group, respectively. In cobinamides, a cyanide group is occupied at both the upper and lower axial position (Banerjee and Matthews, 1990; Banerjee and Ragsdale, 2003).

Small quantities of vitamin B_{12} are required for optimal malaria growth (Caicedo *et al.,* 2010), but it is unknown as to the effect of the vitamin B_{12} derivatives or higher concentrations on parasite growth and on haemozoin formation. As such these vitamin B_{12} derivatives, along with the synthetic porphyrin derivatives, warrant further investigation.

3.2 Objectives

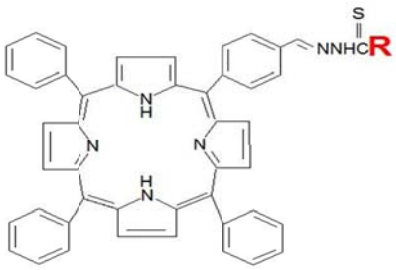
- Assess the antimalarial properties of the novel porphyrin thiosemicarbazide compounds, as well as corrin and its derivatives.
- Determine the ability of the novel porphyrin thiosemicarbazide and corrin derivatives to inhibit the formation of β-haematin.
- Assess the cytotoxic effects of the novel porphyrin thiosemicarbazide and corrin derivatives.
- Evaluate the combined effects of the corrin derivatives with standard antimalarial agents on parasite growth and β-haematin formation.

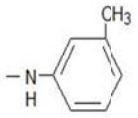
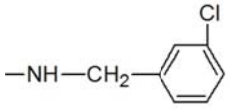
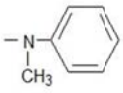
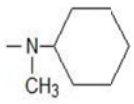
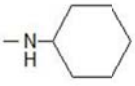
3.3 Methodology

3.3.1 Porphryin thiosemicarbazides

A series of 5-(4-phenyl-N^4-substituted thiosemicarbazone)-10, 15, 20-(trisphenyl) porphyrins (Table 3.1) were synthesized (Bhat *et al.*, 2008) to test for the antimalarial activities *in vitro* as well as its ability to inhibit β-haematin formation. The porphyrin thiosemicarbazides were designed, synthesised and characterised by Prof A. Azam (Department of Chemistry, Jamia Millia Islamia, Jamia Nagar, New Delhi, India)

Table 3.1 The structure and side groups of the synthesized porphyrin thiosemicarbazide molecules - 5-(4-phenyl-N^4-substituted thiosemicarbazone)-10, 15, 20-(trisphenyl) porphyrins (Bhat *et al.*, 2008).



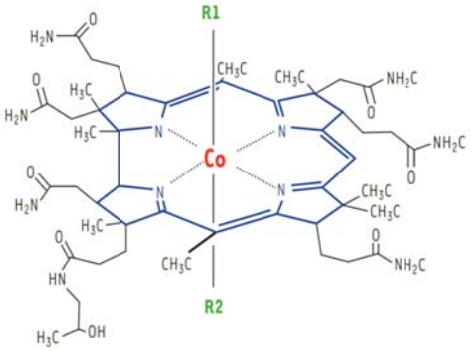
Compound Designation	R-group	Chemical Name
P1		4-(3-Methylphenyl)-1-{[4-(10,15,20-triphenylporphyrin-5-yl)phenyl]methylidene} thiosemicarbazide
P2		4-(4-Chlorohenyl)-1-{[4-(10,15,20-triphenylporphyrin-5-yl)phenyl]methylidene} thiosemicarbazide
P3		4-Methyl-4-phenyl-1-{[4-(10,15,20-triphenylporphyrin-5-yl)phenyl]methylidene} thiosemicarbazide
P4		N'-{[4-(10,15,20-Triphenylporphyrin-5-yl)phenyl] methylidene}pyrrolidine-1-carbothiohydrazide
P5		4-Cyclohexyl-4-methyl-1-{[4-(10,15,20-triphenylporphyrin-5-yl)phenyl]methylidene} thiosemicarbazide
P6		4-Cyclohexyl-1-{[4-(10,15,20-triphenylporphyrin-5-yl)phenyl]methylidene}thiosemicarbazide

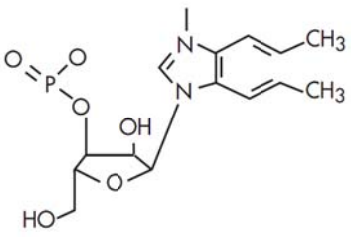
Porphyrin thiosemicarbazide compounds were dissolved in DMSO before being evaluated for *in vitro* antimalarial activity using the ^{3}H-hypoxanthine incorporation assay (Section 2.7) where the test compounds were diluted with the incomplete culture medium (Section 2.6.2) and the final DMSO concentration did not exceed 1%. To test for the effects of the porphyrin thiosemicarbazide compounds on the formation of β-haematin, the BHIA method (Section 2.4.3) was used. The compounds were diluted in DMSO such that the total DMSO concentration for the test did not exceed 25%. For the cytotoxicity study (Section 2.9.6), the porphyrin thiosemicarbazides were diluted with incomplete culture medium (Section 2.9.2) where the final DMSO concentration did not exceed 1%. Due to the limited supply of the porphyrin thiosemicarbazide compounds, no other tests were conducted.

3.3.2 Corrins

Five corrin derivatives, namely adenosylcobalamin (coenzyme B_{12}), aquocobalamin, cyanocobalamin, methylcobalamin and dicyanocobinamide (Table 3.2), were purchased from Sigma-Aldrich® for the assessment of their *in vitro* antimalarial activity and ability to inhibit β-haematin formation.

Table 3.2 The structure of the corrin derivatives with the blue corrin ring structure.



Corrin Derivatives	R1 Group	R2 Group
Adenosylcobalamin	-5' Deoxyadenosyl	
Aquocobalamin	-H_2O	
Cyanocobalamin (Vitamin B_{12})	-CN	
Methylcobalamin	-CH_3	
Dicyanocobinamide	-CN	-CN

Stock solutions of the corrin derivatives were prepared to a concentration of 10 mM in DMSO and stored in -20^{o}C. In the ^{3}H-hypoxanthine incorporation assay, the corrins were diluted in incomplete culture medium and quinine was used as the positive control (Section 2.6.3). In the β-haematin formation inhibition assay, the corrins were diluted in Milli-Q® water, as was the positive control, chloroquine. For the cytotoxicity study (Section 2.9.6), the corrins were diluted with incomplete culture medium (Section 2.9.2) where the final DMSO concentration did not exceed 1%. In the combination studies, in order to potentiate the *in vitro* antimalarial activity and inhibition of β-haematin formation, the active corrins were combined with standard antimalarials such as chloroquine, quinine, primaquine, mefloquine and pyrimethamine.

3.4 Results

3.4.1 Porphyrin thiosemicarbazides

Against the *in vitro P. falciparum* chloroquine-resistant FCR-3 strain, porphyrin **P2** possessed the best inhibitory activity with an IC_{50} = 4.35 ± 0.08 µM, while porphyrins **P4** and **P1** possessed similar inhibitory activities (IC_{50} = 5.35 to 5.66 µM) (Figure 3.3). However, these were not comparable to the potency of quinine, being ~44 fold less active. Only porphyrin **P1** possessed comparable activity (p = 0.5614) to chloroquine when inhibiting β-haematin formation; i.e. 94.4% as effective (Figure 3.3). While the most active porphyrin thiosemicarbazide against the whole parasite, namely **P2** was only 8.1% as effective as chloroquine in inhibiting β-haematin formation. The remaining porphyrin thiosemicarbazide compounds possessed no activity against β-haematin formation (% β-haematin formation range = 93.64 to 100.3%). The porphyrin thiosemicarbazides possessed minimal cytotoxic effects against the kidney epithelial cells when screened at 100 µM (% cell growth range: 70.59-81.21 %); while chloroquine and quinine possessed an IC_{50} value of 245.34 ± 11.77 µM and 335.19 ± 15.03 µM, respectively. The latter indicated a selective inhibitory effect against the intra-erythrocytic *P. falciparum* parasite.

3.4.2 Corrins

None of the corrin derivatives possessed any significant antimalarial activity that was comparable with quinine ($p < 0.001$). Adenosylcobalamin had the most promising antimalarial activity (IC_{50} = 2.65 µM; $p > 0.05$) followed by aquocobalamin ($p < 0.05$) with an IC_{50} value of 8.25 µM (Figure 3.4).

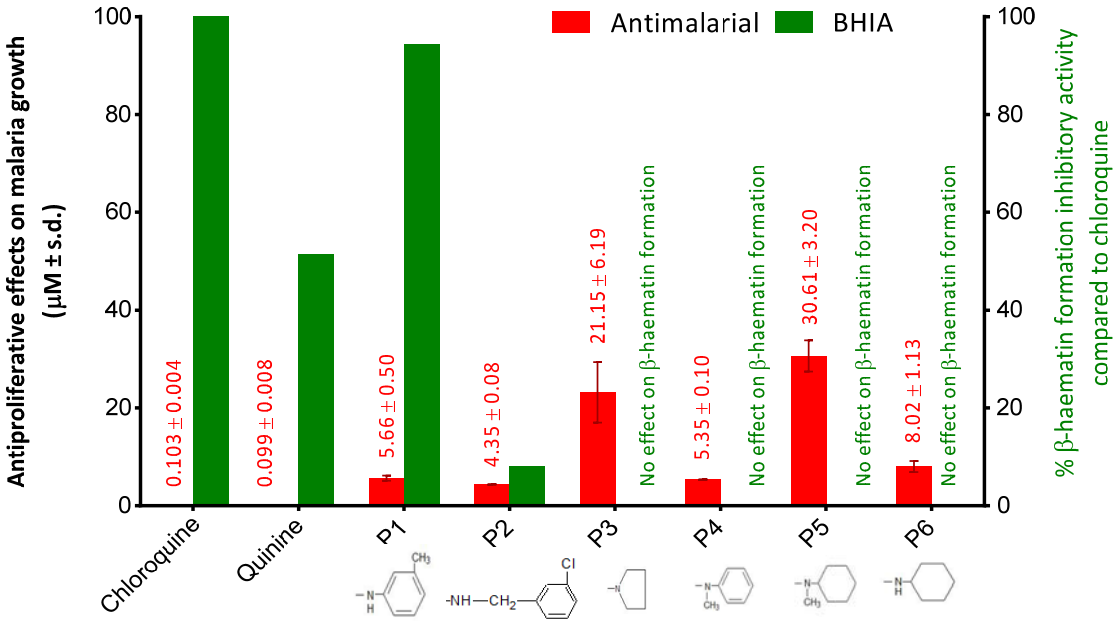


Figure 3.3 The effects of the porphyrin thiosemicarbazide compounds against malaria parasite growth and β-haematin formation.

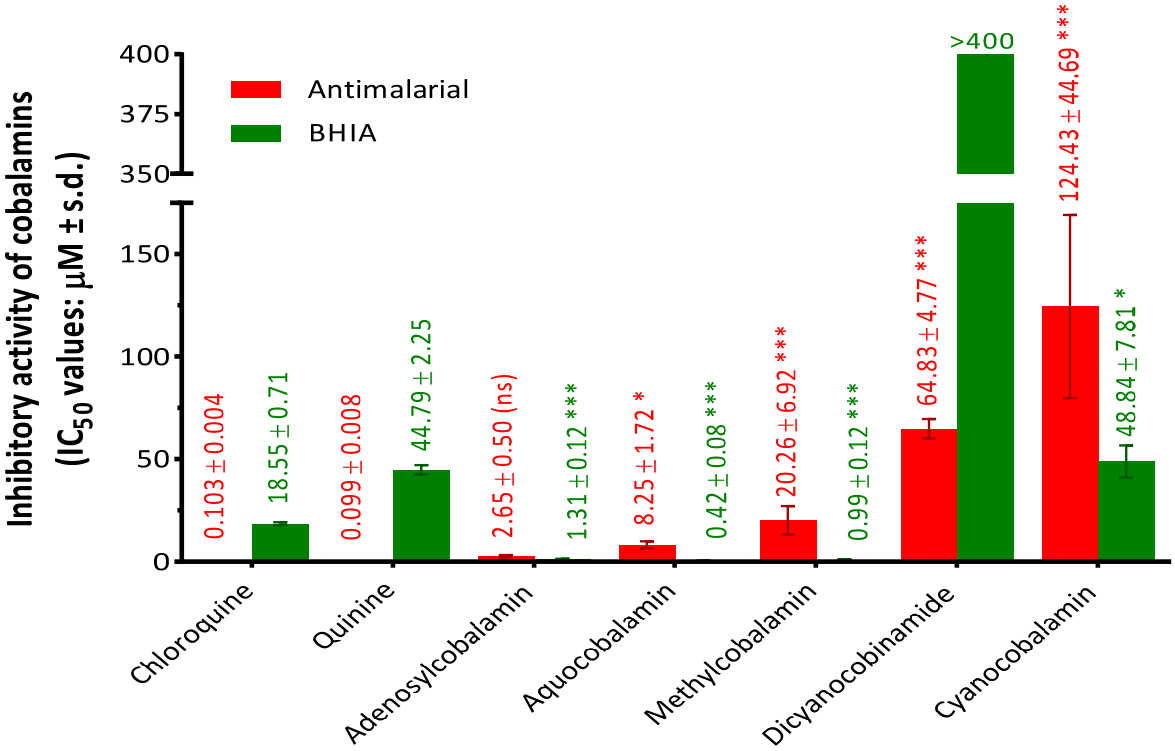


Figure 3.4 Inhibitory activities of corrin derivatives. Quinine was used as the positive control comparison in the antimalarial activity, while chloroquine was used as the positive control in the inhibition of β-haematin formation. *: $p < 0.05$, **: $p < 0.01$, ***: $p < 0.001$. ns = not significantly different from the positive control ($p > 0.05$).

Only dicyanocobinamide was unable to inhibit β-haematin formation, whilst cyanocobalamin possessed a β-haematin formation inhibitory activity that was 38% and 92% similar to that of chloroquine and quinine, respectively. In contrast, methylcobalamin and adenosylcobalamin were respectively, 18 and 14 times more effective than chloroquine. The most active cobalamin to inhibit β-haematin formation was aquocobalamin which was 43 and 106 times more effective than chloroquine and quinine, respectively (Figure 3.4). The corrin derivatives possessed no cytotoxic effect against the kidney epithelial cells at 100 µM [68.76 to 82.18% cell growth], indicating that the cobalamins selectively inhibited *P. falciparum* growth.

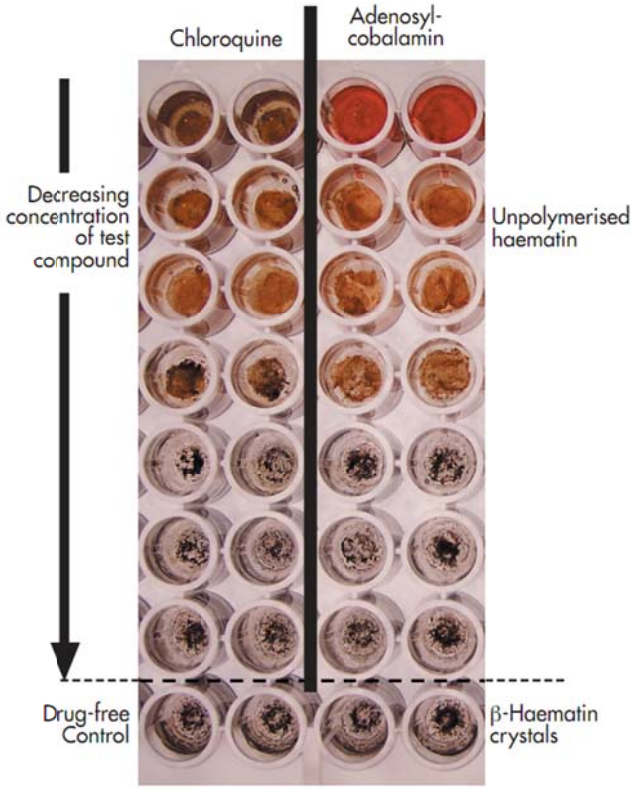


Figure 3.5 β-Haematin formation inhibition assay showing the effects of chloroquine (left) and adenosylcobalamin (right) on the *in vitro* formation of β-haematin.

Since, adenosylcobalamin was the most active corrin derivative against malaria, it was combined with the antimalarial agents to evaluate their combined effect against malaria. Pyrimethamine, chloroquine, quinine and primaquine possessed additive effects when combined with adenosylcobalamin, with ∑FIC values of 0.964, 0.974, 1.004 and 1.085,

respectively (Figure 3.6A). In contrast, an antagonistic effect was observed when adenosylcobalamin was combined with mefloquine (∑FIC = 1.349).

When examining the combined inhibitory effects on β-haematin formation, an additive effect was observed when adenosylcobalamin was combined with quinine and mefloquine (Figure 3.6B). In contrast, chloroquine interacted in a synergistic manner with adenosylcobalamin (∑FIC = 0.522).

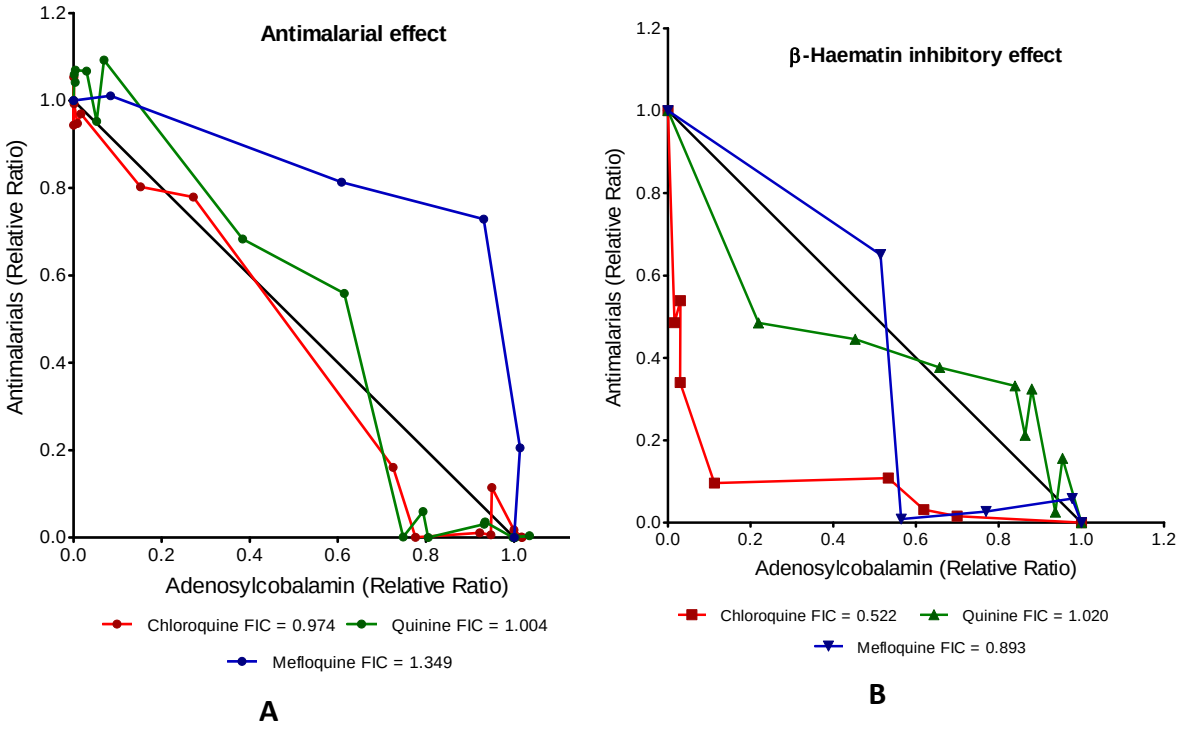


Figure 3.6 Isobolograms depicting the combined effect of adenosylcobalamin with antimalarial agents (**A**) against malaria *in vitro* as well as against the formation of β-haematin (**B**).

3.5 Discussion

Overall, both sets of test compounds had limited ability to inhibit whole parasite growth with variable interactions with β-haematin as compared to chloroquine and quinine. There were a couple of exceptions to this, namely porphyrin **P1** which had promising activity in inhibiting β-haematin formation, but only moderate activity when tested against the whole parasite (Figure 3.3). Even though there was a favourable safety profile for **P1**, for further development of the compound the IC_{50} should ideally be less than 1 µM (Clarkson *et al.*,

2004). Overall, adenosylcobalamin was the most active able to inhibit both β-haematin formation and intra-erythrocytic parasite growth (Figure 3.4). The uptake of these macromolecules is critical for adequate accumulation in the appropriate compartment/s and inhibition of the proposed target and may have been a limiting factor.

3.5.1. Porphyrin thiosemicarbazides

3.5.1.1 Uptake and accumulation of porphyrin thiosemicarbazides

The micromolar IC_{50} range of porphyrin thiosemicarbazides and corrins required to inhibit the *in vitro* malaria parasite may in part be attributed to their large molecular size, thereby limiting uptake and concentration within the various compartments of the parasite. Bearing in mind that the compounds have to transverse four membranes to enter the parasitic food vacuole, which was the proposed target of these compounds (Figure 1.3). The limited amount of compound to enter and inhibit the parasite could have been facilitated by the parasites capacity to incorporate new permeation pathways into the erythrocytic membranes for the uptake or extrusion of molecules (Kirk, 2001; Martin *et al*., 2009). The presence of a parasitophorous duct has been proposed for the uptake of larger molecules (Pouvelle and Gysin, 1997; Goodyer *et al*., 1997), but this has not been accepted by all (Kirk, 2001). The presence of a parasitophorous duct has been proposed to link the extracellular environment with the parasitophorous vacuole which immediately surrounds the parasite, and these compounds could then be endocytosed into the food vacuole of the parasite to interact with the haem units, an important addition to the derivative due to their biological activities. Although the aromatic and cyclic substituents were better inhibitors against *E. histolytica*, they did not exhibit any potent inhibitory activity against *P. falciparum* nor on β-haematin formation (Figure 3.3). Other thiosemicarbazide derivatives have been shown to possess variable antimalarial activity where this activity can be potentiated by associated components in the compound (Table 5.4; Klayman *et al*., 1983). The *in vitro* effect of several synthetic porphyrin compounds have been reported to possess antimalarial activity at micromolar concentrations, as also observed in this study (Figure 3.3). These include the protoporphyrin IX compounds that contained silver, palladium, cobalt and manganese, as well as gallium deuteroporphyrin IX (GaDPIX) and gallium hematoporphyrin IX (GaHPIX) (IC_{50} values range: 15.5 to 77 µM) (Begum *et al*., 2003).

3.5.1.2: Mechanism of action: inhibition of β-haematin formation

Of the porphyrin thiosemicarbazide derivatives investigated in the current study, only one compound with a 3-methylphenyl substitution (**P1**) possessed any β-haematin formation inhibition that was similar in activity to chloroquine (Table 3.1; Figure 3.3). The proposed mechanism of action for this compound could be due to the a methyl group attached to N(4) in the cycloalkyl moiety which could interfere with the ferriprotoporphyrin IX subunits from forming the β-haematin crystalline structure (Bhat *et al.,* 2008). It was proposed that the orientation of this compound and that of the methyl group could possibly facilitate cofacial π–π binding to occur between the porphyrin thiosemicarbazide structure and the ferriprotoporphyrin IX unit. The promising activities of **P1** to inhibit β-haematin formation could also be attributed to the electron-withdrawing group attached to it (Bhat *et al.,* 2008).

Synthetic protoporphyrins IX, which contain metal ions such as Ga(II), Sn(IV), Zn(II), and Mg(II) within the porphyrin structure have been reported to inhibit the formation of β-haematin comparable to that of chloroquine. As with the porphyrin thiosemicarbazides in this study, the protoporphyrins IX were unable to effectively inhibit parasite growth (at least a 1000 times less active) (Begum *et al*., 2003).

It has been demonstrated that non-iron porphyrins inhibit β-haematin formation via cofacial π-π links that form drug-haem complexes via the centre-metal coordination to the porphyrin ligand. It has been found that the potency of the complexes increase when there are hydroxyl groups associated with the metalloporphyrin (Bascilio *et al.,* 1997). It is postulated that compounds able to form both π-π links and bind between hydroxyl groups and haematin ions are best suited to form drug-haem complexes, thereby able to disrupt interactions within the polymer that are critical for the stability of haem polymerisation – resulting in parasite death (Begum *et al*., 2003). The drug-haem complex is proposed to induce lipid peroxidation of the parasite membranes, resulting in parasite death in a similar manner to that of chloroquine (Bascilio *et al.,* 1997; Cole *et al.,* 2000).

Mg(II)PPIX, Zn(II)PPIX and Sn(IV)PPIX have been shown to be six times more active than chloroquine, but unable to completely prevent the formation of the Fe-(O)-propionate linkage. However, these porphyrins were effective in inhibiting haemozoin formation when the π-π adducts to the haem substrate were formed (Cole *et al*., 2000). In contrast, Co(III)PPIX, Cr(III)PPIX and Mn(III)PPIX prevented the formation of the Fe-(O)-propionate linkage, but possessed poorer inhibition of the haemozoin formation (3-4 fold less active

than chloroquine). It could be interpreted that Fe-(O) propionate bonds may not be the dominant oligomerisation interaction within β-haematin (Cole *et al*., 2000).

The precise mechanism of inhibition of the porphyrin thiosemicarbazides that were able to inhibit the intracellular parasite was not fully elucidated and the interaction of these derivatives undoubtedly consists of an interplay between multiple interactions within the β-haematin crystal.

3.5.2 Corrins

Adenosylcobalamin and aquocobalamin were the most active of the five test cobalamins, with these two eliciting promising antimalarial activity and a potent ability to inhibit β-haematin formation; whilst displaying favourable safety effects on the human kidney epithelial cells (Figure 3.4). If an adequate concentration of these cobalamins could accumulate into the parasite and inhibit parasite growth in a similar manner as β-haematin formation, they would be a therapeutic advantage against resistant malaria.

3.5.2.1 Uptake of corrins

In circulation, cobalamins are bound to two plasma binding proteins, namely transcobalamin or haptocorrin. Only 20% of the ingested cobalamin is bound to transcobalamin and taken up for cellular utilisation. In contrast, haptocorrin binds ~80% of the plasma cobalamins, but does not facilitate cellular uptake. Specific membrane receptors recognise the protein portion of the transcobalamin-cobalamin complex (Figure 3.2); whereas free cobalamin or haptocorrin-bound cobalamin is not taken up by the cell (von Castel-Dunwoody *et al*., 2005).

The lack of transcobalamin within the *in vitro* assay to facilitate cobalamin uptake indicates that the addition of high concentrations of cobalamins were either unbound in the plasma or bound to haptocorrin. The latter is found in high concentrations in various body fluids including human plasma (Jensen *et al*., 1977), which was added to the culture media to sustain optimal parasite growth (Section 2.6.2).

Mature erythrocytes also lose the ability to incorporate transcobalamin II-bound cobalamin. The unbound cobalamins and excess cobalamins in supraphysiological concentrations could passively diffuse into the erythrocytes independent of the receptor-mediated endocytosis (Voet and Voet, 2011). Cobalamins are hydrophilic molecules which would be difficult to diffuse through the digestive vacuole membrane and accumulated via

pH trapping which chloroquine and quinine are both proposed to have entered the digestive vacuole. The possible processes of cobalamin accumulation are: (i) pass diffusion of the small hydrophobic molecules across the lipophilic membranes (Kirk, 2001); (ii) pH trapping of the protonated form of the chloroquine and quinine (Egan, 2003); and (iii) the molecules (already present in the red blood cell cytoplasm) are taken up into the digestive vacuole along with haemoglobin uptake by endocytosis (Figure 3.7) (Chemaly *et al.,* 2007). Similarly, porphyrin compounds could be diffused into the erythrocyte cytoplasm since it is not bound to any proteins to facilitate its transport into the parasite via channel specific pathways and or receptor-mediated endocytosis. Like with the cobalamins, porphyrin thiosemicarbazides would be endocytosed from the erythrocyte cytoplasm, along with haemoglobin, into the digestive vacuoles (Figure 3.7).

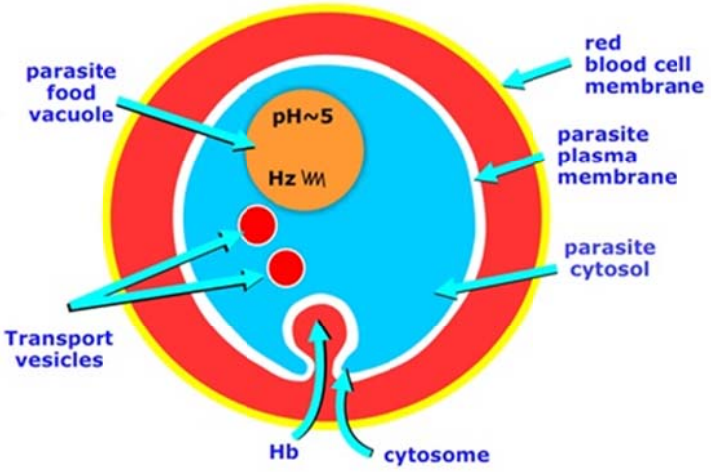


Figure 3.7 The uptake and ingestion of the host haemoglobin by the parasite. It is also a possible route whereby the porphyrins and corrins could be endocytosed along with the host haemoglobin into the parasite. Hb = haemoglobin, Hz = haemozoin (Chemaly *et al.,* 2007).

The observed antimalarial property of cyanocobalamin is most likely that the cyanobalamin is diffused into the erythrocytes and converted to methycobalamin in the erythrocyte cytoplasm where methylcobalamin is endocytosed into the digestive vacuole along with the haemoglobin. The rates of cyanocobalamin uptake and conversion into methylcobalamin and the rates (and frequency) in which methylcobalamin get endocytosed along with haemoglobin would be the rate limiting steps that would determine the efficacy and potency of cyano-/methylcobalamin against the parasite.

3.5.2.2 Accumulation of corrins and antimalarial activity

The *in vitro* inhibitory activity of all the cobalamins on the whole intra-erythrocytic parasite was much lower than that of chloroquine and quinine, with adenosylcobalamin having the greatest antimalarial activity in the micromolar range (Figure 3.4). The lower potency of the cobalamins is most likely due to the concentration that was able to accumulate in the various compartments and the proposed target site, namely the parasitic food vacuole. This contrasts with that of the quinolines which are able to accumulate in the acidic vacuole to a high concentration (Figure 3.8). This has been reported to be due to the weak basic nature of the quinolines that enables them to move along a pH gradient into the acidic digestive vacuole, where they are trapped in the deprotonated form, resulting ultimately in parasite death (Fidock *et al*., 2008; Warhurst, 2000). At the slightly acidic pHs in the digestive vacuole, cyanocobalamin would be entirely in the unprotonated base-on form and is neutral (accumulation ratio 1.0), adenosylcobalamin and methylcobalamin are mainly in the unprotonated base-on form (neutral) and aquocobalamin is entirely in the unprotonated base-on form with a charge of +1 (Table 3.3). For cyanocobalamin, pH trapping is not expected, while pH trapping is expected to occur to only a small extent for adenosylcobalamin and methylcobalamin. However, aquocobalamin (predicted accumulation ratio of 1.3×10^2) is present in the parasite cytoplasm (pH 6.8-7.2) to some extent as hydroxocobalamin (17% neutral hydroxocobalamin and 83% aquocobalamin), so pH trapping is expected to take place with aquocobalamin/hydroxocobalamin (Chemaly *et al.,* 2007).

3.5.2.3 Mechanism of action: inhibition of β-haematin formation

In contrast to the micromolar IC_{50} values required to inhibit the intra-erythrocytic parasite (adenosylcobalamin > aquocobalamin > methylcobalamins > dicyanocobinamide > cyanocobalamin), the effect of the corrins at nanomolar values indicated a potent interaction between the corrins and uncomplexed haem units (aquocobalamin > methylcobalamins > adenosylcobalamin > cyanocobalamin > dicyanocobinamide) (Figure 3.4). Alhtough there is a general trend with adenosyl-, aquo- and methyl-cobalamin being much more active than the cyanocobalamins, there was no correlation between the effect of the corrins on the intra-erythrocytic parasite and β-haematin formation ($r^2 = 0.01966$).

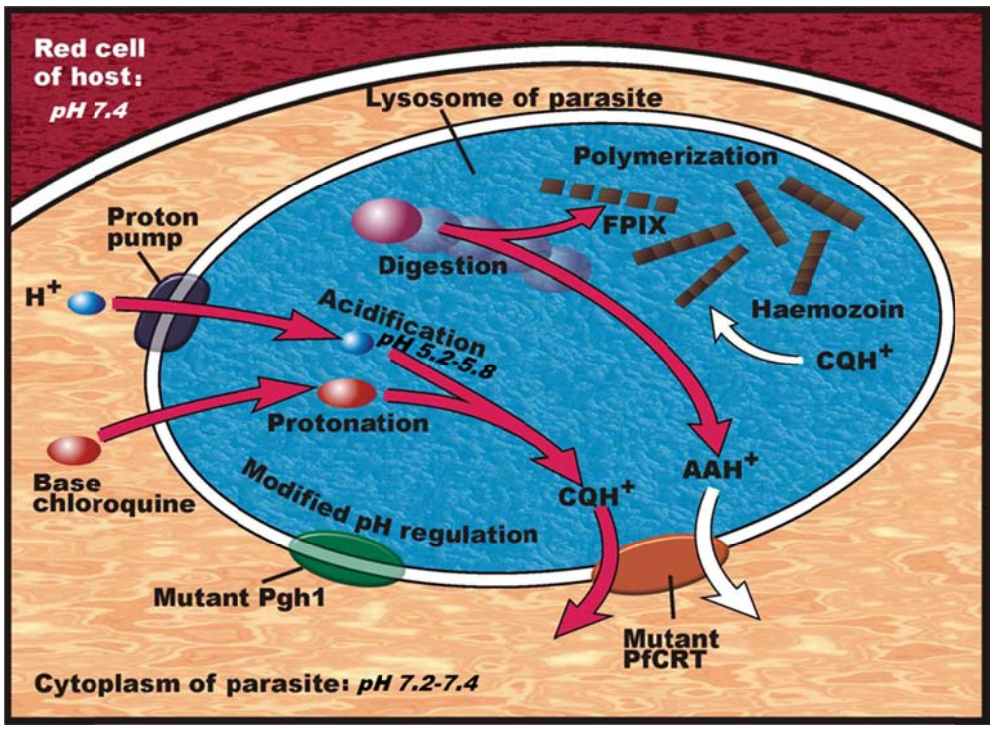


Figure 3.8: The effect of chloroquine (CQ) on haem (FPIX) detoxification in the lysosome of a chloroquine-resistant malaria parasite (Warhurst, 2000). Where PfCRT = *Plasmodium falciparum* chloroquine-resistant transport; Pgh1 = p-glycoprotein homologue 1 and AA = amino acid.

Table 3.3 pK_a values, accumulation ratios and accumulation ratios relative to chloroquine of corrin derivatives (Chemaly *et al.*, 2007).

Compound	pK_{a1}	pK_{a2}	Accumulation ratio ($[Q]_v/[Q]_c$)	Accumulation ratio relative to chloroquine
Adenosylcobalamin	3.67	-	1.0	4.3×10^{-5}
Aquocobalamin	-2.13	8.10	1.3×10^{2}	5.7×10^{-5}
Cyanocobalamin	0.03	-	1.0	4.3×10^{-3}
Dicyanocobinamide	-	-	1.0	4.3×10^{-5}
Methylcobalamin	2.90	-	1.0	4.3×10^{-5}
Chloroquine	8.55	9.81	2.3×10^{4}	1.0
Quinine	5.07	9.70	2.2×10^{2}	9.6×10^{-2}

The corrin ring and the side-chains of methyl-cobalamins and cyanocobalamin have been shown to be very flexible (Brown *et al.*, 1998) and even though the corrin ring is not as flat as the porphyrin ring, cobalamins could conceivably bind with the Fe(III)-protoporphyrin ring of β-haematin/haemozoin by cofacial π-π interactions, similarly to porphyrins (Chemaly *et al.,* 2007). The corrin's effectiveness (adenosyl-, aquo- and methyl-cobalamins) against β-haematin formation could possibly have been due to the cofacial π-π interactions that could take place between the lower face of the methyl- and adenosylcobalamins in their base-off forms (in either protonated or unprotonated forms) and the Fe(III)PPIX ring (Figure 3.9). It is unlikely that the interaction could have been between the upper face of either the methyl- and adenosyl-cobalamin, due to steric hindrance from the upward-pointing ligands (Chemaly *et al.,* 2007). The water ligand on the aquocobalamin could either be substituted by an acetate ligand with the equilibrium constant K = 4.5 (Firth *et al*., 1969). It is possible that the carboxylate group on a Fe(III)PPIX unit could displace the water ligand from aquocobalamin and coordinate to Co(III). Thus, the lower faces of methylcobalamine, adenosylcobalamin and the upper face of aquocobalamin could stack with the Fe(III)-protoporphyrin ring (Chemaly *et al.,* 2007). In contrast, the moderate and inactive properties of the cyanocobalamins to inhibit β-haematin formation could be due to the unavailability of both its upper and lower faces for π-π stacking. It is therefore possible for the lower faces of methyl- and adenosylcobalamins and the upper face of the aquocobalamins to stack with the Fe(III) protoporphyrin rings (Chemaly *et al.,* 2007).

Dicyanocobinamide showed no inhibition of β-haematin formation (Figure 3.4), which implied that the 5,6-dimethylbenzimidazole/α-*D*-ribofuranose/ phosphate side-chain was needed for inhibition of β-haematin formation. It was postulated that the cobalamins could potentially inhibit β-haematin formation using either the corrin ring or by hydrogen-bonding using their 5,6-dimethylbenzimidazole/a-D-ribofuranose/phosphate side-chain or both (Chemaly *et al.,* 2007). The 5,6-dimethylbenzimidazole ring could, in theory, interact with the Fe(III)-protoporphyrin ring through non-covalent cofacial π-π interactions, as in the quinoline antimalarials. Compounds containing the 5,6-dimethylbenzimidazole moiety have been found to have antimalarial activity, but the mechanism of action is unknown (Chemaly *et al.,* 2007). It is difficult to envisage the 5,6-dimethylbenzimidazole ring in the base-on cobalamins, forming cofacial π-π interactions because the nitrogen is coordinated to Co(III) and thus only the base-off forms (Figure 3.9) are expected to act in this way. However, adenosylcobalamin and methylcobalamin at pH 4.6-4.8 have small amounts of the

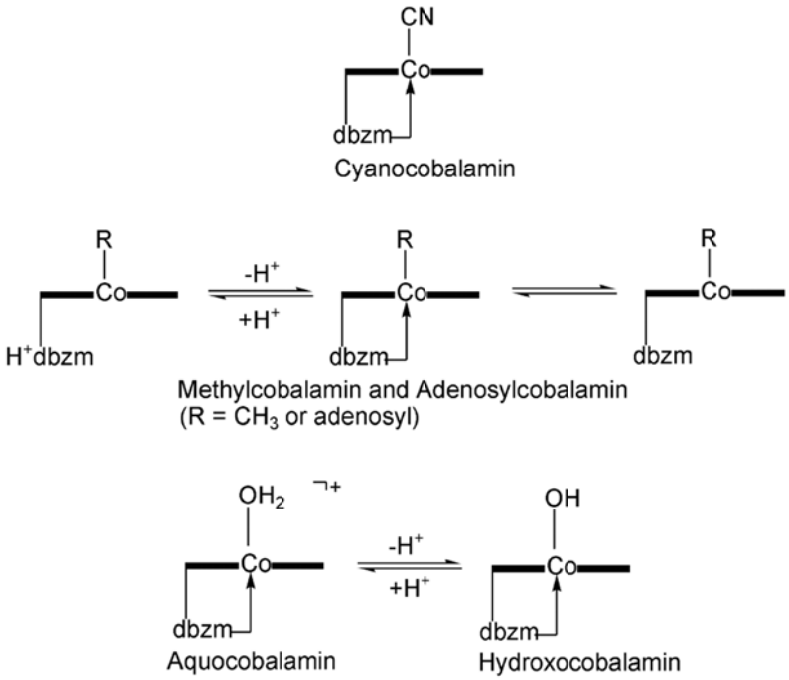


Figure 3.9 Equilibria of base-on, base-off and protonated base-off forms of cobalamins (dbzm = 5,6-diemethylbenzimidazole base) (Chemaly *et al.,*. 2007).

unprotonated base-off form (~10% and ~5%, respectively) and the protonated base-off form (~6% and ~1%, respectively) present in solution.

3.5.2.4 Mechanism of action: methionine synthase co-factor

Methionine synthase is the only cobalamin-dependent enzyme in the intra-erythrocytic *P. falciparum* parasite (Banerjee and Matthews, 1990 and Krungkrai *et al.,* 1989).The enzyme was demonstrated to be dependent on methylcobalamin or adenosylcobalamin, but not cyanocobalamin or aquo-/hydroxocobalamin (Banerjee and Matthews, 1990). Methionine synthase is important in *P. falciparum* metabolism in that it provides a salvage pathway for tetrahydrofolate by catalysing the methylation of homocysteine to methionine and tetrahydrofolate, which is then converted to 5,10-methyltetrahydrofolate, a precursor in nucleic acid synthesis (Krungkrai *et al.,* 1989; Krungkrai *et al.,* 1990). Methionine is also the precursor of *S*-adenosyl-methionine, which is the cofactor involved in a large number of methylation reactions (Figure 3.10). Methionine is an essential amino acid for the optimal growth of *P. falciparum* (Divo *et al.,* 1985). When cultured *in vitro*, an exogenous source of cobalamin must be supplied in the RPMI-1640 culture medium (3.7 nM) (Schuster, 2002), as

there is an insufficient amount in the host RBCs (0.08–0.4 nM) and plasma (0.3 nM) (Divo *et al.,* 1985) to sustain a continuous culture of viable parasites.

The standard antimalarial agent, pyrimethamine is known to inhibit dihydrofolate reductase (Winstanley *et al.*, 1995) and to inhibit whole parasite growth of the chloroquine-resistant FCR-3 strain (IC_{50} value: 0.102 ± 0.007 µM). When pyrimethamine and excess cobalamin were concurrently incubated with the parasite, an additive interaction was observed (ΣFIC values of 0.964). This indicated that the two compounds worked complementary to each other in the folic acid pathway (Figure 3.10).

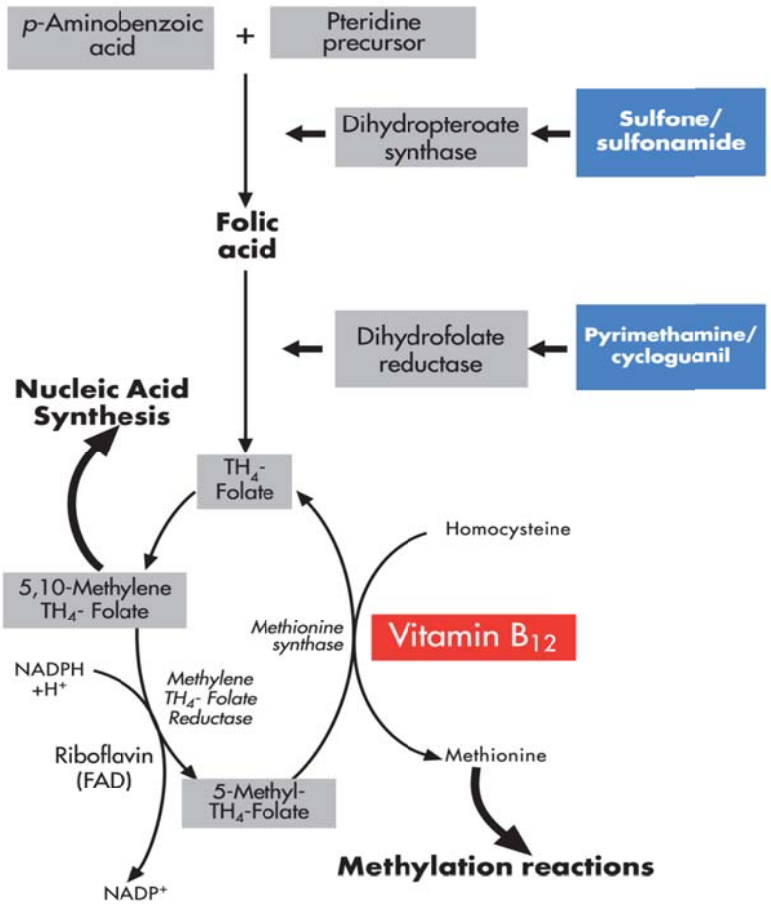


Figure 3.10 The folate scavenging pathway in the malaria parasite. Methionine synthase has been identified where it is the only cobalamin-depended enzyme that is vital in the synthesis of the DNA precursor N^5,N^{10}-methylene-tetrahydrofolate (TH_4) in *P. falciparum* (Winstanley *et al.*, 1995).

3.5.2.5 Combination interactions

The synergistic interaction observed between adenosylcobalamin and chloroquine when inhibiting β-haematin formation, could be due to the inhibition of a common target and complementing each other's activity by binding to different sites of Fe(III)-protoporphyrin-IX (Figure 3.6B). However only an additive effect was observed when this latter combination was incubated with the whole parasite. The difference in activity between the potential target and whole parasite could be due to the lower accumulation of the adenosylcobalamin / chloroquine in the parasite food vacuole (Figure 3.6A). Mefloquine is proposed to inhibit parasite growth in a similar manner to chloroquine, but not as potently (Cowman *et al*., 1994). In contrast to the additive interaction between chloroquine and adenosylcobalamin an antagonistic interaction was observed between mefloquine and adenosylcobalamin when incubated with the whole parasite, as well as with the potential β-haematin drug target. Competition at the target site or at a transporter level may result in this interaction.

3.6 Conclusions

Overall, the effect of the porphyrin thiosemicarbazide derivatives on the intra-erythrocytic parasite did not correlate to the effect on inhibiting β-haematin formation and the variations in structural features did not improve pharmacological activity. Even though there was a favourable safety index, these derivatives do not warrant further investigation. In contrast, although vitamin B_{12} is required for optimal biochemical functions, excess levels of the corrin appeared to accumulate and inhibit β-haematin formation. The accumulation of adenosylcobalamin could be optimised such that the effect on the whole parasite can mimic the very potent inhibitory effect on β-haematin formation. Formulations or structural alterations to enhance uptake into the food vacuole could be investigated for this pharmacokinetic improvement. This could be accomplished by linking them to a β-glucoside to facilitate the transport of the macromolecules via the hexose transporter system into the parasite (Suzuki *et al*., 2007). Or they could be encapsulated into peptide-based nanostructures for optimal deliver to the target site within the malaria parasites (Mishra *et al*., 2008).

Chapter 4

8- and 4-Hydroxyquinolines

4.1 Introduction

Quinoline or 1-aza-napthalene or benzo[*b*]pyridine is a nitrogen containing heterocyclic aromatic compound with the chemical formula C_9H_7N. This weak tertiary base undergoes both electrophilic and nucleophilic substitution reactions.

The quinoline nucleus occurs in several natural compounds (cinchona alkaloids, such as quinine) and pharmacologically active substances displaying a broad range of biological activity; including analgesic, anti-inflammatory, anticancer, antiviral and cardiovascular activity (Table 4.1). It has been reported to be nontoxic to humans following oral absorption and inhalation (Kumar *et al*., 2009).

Table 4.1 Pharmacological activities of quinoline-based derivatives.

Activity	Target
Analgesic	Antagonism at vanilloid receptors[a]; selective agonists at cannabinoid CB_2 receptors[b].
Anti-inflammatory	Inhibitors of lysozyme and β-glucuronidase release[c]; treatment of osteroarthritis as amino-acetamide inhibitors of aggrecannase-2[d].
Anticancer	CSF-1R (Colony stimulating factor 1 receptor) kinase inhibitor[e]; histone acetyltransferase (HAT) inhibitors[f]; insulin like growth factor receptors (IGF-1R)[g,h]; tyrosine kinase inhibitors[i]; c-Met kinase inhibitor[j].
Antiviral	HIV-1 Tat-TAR (Tat protein-trans-activation response element) interaction inhibitor[h].
Cardiovascular	Liver X receptor agonist in conditions of dyslipidaemia with good binding affinity for LXRβ and LXRα[k,l]; HMG-CoA (3-hydroxy-3-methylglutaryl-coenzyme A) reductase inhibitors[m]; angiontenin II receptor antagonists[n,o]; cholesteryl ester transfer protein inhibitor[p]; platelet aggregation inhibitor (P2Y1 receptor antagonists)[q].

[a]Gomtsyan *et al.* (2005); [b]Manera *et al.* (2007); [c]Chen *et al.* (2006); [d]Gilbert *et al.* (2008); [e]Scott *et al.* (2009); [f]Mai *et al.* (2009); [g]Miller *et al.* (2009); [h]Chen *et al.* (2009); [i]Assefa *et al.* (2003); [j]Wang *et al.* (2011); [k]Bernotas *et al* (2009); [l]Hu *et al.* (2007); [m]Cai *et al*. (2007); [n]Lloyd *et al*. (1994); [o]Srimal *et al.* (1990); [p]Rano *et al*. (2009); [q]Ramos *et al*. (2008).

Quinoline-based derivatives possess other pharmacological activities: anti-protozoal activities against *Trypanosoma cruzi* (Ma *et al*., 2009; Franck *et al.,* 2004), *Leishmania* spp. (Fournet *et al.,* 1993; Fakhfakh *et al*., 2003), African trypanosomiasis and Chagas' disease (Fakhfakh *et al.* 2003). As antifungal agents, the non-azole quinoline-based derivatives have

also been evaluated against *Aspergillus niger*, *A. flavus*, *Monascus purpureus* and *Penicillium citrinum* (Kumar *et al*., 2011; Kumar *et al*., 2009). Based on the antimicrobial and antimalarial activity of other hydroxyquinolines such as quinine, these compounds warranted further investigation.

4.2 Hydroxyquinolines

4.2.1 8-Hydroxquinoline derivatives

4.2.1.1 Antimicrobial properties

The 8-hydroxyquinoline molecule also known as 8-quinolinol, 8-oxychinoline and oxine is a planar molecule that contains two hexagonal sided rings with a nitrogen atom in position one and a hydroxyl group on the 8th carbon (Phillips, 1956). The two hexagonal sided rings are lipophilic, whereas the hydroxyl side group is hydrophilic. The 8-hydroxyquinoline molecule has a wide variety of therapeutic applications, where the chemical base and derivatives are used as antibacterial, antiprotozoal agents and as fungicides and insecticides in agriculture (SAMF, 2014; Phillips, 1956).

4.2.1.2 Metal chelating properties

Out of the possible seven quinolinols this structure can generate, only 8-hydroxyquinoline possesses the ability to chelate metal ions (Phillips, 1956). It has been proposed that 8-hydroxyquinolines could be used in the treatment of *Mycobacterium tuberculosis* and malaria with its iron-chelating antimicrobial actions, depriving the microbes essential nutrient (Hongmanee *et al*., 2007; Scheibel and Adler, 1980). Inflammation and neurodegenerative diseases such as Alzheimer's disease where 8-hydroxquinolines, the strong iron chelator, exhibited strong free-radical-scavenging capability with monoamine oxidase B inhibitory activities and neuroprotective activity (Zheng *et al.,* 2005). In addition to the metal chelator being active, Gershon and Parmegiani (1963) and Daniel *et al*. (2005) demonstrated the antifungal/antibacterial and anticancer activities of copper-8-hydroxquinoline chelate complexes.

Iron plays a vital role in human metabolism and is essential for several biologic systems, including haematopoiesis, oxygen delivery, neurological function, immune function, and physical development. Red blood cells are the primary pool of iron in the body. The

continuous turnover of red blood cells via erythropoiesis presents the greatest demand for iron at about 20 mg/day. Under most circumstances, the human body is excellent at conservation, but iron deficiency does occur when there is an imbalance among requirements, losses and intake (Brittenham, 2008).

Malaria parasites require iron for its iron-dependent metabolic pathways during the trophozoite stage of the life cycle to sustain DNA synthesis, pyrimidine synthesis, glycolysis, pentose phosphate shunt, CO_2 fixation, proteolysis of haemoglobin, haem synthesis and mitochondrial electron transport (Mabeza *et al*., 1999). Malaria parasites utilize iron, possibly from the intra-erythrocytic labile pool of ferrous iron and not from the abundant supplies available in erythrocyte haemoglobin, the haem portion of which is quickly degraded to nontoxic and non-iron-bioavailable haemozoin or from the plasma via transferrin (Prentice *et al.*, 2007).

The number of different substitutions which can be applied to the 8-hydroxyquinoline backbone are numerous and provides an ideal starting point for derivatisation and optimisation. As such 8-hydroxyquinoline-base structure and 14 structural derivatives were selected to evaluate their *in vitro* antimalarial activity, as well as their ability to chelate iron and inhibit the formation of β-haematin as a possible mechanism of action.

4.2.2 4-Hydroxquinolines

The 4-hydroxyquinoline has the hydroxyl function group substituted on carbon 4 (C-4) position of the quinoline-base (Andersson and MacGowan, 2003). 4-Hydroxyquinolines are a family of synthetic broad-spectrum agents used as antibacterial agents (Oliphant and Green, 2002). Structurally resembling ciprofloxacin and norfloaxine, alkyl hydroxyquinoline-*N*-oxides were found to be effective against both Gram-positive and Gram-negative bacteria (Hooper and Wolfson, 1991).

4-Hydroxyquinoline derivatives were also studied extensively for their dehydrogenase inhibitions (Baker and Bramhall, 1972a; Baker and Bramhall, 1972b; Baker and Bramhall, 1972c; Baker and Bramhall, 1972d).

A novel class of 4-hydroxyquinolines (4-oxo-dihydroquinolines) has broad spectrum antiviral activity targeting the *Herpes* virus DNA polymerase (Siakallis *et al.*, 2009). It has a high specificity index for inhibiting DNA polymerase belonging to the *Herpes viridae* family.

Suzuki *et al*. (2007) synthesised a series of 4-hydroxyquinoline-*β*-glucosides which utilised the hexose transport pathway for the uptake of the hexose analogues as a novel drug delivery system. One particular compound, 4-(*β*-D-glucosyloxy)-quinoline, was shown to possess *in vitro* antimalarial activities (IC_{50} = 0.15 µg/ml) similar to that of quinine. Thus, indicating that the 4-hydroxyquinoline-base structure has some merit to further investigate.

The 4-hydroxyquinoline base and 19 derivatives were selected for *in vitro* assessment of their activity against *P. falciparum* and against β-haematin formation; as these derivatives have (i) a quinoline base and (ii) a C-4 substitution with an hydroxyl functional group which are proposed to increase its efficacy by increasing its permeability through parasite membranes and (iii) the similar structural/positional substitutions as compared to quinine, chloroquine and mefloquine.

4.3 Objectives

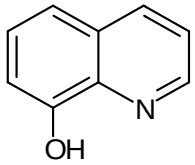
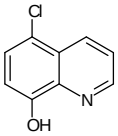
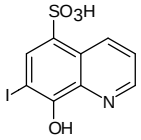
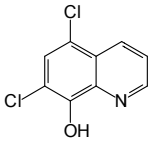
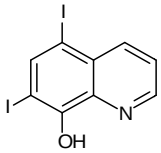
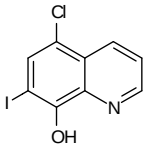
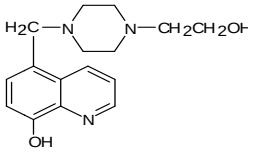
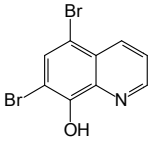
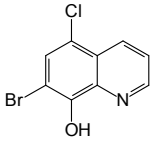
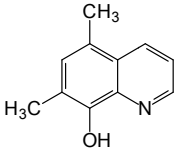
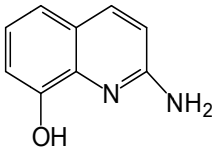
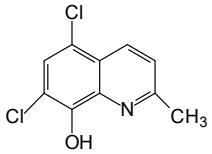
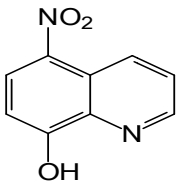
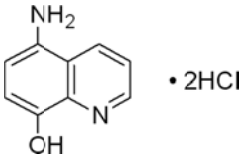
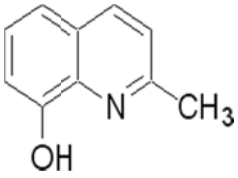
- Evaluate the effectiveness of 8-hydroxy- and 4-hydroxy-quinoline-based compounds in inhibiting *in vitro* β-haematin formation in comparison to chloroquine and quinine.
- Correlate the β-haematin inhibitory activity to their *in vitro* inhibitory effects against *P. falciparum*.
- Elucidate whether the compounds retained ability to chelate iron and scavenge free radicals.
- Assess possible toxic properties against a human kidney epithelial cell line and human RBCs.

4.4 Methodology

4.4.1 8-Hydroxquinoline derivatives

A series of 8-hydroxyquinolines (Table 4.2) were purchased from Sigma-Aldrich®. The compounds were dissolved in DMSO in 20 mM aliquots stored at -20^{o}C (Section 2.7.2) before being diluted in experimental medium to evaluate their effects on the malaria parasite (Section 2.7), human kidney epithelial cells (Section 2.9.6), as well as human RBC membrane integrity p (Section 2.8.2). For the β-haematin formation inhibition assay (Section 2.4.3), anti-oxidant assay (Section 2.10.2) and iron chelation assay (Section 2.11.1), the 8-hydroxyquinolines were dissolved and diluted in DMSO.

Table 4.2 The chemical names, chemical structures and the abbreviations of the tested 8-hydroxyquinoline derivatives.

8-Hydroxyquinoline  8-OH	**5-Chloro-8-hydroxyquinoline**  5-Cl-8OH	**8-Hydroxy-7-iodoquinoline-5-sulphonic acid**  7-I-5-SO_3H-8OH
5,7-Dichloro-8-hydroxyquinoline  5,7-DiCl-8OH	**5,7-Diiodo-8-hydroxyquinoline**  5.7-DiI-8OH	**5-Chloro-8-hydroxy-7-iodoquinoline**  5-Cl-7-I-8OH
5-[[4-(2-Hydroxyethyl)-1-piperazinyl] methyl]-8OH  VK28	**5,7-Dibromo-8-hydroxyquinoline**  5,7-DiBr-8OH	**7-Bromo-5-chloro-8-quinolinol**  7-Br-5-Cl-8OH
5,7-Dimethyl-8-hydroxyquinoline  5,7-DiCH_3-8OH	**2-Amino-8-hydroxyquinoline**  2-NH_2-8OH	**5,7-Dichloro-8-hydroxy-2-methylquinoline**  5,7-DiCl-2-CH_3-8OH
8-Hydroxy-5-nitroquinoline  5-NO_2-8OH	**5-Amino-8-hydroxquinoline dihydrochloride**  5-NH_3-8OH-DiHCl	**2-Methyl-8-quinolinol**  2-CH_3-8OH

4.4.2 4-Hydroxquinoline derivatives

A series of PN, MN and ON derivatives (Table 4.3) were synthesized by Prof S. van Dyk (North-West University, Potchefstroom Campus). The *in vitro* tritiated-hypoxanthine assay and the *in vitro* cytotoxicity assay using the human kidney epithelial cell line were conducted by Prof R. van Zyl (The University of the Witwatersrand). The PN1, MN1 and ON1 series (diethyl-nitroanilinemethylenemalonates; intermediate 1) were the precursors to 4-hydroxyquinolines, the substitutions were on positions 2-, 3- and 4- (Table 4.3). The PN2, MN2 and ON2 series (intermediate 2) were the nitro-4-hydroxyquinoline-3-carboxylates, with the PN3, MN3 and ON3 series (intermediate 3) the nitro-4-hydroxyquinolines-3-carboxylic acids. The PN4, MN4 and ON4 series were nitro-substituted, while the PN5, MN5 and ON5 series were substituted with an amine. The PN6, MN6 and ON6 series (N,N-dipropylamino-4-hydroxyquinolines), PN7, MN7 and ON7 series (N,N-diethylamino-4-hydroxyquinolines) and the PN8, MN8 and ON8 series (N,N-dibutylamino-4-hydroxyquinolines) consisted of double amines substituted at positions 6-, 7- and 8-. A hydrochloride salt was added to the N,N-dipropyl-, -diethyl- and –dibutylamino-4-hydroxyquinolines to improve hydrophilicity. The 4-hydroxyquinolines were dissolved in DMSO with a stock concentration of 10 mM and stored at -20^{o}C (Section 2.7.2). The stocks were used to evaluate their ability to inhibit β-haematin formation (Section 2.4.3); in the tritiated hypoxanthine incorporation assay (Section 2.7) to evaluate their effects on the whole malaria parasite and the MTT assay to elucidate the cytotoxic effects of the derivatives on human kidney epithelial cells (Section 2.9.6).

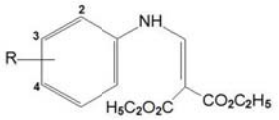
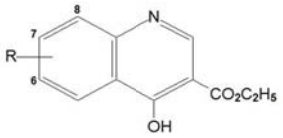
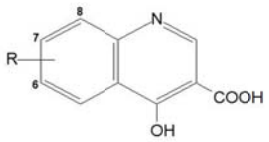
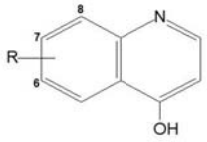
4.5. Results

4.5.1 Pharmacological properties of 8-hydroxyquinolines

4.5.1.1 Inhibition of β-haematin formation

All of the 8-hydroxyquinoline derivatives possessed no comparable ability to inhibit β-haematin formation to that of the positive standard, chloroquine (Table 4.4).

Table 4.3 The β-haematin inhibitory and antimalarial activities of the 4-hydroxyquinoline derivatives, with their respective cytotoxicity (van Dyk, 2001).

Intermediate 1 (PN1, MN1, ON1 series)	Intermediate 2 (PN2, MN2, ON2 series)
	
Intermediate 3 (PN3, MN3, ON4 series)	**4-Hydroxyquinoline**
	

Compound designation		R-group	β-Haematin activity (% inhibition ± S.D. at 1:1 ratio)†	Antimalarial activity (IC_{50}: µM ± S.D.)‡	Toxicity profile (IC_{50}: µM ± S.D.)‡	Safety index
PN	1	–NO	ND	73.90 ± 16.36	1235.06 ± 186.49	16.71
MN			ND	270.03 ± 48.90	1001.17 ± 303.96	3.71
ON			ND	397.95 ± 196.30	1495.19 ± 529.03	3.76
PN	2	–NO	ND	276.03 ± 46.03	1434.89 ± 41.68	5.20
MN			ND	113.47 ± 30.92	451.68 ± 92.6	3.98
ON			ND	50 ± 18.44	212.94 ± 34.31	4.26
PN	3	–NO	ND	27.69 ± 7.69	18.59 ± 0.06	0.67
MN			ND	260.04 ± 69.79	1495.43 ± 321.67	5.75
ON			ND	59.06 ± 28.33	252.91 ± 194.36	4.28
PN	4	–NO	[0.01 ± 0.01%]	115.05 ± 19.63	164.68 ± 101.68	1.43
MN			[0.01 ± 0.01%]	56.21 ± 8.05	384.05 ± 51.47	6.83
ON			[0.01 ± 0.01%]	53.16 ± 14.32	248.58 ± 34.89	4.68
PN	5	$–NH_2$	[0.01 ± 0.01%]	108.31 ± 15.5	2344.19 ± 73.5	21.64
MN			[0.01 ± 0.01%]	540.31 ± 62.94	1244.5 ± 325	2.30
ON			[0.01 ± 0.01%]	316.25 ± 30.43	3855.56 ± 719.81	12.19
PN	6	$–N(C_3H_7)_2$	**0.89***	47.75 ± 20.00	1047.46 ± 259.67	21.94
MN			[0.01 ± 0.01%]	109.71 ± 45.16	4147.79 ± 538.36	37.81
ON			[0.01 ± 0.01%]	49.016 ± 15.29	4932.17 ± 559.92	**100.62**
PN	7	$–N(C_2H_5)_2$	**0.65***	45.51 ± 18.33	1283.84 ± 494.4	28.21
MN			[0.01 ± 0.01%]	192.92 ± 53.61	5695.69 ± 375.69	29.52
ON			[0.01 ± 0.01%]	118.19 ± 42.96	1332.45 ± 129.07	11.27
PN	8	$–N(C_4H_9)_2$	**1.39***	17.50 ± 5.22	178.86 ± 27.61	10.22
MN			[0.01 ± 0.01%]	33.93 ± 20.99	644.6 ± 76.65	19.00
ON			[0.01 ± 0.01%]	57.46 ± 24.49	392.94 ± 120.26	6.84
PN	6S	$–N(C_3H_7)_2·HCl$	[0.01 ± 0.01%]	14.05 ± 4.46	264.85 ± 24.31	18.86
MN			ND	498.57 ± 92.55	3967.99 ± 83.96	7.96
ON			**2.04***	294.40 ± 49.52	619.11 ± 59.25	2.10
PN	7S	$–N(C_2H_5)_2·HCl$	ND	51.64 ± 7.41	77.09 ± 2.32	1.49
MN			ND	573.70 ± 140.12	3760.13 ± 192.4	6.55
ON			ND	107.29 ± 11.52	972.83 ± 199.25	9.07
PN	8S	$–N(C_4H_9)_2·HCl$	**14.23***	**2.92 ± 1.56**	398.28 ± 90.44	**136.52**
MN			[0.01 ± 0.01%]	35.66 ± 17.63	442.98 ± 24.28	12.42
ON			ND	28.46 4.76	500.62 ± 83.63	17.59
Chloroquine			18.55 ± 0.71**	0.10 ± 0.01	245.34 ± 11.77	2378.64
Quinine			44.79 ± 2.25**	0.10 ± 0.01	335.19 ± 15.03	3385.76

†The 1:1 ratio of test compound to haemin at 191.73µM

*Percentage activity relative to chloroquine; **IC_{50} values of the BHIA result (µM ± s.d.); ‡ van Dyk, 2001

ND- not determined due to insufficient compound available

4.5.1.2 Antimalarial and β-haematin formation inhibitory activities

The base 8-hydroxyquinoline was found to be quite active compared to the derivatives tested and four fold less active than quinine (Table 4.4). Of the fifteen derivatives, the two amino-substituted compounds were the more active, with 5-amino-8-hydroxyquinoline the most active (IC_{50}: 0.12 μM), with an antimalarial activity equivalent to that of chloroquine and quinine (p>0.05). The amino-substitution at position 5 has yielded a nine fold increase in antimalarial activity than when at position 2 (IC_{50}: 1.08 μM, p>0.05).

The promising antimalarial activity observed against the whole parasite was not due to inhibition of haemozoin formation as observed by the lack of inhibition of β-Haematin formation at 100 μM (Table 4.4).

4.5.1.3 Ferrous ion chelation activities

All the 8-hydroxyquinoline derivatives possessed ferrous ion chelation properties, with 2-methyl-8-hydroxyquinoline being the most effective (6.70 μM), and approximately 1.4 fold less active as the positive control, EDTA (4.79 μM) (Table 4.4). The remaining 8-hydroxyquinoline derivatives were between 4 to 12 fold less active than EDTA.

4.5.1.4 Free radical scavenging activities

Only three of the fifteen 8-hydroxyquinoline derivatives possessed any free radical scavenging properties (Table 4.4). When compared to the positive control, ascorbic acid, 2-amino- and 5,7-dichloro-8-hydroxyquinolines were 68% and 78% as active (p>0.05). In contrast, 5-amino-8-hydroxyquinoline was 16% more effective than ascorbic acid (p>0.05) at scavenging free radicals.

4.5.1.5 Haemolytic activity

Variable degrees of haemolysis were observed for the 8-hydroxyquinoline derivatives when screened at 100 μM in the range of 0.16 to 23.66%, with 8-hydroxy-5-nitroquinoline being most lytic (Table 4.4). In comparison to the 100% haemolysis control, 0.2% (v/v) Triton X-100™, chloroquine and quinine only induced 0.32% and 0.80% haemolysis at 100 μM, respectively.

Table 4.4 The inhibitory properties of 8-hydroxyquinolines.

8-OH Derivatives	Antimalarial activity (IC_{50}: µM ± S.D.)	β-Haematin formation inhibition [% at 100 µM]	Iron chelation (IC_{50}: µM ± S.D.) [% at 100 µM]	Free radical scavenging (IC_{50}: µM ± S.D.) [% at 100 µM]	Haemolysis [% at 100 µM]	Cell viability (IC_{50}: µM ± S.D.)	Safety index
5-NH_2-8OH	**0.12 ± 0.01**	[0.1 ± 0.01%]	[9.12 ± 1.12]	19.41 ± 1.42	[2.94 ± 0.35]	9.76 ± 1.46	**81.33**
8-OH	**0.41 ± 0.16**	[0.1 ± 0.01%]	30.59 ± 8.52	[18.31 ± 1.24%]	[0.30 ± 0.24]	5.03 ± 0.56	12.27
2-NH_2-8OH	1.08 ± 0.52	[0.1 ± 0.01%]	33.97 ± 9.54	**29.84 ± 5.21**	[0.16 ± 0.13]	10.81 ± 2.28	10.01
5-Cl-8OH	1.12 ± 0.26	[0.1 ± 0.01%]	35.27 ± 9.39	[3.45 ± 0.52%]	[0.99 ± 0.24]	7.48 ± 0.98	6.68
5,7-DiCl-2-CH_3-8OH	1.36 ± 0.56	[0.1 ± 0.01%]	43.28 ± 9.95	[24.07 ± 1.65%]	[12.23 ± 0.58]	2.79 ±.0.80	2.05
5,7-DiCl-8OH	1.81 ± 0.71	[0.1 ± 0.01%]	55.09 ± 13.49	[11.26 ± 0.29%]	[16.40 ± 2.55]	8.27 ± 0.96	4.57
2-CH_3-8OH	3.29 ± 1.52	[1.41 ± 3.53]	**6.70 ± 1.62**	[20.39 ± 1.98%]	[0.60 ± 0.34]	10.98 ± 1.54	3.34
5,7-DiBr-8OH	3.34 ± 0.55	[0.1 ± 0.01%]	59.43 ± 15.84	[6.47 ± 0.15%]	[17.50 ± 1.98]	17.03 ± 0.66	5.10
7-Br-5-Cl-8OH	3.63 ± 0.97	[0.1 ± 0.01%]	50.37 ± 9.65	[8.57 ± 0.88%]	[17.43 ± 2.56]	10.71 ± 0.92	2.95
5,7-DiCH_3-8OH	4.57 ± 1.26	[0.1 ± 0.01%]	53.67 ± 27.74	**27.40 ± 2.71**	[0.20 ± 0.17]	3.42 ± 0.84	0.75
5-NO_2-8OH	4.55 ± 1.02	[0.1 ± 0.01%]	21.79 ± 1.49	[10.64 ± 0.37%]	[23.66 ± 3.87]	4.88 ± 0.87	1.07
5.7-DiI-8OH	7.04 ± 2.37	[0.1 ± 0.01%]	59.93 ± 13.22	[14.11± 1.16%]	[15.77 ± 1.41]	22.63 ± 2.88	3.21
VK28	10.02 ± 3.35	[0.1 ± 0.01%]	51.39 ± 16.94	[14.25 ± 4.26%]	[0.95 ± 0.06]	**56.78 ± 2.59**	5.67
5-Cl-7-I-8OH	13.76 ± 1.41	[0.1 ± 0.01%]	51.30 ± 7.51	[17.97 ± 0.44%]	[14.40 ± 2.49]	21.52 ± 1.03	1.56
7-I-5-SO_3H-8OH	41.57 ± 7.66	[0.1 ± 0.01%]	54.35 ± 22.48	[9.08 ± 0.81%]	[0.74 ± 0.17]	[53.35 ± 1.06%][2]	3.10
Chloroquine	0.103 ± 0.004	18.55 ± 0.71[1]	ND	ND	[0.32 ± 0.06]	245.34 ± 11.77	2378.64
Quinine	0.099 ± 0.008	44.79 ± 2.25[1]	ND	ND	[0.80 ± 0.20]	335.19 ± 15.03	3385.76
EDTA	ND	ND	4.79±0.52	ND	ND	ND	ND
Ascorbic acid	ND	ND	ND	22.52 ± 4.89	ND	ND	ND

[1] IC_{50}: µM ± S.D.; [2] percentage cell viability at 129 µM; ND = not determined

4.5.1.6 Cytotoxic activities

Of the 8-hydroxyquinoline derivatives screened to evaluate their potential toxicity, 14 were found to be toxic at concentration less than 129 µM. These compounds were 4 to 88 times more toxic than chloroquine and 6 to 120 times more toxic than quinine against the *in vitro* human kidney epithelial cell line. Where 5,7-dichloro-8-hydroxy-2-methylquinoline was the most and 8-hydroxy-7-iodoquinoline-5-sulphonic acid the least toxic when screened at 129 µM (Table 4.4).

4.5.2 4-Hydroxyquinoline derivatives

The 4-hydroxyquinoline derivatives possessed no β-haematin inhibition activity (range: 0.01 – 14.23%) compared to that of chloroquine (Table 4.3). Of the 24 derivatives screened for β-haematin inhibition activity, only 5 showed a minimal inhibitory effect. The most active compound against β-haematin formation inhibition was PN8S with a 14.23% activity when compared to chloroquine. In contrast these compounds have been reported to possess variable antimalarial and cytotoxic effects (Table 4.3; van Dyk, 2001).

4.6 Discussion

4.6.1 8-Hydroxyquinoline derivatives

4.6.1.1 Inhibition of β-haematin formation

The inability of the 8-hydroxyquinoline derivatives to inhibit the formation of β-haematin (Table 4.4) was probably due to the fact that 8-hydroxyquinoline does not associate with haem under acid reaction conditions (Egan *et al,.* 1994; Egan *et al*., 1997). The inactivity was also further shown by Paraskevopoulos (2008), where the 8-hydroxyquinoline base or pantothenic acid or adenosine derivatives at C4 demonstrated no inhibitory activity against β-haematin formation. It was proposed that the 8-hydroxyquinolines were not able to dissociate after binding of the metal ions as per the mechanism of action as suggested by Albert *et al.* (1953) and Scheibel and Adler (1980).

4.6.1.2 Antimalarial activity related to structure

Overall, the 8-hydroxyquinolines possessed promising activity all inhibiting in the micromolar range, which may be attributed to their favourable lipid/water partition coefficient allowing them to move through the RBC and parasitic membranes; as well as

their high stability and binding constants which allowed them to compete with naturally occurring chelators in the RBC and parasite (Scheibel and Adler, 1980). 8-Hydroxyquinoline was reported to inhibit the FCR-4/6252 knobless strain of *P. falciparum* in a dose-response manner, where there was a rapid onset of parasite inhibition, with 6.89 to 689 µM decreasing parasite growth by 62-76% after 48 hours of treatment and 100% growth after 96 hours (Scheibel and Adler, 1980).

Of the fifteen 8-hydroxyquinoline derivatives tested, the two amino-derivatives possessed the most promising activity (Table 4.4). The single amino-substitution at position 5 was more active against malaria than the chloro- ($p<0.05$) or nitro-substitution ($p<0.001$) in the same position. Similarly if the amino group was at position 2, a greater antimalarial activity was observed than when a methyl-substitution was placed at the same position, such that the IC_{50} values were 1.08 and 3.29 µM, respectively ($p<0.01$). The presence of a single amine- or methyl- substitution at C2 was shown to possess less cytotoxicity when compared with the 8-OH base compound. This resulted in a highly favourable safety index for 5-amino-8-hydroxyquinoline (81.33), indicating that the inhibitor effect on the growth of the malaria parasite is distinct from that observed for the human cell line. The mechanism of action of 5-amino-8-hydroxyquinoline is not due to inhibition of haemozoin formation, iron chelation and scavenging free radicals are unlikely the primary mechanism of action (Table 4.4). Alternative mechanisms of action warrant further investigation and may be linked to their ability to chelate other divalent metals (Section 5.6.1.3).

A single chloro-substitution was observed to be slightly more effective as an antimalarial as compared to the double chloro-substitution (1.12 > 1.81 µM). Whilst, a bromo-substitution at C7 (3.34 µM) possessed increased antimalarial activity over the iodo-substitution at C7 (7.04 µM). Winter *et al.* (2006) also demonstrated that a chlorine substitution yielded better antimalarial activities than a bromine substitution (compounds no. 11> 10 and compounds no. 16 > 15, Figure 4.1); as well as by increasing the length of the haloalkyl and haloalkoxy chain length that terminated with trifluoro-functional groups would also increase its antimalarial properties (410 000 fold over 8-hydroxyquinoline; approximated 1 picomolar vs 0.41 micromolar).

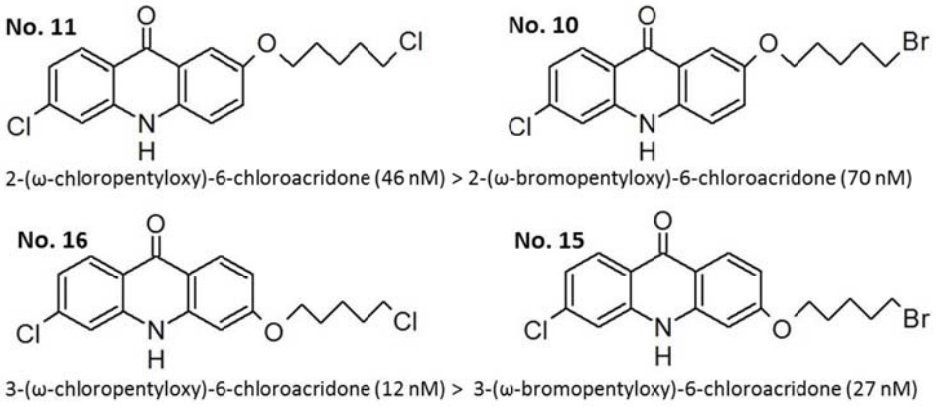


Figure 4.1 The antimalarial activity comparisons of chloro- and bromo-substitution on the acridone base structure (Winter *et al*., 2006).

A dichloro- substitution was observed to be more active than dimethyl-, dibromo-, and diiodide-substitutions (IC_{50} values: 1.81 > 3.29 > 3.34 > 7.04 µM, respectively); where only the dichloro-substitution had a significant difference ($p<0.001$) over the diiodo-substitution. The addition of a methyl group at position 2 to the dichloro-substitution derivative increased the efficacy by 25% against the whole parasite (IC_{50} = 1.36 µM; $p>0.05$); whilst the 2-methyl derivative was as active as the 5,7-dichloro derivative ($p>0.05$)(Table 4.4). Scheibel and Adler (1980) also investigated the effects of 2-methyl-8-hydroxyquinoline against the FCR-4/6252 knobless *P. falciparum* strain and found that the addition of a methyl-group at position 2 decreased the antimalarial effect in comparison to 8-hydroxyquinoline. Where the latter at 6.28 µM, inhibited 100% growth after 96 hours, 2-methyl-8-hydroxyquinoline only inhibited 68% growth. The decrease in antimalarial activity was proposed to be related to the decreased metal binding affinity of 2-methyl-8-hydroxyquinoline (Section 4.6.1.3). In contrast, Scheibel and Adler (1980) reported that 5-methyl-8-hydroxyquinoline inhibited 94% parasite growth after 96 hours, indicating that the position of the methyl group greatly affected the inhibitory effect on the whole parasite. The reported IC_{50} values for 5-methyl-8-hydroxyquinoline and 2-methyl-8-hydroxyquinoline were 62.8 µM and >628 µM, respectively after 48 hours with an initial parasitaemia of 1.2% (Scheibel and Adler, 1980); compared to this study where the IC_{50} value for the latter derivative was 3.29 µM after 48 hours, where the tritiated hypoxanthine incorporation assay was initiated at 0.5% parasitaemia (Table 4.4).

The two derivatives with different halogens bound at positions 5 and 7, namely 7-bromo-5-chloro-8-hydroxyquinoline and 5-chloro-7-iodo-8-hydroxyquinoline (clioquinol) did not significantly improve the antimalarial effects of the mono- or di-chloro/iodo/bromo-derivatives (Table 4.4), but the addition of the iodine group at position 7 did significantly (p<0.001) decrease the activity compared to the 5-chloro-, 5,7-dichloro- and 5,7-diiodo-derivatives. In contrast, the more complex structure of VK28 (5-[4-(2-hydroxyethyl) pierazine-1-ylmethyl]-quinole-8-ol) did not greatly improve the antimalarial activity in comparison to the simpler structure of 5-chloro-7-iodo-8-hydroxyquinoline (clioquinol), which are both under investigation for use in neurodegenerative disorders (Section 4.2.1.2).

The importance of the chlorine-substitution at position 5 was again highlighted when the antimalarial activity of 5-chloro-7-iodo-8-hydroxyquinoline was compared with 8-hydroxy-7-iodoquinoline-5-sulphonic acid, where the antimalarial activity of the latter derivative was 3.4 fold lower than the former (Table 4.4).

The iodo-derivatives are proposed to have a different mechanism of action to the remaining halogen and non-halogenated 8-hydroquinoline derivatives. It has been found that 5-chloro-7-iodo-8-hydroxyquinoline and diiodo-8-hydroxyquinoline owe much of their activity to the low release of iodine from the structure and to a lesser degree to its ability to chelate metal ions; which contrasts with 8-hydroxyquinoline which appears to be mainly due to metal chelation (Scheibel and Stanton, 1986). 5-Chloro-7-iodo-8-hydroxyquinoline is used in the treatment of intestinal amoebiasis, but it has been found that following substantial absorption of the drug from the gastro-intestinal tract that there is increased plasma iodine levels (Jack and Riess, 1973), which could inhibit the intra-erythrocytic stages of the parasite.

Although 8-hydroxyquinoline inhibited the intracellular parasite, it did so at micromolar concentrations and ideally nanomolar concentrations would warrant further investigations. It was proposed that this concentration dependant effect may be attributed to: (i) formation of the ligand/metal complex that does not kill the parasite; (ii) decreased tendency to dissociate inside the cells/parasites to the active 1:1 complex and free chelator (Figure 4.2) and (iii) decreased partition co-efficient which did not correlate with antimalarial activity (Scheibel and Adler, 1980).

Proposed mechanisms of action of 8-hydroxquinoline derivatives included metal chelation, oxidation of enzymes and/or halogen toxicity. In malaria it was proposed to be by

either exhibiting its pharmacological effects through the oxidation of sulfhydryl groups of the glycolytic enzymes, directly, and proportionally concentration dependent inhibiting glycolysis of the parasites in culture, or affect biosynthetic metalloprotein oxidase (Scheibel and Adler, 1980).

4.6.1.3 Mechanism of action: metal chelation

8-Hydroxyquinoline derivatives are known to be non-specific metal chelators with high binding constants which are able to penetrate through cellular membranes and compete with naturally occurring chelators in the cell (Scheibel and Adler, 1980). This was shown to be true in this study when the derivatives competed with the selective chelators, 2,2-bipyridyl for ferrous ions; where the iron chelating IC_{50} values for the derivatives ranged between 6.7 and 59.93 µM in comparison to the non-specific chelator, EDTA (4.79 µM) (Table 4.4). 8-Hydroxyquinoline derivatives are known to chelate several cations to varying degrees compared to therapeutically administered chelators, such as EDTA and desferrioxamine (Table 4.5). Where the latter two chelators had a higher affinity for ferric over ferrous ions, and 8-hydroxyquinolines had a higher affinity for ferric ions than either of these two therapeutic agents. Scheibel and Adler (1980) reported that the addition of equimolar concentrations of cobalt did not antagonise the antiparasitic effect of 5-methyl-8-hydroxyquinoline at 6.28 and 62.8 µM; nor did the addition of equimolar concentrations of iron potentiate the inhibitory effect of 5-methyl-8-hydroxyquinoline at 0.628 and 6.28 µM.

Table 4.5 Metal affinity constants for selected ligands (Gaeta and Hider, 2005).

Ligand	Fe(III)	Al(III)	Ga(III)	Cu(II)	Zn(II)	Fe(II)
DFO	30.6	25	27.6	14.1	11.1	7.2
2,2'-Bipyridyl	16.3	-	7.7	16.9	13.2	17.2
EDTA	25.1	16.5	21	18.8	16.5	14.3
8-Hydroxyquinoline	37.7	-	40.5	22.9	15.8	-

Factors that have been proposed to interfere with ion chelation by 8-hydroxyquinoline derivatives included the availability of electrons from the nitrogen atom or with the ionization of the hydroxyl group (Scheibel and Adler, 1980).

Scheibel and Adler (1980) have proposed that the decreased antimalarial activity of the methyl-substitution at position 2 maybe be affected by the derivative's lesser affinity for

binding cations and divalent cations when compared with the base structure base of 8-hydroxyquinoline. In this study there was no correlation between the antimalarial activity and iron chelating ability of the 8–hydroxyquinolines (r^2 = 0.1205). The smaller crystal radius of the divalent cations may have contributed to the lower binding affinity, and the methyl-substitution may have caused possible structural steric hindrance resulting in decreased ion binding affinity. Of the seven possible isomeric mono-hydroxyquinolines, only 8-hydroxyquinoline is capable of forming a non-ionised complex with divalent metallic ions through chelation (Rubbo *et al*., 1950). Therefore when Scheibel and Adler (1980) tested 5-hydroxyquinoline, the observable antimalarial activities at 68.9 µM were 0% and 50% inhibition after 48 and 96 hours, respectively. By virtue of the location of the hydroxyl group in relation to the basic ring nitrogen, 8-hydroxyquinoline is able to chelate divalent cations. The movement of the hydroxyl group from position 8 to position 5 eliminated the ability for the hydroxyquinoline to chelate; the antimalarial activity of 5-hydroxyquinoline at high concentrations was probably facilitated by a different mechanism. The hydroxyl group is proposed to dissociate as an anion, while the nitrogen supplies electrons forming a coordinate bond between metal and 8-hydroxyquinoline (Albert *et al*., 1947). The mechanism of action of the 8-hydroxyquinolines was proposed to be dependent on the presence of one or more Cu^{2+}, Fe^{2+} and Fe^{3+} with the 8-hydroxyquinoline-metal complex forming in a 1:1 and/or 2:1 ratio (Figure 4.2). The latter complex possessed a favourable lipid/water partition, allowing the uptake of both complexes into both the RBCs, as well as the intracellular malaria parasite (Albert *et al*., 1953; Sheibel and Adler, 1980).

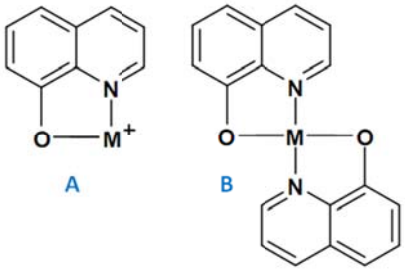


Figure 4.2 8-Hydroxyquinoline and its metal complex. **A** depicts the 1:1 8-hydroxyquinoline:Metal hydrophilic complex (M = Cu^{2+} or Fe^{2+}) and **B** depicts 2:1 1 8-hydroxyquinoline:Metal lipophilic complex where M = Cu^{2+} or Fe^{2+} (Albert *et al*., 1953; Scheibel and Adler, 1980).

In 1953, Albert *et al*. proposed that the lipophilic 1:2 chelate of Cu(II)-8-hydroxyquinoline (Figure 4.2) crosses the lipid membranes and reaches the interior of the cell before dissociating into a 1:1 half chelate and free 8-hydroxyquinoline. The toxic half chelate then competitively binds/blocks the metal-binding sites on enzymes and initiates oxidative chain reactions which inactivate labile enzymes and kill the cell, such as inhibiting the biosynthesis of pteridines and its precursors. It is also proposed to elicit its antimalarial properties through the oxidation of sulfhydyl groups of glycolytic enzymes or affecting some vital metalloprotein oxidase enzymes specifically in the parasite as the 8-hydroxyquinoline derivatives were found to have little effect on the same processes in normal RBCs (Scheibel and Adler, 1980). Whilst, the free 8-hydroxyquinoline reverts intracellularly to a 1:1 complex which may exert its biological effects by binding to the metallic prosthetic groups from enzymes.

The proposed mechanism of action of the 5-substituted-8-hydroxyquinolines (methyl- and nitro-substitution) involved the inhibition of redox enzymes such as the superoxide dismutase, catalase, and glutathione peroxidase and reductase such that the derivatives reduced the natural resistance to oxidative damage resulting in parasite death (Scheibel and Adler, 1981). This was proposed to not be the primary mechanism of action. Overall it has been postulated that one of the main mechanism of action for 8-hydroxyquinoline and several of the derivatives was through their inhibitory actions as metal-chelators (Albert *et al.,* 1953; Scheibel and Adler, 1980).

4.6.1.4 Mechanism of action: pro- or anti-oxidant

Many phenolic compounds, derived from either natural sources or synthetic methods, have been reported as potent anti-oxidants (Ma *et al*., 2000). An effective anti-oxidant activity of phenolic compounds is dependent on the stability of the phenoxyl radical formed in the reaction, as well as the position of a substituent which affects the phenoxyl radical. However, the anti-oxidant activity was only observed for three of the derivatives, namely 5-amino- and 2-amino-8-hydroxyquinolines and 5,7-dimethyl-8-hydroxyquinoline (Table 4.4).

This is in contrasts to the reports that numerous 8-hydroxyquinolines derivatives are potent anti-oxidants, which arises from their chelating ability (Fernández-Bachiller *et al*., 2010). The phenolic hydroxyl group of the 2-vinyl-8-hydroxyquinoline derivatives has been

demonstrated to possess anti-oxidant activities in hydrogen peroxide-induced oxidative stress by reacting to the free radicals. The study conducted by Wang *et al*. (2011) also discovered that certain 2-vinyl-8-hydroxyquinoline derivatives protected the bone mesenchymal stem cells from oxidative stress damage, as well as induced proliferation of these stem cells.

In an *in vivo* study, it was reported that the combined administration of 5-chloro-7-iodo-8-hydroxyquinoline (clioquinol) and vitamin B_{12} fully rescued the lead-induced neurotoxicity; whilst clioquinol alone did not reverse the lipid peroxidation and vitamin B_{12} alone was only partially effective (Chen *et al.*, 2006).

VK28 (5-[4-(2-hydroxyethyl) pierazine-1-ylmethyl]-quinole-8-ol) has iron (III) binding capacity similar to that of desferroxamine and it does not cross the blood brain barrier when injected intraventricularly, possessed neuroprotective activity against dopaminergic neurodengeneration-induced in mice. The neuroprotective action of VK-28 was most likely to be its anti-oxidant properties as an iron chelator, since intranigral or intraventricular 6-hydroxydopamine initiated an increase in total iron in the substantia nigra and striatum, which may have increased hydroxyl radical production via the Fenton reaction (Shachar *et al*., 2004).

These anti-oxidant properties, although not entirely replicated with the $DPPH^{\bullet}$ free radical scavenging activity in this study, have been investigated for the therapeutic properties in neurogenerative diseases (Prachayasittikul *et al*., 2013).

4.6.1.5 Cytotoxic effect

Fourteen of the 8-hydroxyquinoline derivatives were highly effective in inhibiting cellular viability and growth (IC_{50} range: 2.79–56.78); with 5,7-dichloro-8-hydroxy-2-methylquinoline the most toxic (IC_{50} = 2.79 µM) and only 8-hydroxy-7-iodoquinoline-5-sulphonic acid not affecting cell growth i.e. the safest (IC_{50} > 129 µM).

Structural analysis indicated that a nitro- functional group substitution at C5 possessed slightly more cytotoxicity ($p < 0.05$) than the base 8-OH compound with 8-hydroxy-5-nitroquinoline (4.88 µM) > 8-hydroxyquinoline (5.03 µM); while a chloro- and amine-substitution at C5 did not increase the cytotoxicity effect of the derivatives (IC_{50} 7.48 µM and 9.76 µM, respectively). Substitutions at both C5 and C7 with dichloro-, dibromo-, diiodo,

and dimethyl- functional groups illustrated that the dimethyl substitution increased its cytotoxic effect when compared with 8-OH ($p < 0.05$) (Table 4.4). The increase in the molecular weight and atomic number of the substituents on the functional group, notably decreased the cytotoxic effect ($I < Br < Cl < CH_3$) and the same effect was also observed with chloro- substitution at C5 and chloro-, bromo- and iodo- substitutions at C7 ($Cl > Br > I$). A methyl- functional group bound at C2 in 5,7-dichloro-8-hydroxyquinoline significantly increased ($p < 0.05$) its cytotoxic effect when compare with 8-OH.

Based on the metal chelating properties of the derivatives, the cytotoxic effect on the human kidney epithelial cells could be due to the formation of half-chelate complexes (Figure 4.2A), where it competitively bind/block the metal-binding sites on various enzymes, such as inhibiting the biosynthesis of pteridines and its precursors for cell growth (Albert *et al*., 1953). 8-Hydroxyquinoline is also a known inhibitor of ribonucleotide reductase in yeast (Fraser and Creanor, 1975), where this iron-dependent enzyme is essential for optimal viability in healthy and cancer cells (Cerqueira *et al*., 2007) as well as in malaria (Gamboa de Domínguez and Rosenthal, 1996).

The toxicity associated with iron chelators may be due to a number of factors, such as inhibiting iron-containing metalloenzymes, lack of metal selectivity, redox cycling of iron-complexes between iron(II) and iron(III) and the kinetic lability of the iron complex leading to iron redistribution (Gaeta and Hider, 2005). The 8-hydroxyquinoline chelators contain both oxygen and nitrogen atoms and hence possess intermediate properties between those of the di-nitrogen ligands and the di-oxygen ligands (Hider & Hall, 1991; Liu& Hider, 2002b). More importantly, because 8-hydroxyquinoline is monobasic, it forms neutral 3 : 1 complexes with iron(III) and neutral 2 : 1 complexes with both copper(II) and zinc(II). Thus, in principle, it can remove these metals from cells. However, because 8-hydroxyquinoline binds both iron(III) and iron(II) relatively tightly, iron can redox cycle between these two oxidation states with relative ease, thereby generating toxic oxygen radicals which via lipid peroxidation could kill the cells (Gaeta and Hider, 2005).

Various mechanism of action of 8-hydroxyquinoline derivatives have been proposed. Where Shen *et al*. (1999) demonstrated that 7-substituted-8-hydroxyquinoline derivatives possessed substantial cytotoxic activity against leukaemia; where the proposed mechanism of action against myeloma cells was related to the blockade of voltage-gated K^+ channels. Li *et al.* (1995) discovered that the cytotoxicity of 5-amino-8-hydroxyquinoline against

myeloma and leukaemia cells could act as a non-competitive proteasome inhibitor. Whilst metal complexes of 8-hydroxyquinoline-2-carboxaldehyde thiosemicarbazone (Figure 4.3) inhibited a cisplatin-resistant neuroblastoma cell line (SK-N-DZ) in a dose-dependent manner by arresting the cell cycle and inducing apoptosis by increasing p53 protein expression (Zheng *et al*., 2005).

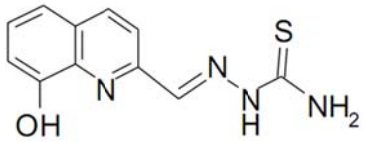


Figure 4.3 Structure of 8-hydroxyquinoline-2-carboxaldehyde thiosemicarbazone (Zheng *et al*., 2005).

In addition to the cytotoxic properties of the 8-hydroxyquinoline derivatives, 5-methyl-8-hydroxyquinoline was found to be one of the more mutagenic inhibitors of *Plasmodium falciparum* and kidney epithelial cells. When tested in the forward mutation assay with *Salmonella typhimurium,* 5-methyl-8-hydroxyquinoline was more than 30 times more mutagenic than chloroquine (Batzinger *et al*., 1978). Therapeutic use would require reduced genetic toxicity which would require suitable structural alterations.

The toxicity profile of the 8-hydroxyquinoline derivatives was further characterised by investigating their effect on the membrane stability of RBC by measuring haemolysis (Table 4.4). It was found that there was minimal lytic potential by the 8-hydroxyquinoline derivatives, which has been shown to be due to the protective free radical scavenging anti-oxidant properties of the phenol group of the 8-hydroxyquinoline derivatives (Ma *et al*., 2000).

Unfortunately, many halogenated hydroxyquinolines possess neurotoxic side effects (Tsubaki *et al*., 1971; Oakley, 1973). In the 1970s, 5-chloro-7-iodo-8-hydroxyquinoline (clioquinol) was used as an antibiotic/antiprotozoal but was banned due to the adverse side effect of subacute myelo-optic neuropathy (SMON) being reported in Japanese and was attributed to vitamin B12 deficiency. However the causal relationship between clioquinol and SMON was never proven (Bush and Masters, 2001). In an unpublished phase one clinical trial data, co-administration of vitamin B_{12} with 5-chloro-7-iodo-8-hydroxyquinoline revealed no adverse systemic, neurological and cognitive effects (Shachar *et al*., 2004). It

has been proposed that these side effects may be avoided by the use of nonhalogenated analogues, for instance the brain permeable VK-28 (Warshawsky *et al*., 2000).

Overall the 8-hydroxyquinoline inhibited the intracellular parasite at micromolar concentrations which without further structural alterations to improve the antimalarial activity they do not warrant further investigations. Researchers have attempted to potentiate the antimalarial properties of 8-hydroxyquinoline derivatives by using them in combination with standard antimalarials or by altering the side chain structures that could act via different mechanisms.

4.6.2 4-Hydroxyquinoline

4.6.2.1 β-Haematin inhibitory activity of the 6-, 7- and 8-dialkylamino 4-hydroxyquinolines

There is no significant β-haematin formation inhibition, only the 6-substituted-N,N-dibutylamino-4-hydroxyquinoline with the added hydrochloride salt (PN8S) that possessed 14% inhibition compared to chloroquine (Table 4.3). Inhibition of haemozoin formation is unlikely to be the primary mechanism of antimalarial action of the 4-hydroxyquinoline derivatives, but possibly that of enzyme inhibition compared to the action of chloroquine.

4.6.2.2 Antimalarial and cytotoxicity activities of the 6-, 7- and 8-dialkylamino 4-hydroxyquinolines

The 4-hydroxyquinoline intermediates of synthesis and 4-hydroxyquinoline derivatives were evaluated against the *P. falciparum* FCR-3 strain for their *in vitro* antimalarial activities, as well as their cytotoxicity profile against HEK293 cells (van Dyk, 2001). None of the derivatives possessed any antimalarial activities comparable with chloroquine ($P < 0.0001$) and quinine ($P < 0.0001$). The increased antimalarial activity for the dialkylamino substitution at position 6 (PN5 to PN8) were greater than substitutions at positions 8 (ON5 to ON8) and 7 (MN5 to MN8); with IC_{50} values ranging from 17.5 to 108.3 µM for the PN series, 49.0 to 316.3 µM for the ON series and 33.9 to 540.3 µM for the MN series (Table 4.3). Lengthening of the carbon chains on the dialkylamino substituents also increased the antimalarial activities of the 4-hydroxyquinoline derivatives where PN8>PN7>PN6>PN5, MN8>MN6>MN7>MN5 and ON6>ON8>ON7>ON5.

As for cytotoxic effect of the 4-hydroxyquinoline derivatives on the human kidney epithelial (HEK293) cells, the 6-dialkyamino-4-hydroxyquinolines were more toxic when compared with 7- and 8-substituted 4-hydroxyquinolines with the dialkylamino substituents. The cytotoxic effects of the PN5 to PN8 derivatives were 178.8 to 2344.2 μM, for the MN5 to MN8 derivatives were 644.6 to 5695.7 μM and for the ON5 to ON8 derivatives were 392.9 to 4932.2 μM (Table 4.3). It was also observed that as the four carbon side chain length substitution increased, so did the cytotoxic effects of the derivatives.

A nitro-substitution on positions 6, 7 and 8 possessed greater antimalarial activity when compared to the amino-substitution. However, substitutions at positions 8 and 7 yielded better antimalarial activities with ON4>ON5 ($p = 0.0194$) and MN4>MN5 ($p = 0.0002$), than substitutions at position 6 (ON4>MN4>PN4, 53.16>56.21>115.05 μM). This is in agreement with the study by Bhattacharjee (2001) where it was demonstrated that a nitro-substitution at C7 greatly increased its haematin polymerisation inhibition, as well as *in vitro* antimalarial activities against the *P. falciparum* (NF54 strain); where PN4 was not significantly more active than PN5 ($P = 0.694$). Correspondingly, the nitro-substitution also increased the cytotoxic profiles when compared with amino-substitutions, such that PN4>PN5 (164.68>2344.19 μM), MN4>MN5 (384.05>1244.5 μM) and ON4>ON5 (248.58>3855.56 μM) (Table 4.3).

Antimalarial and cytotoxic activities for the intermediates of synthesis were also investigated. Except for the PN, MN and ON1 derivatives, where the substitutions were at positions 2-, 3-, and 4-, and the intermediates 2 and 3 had their nitro-substitutions at the same positions as the derivatives with carboxylate (PN2, MN2 and ON2), carboxylic acid (PN3, MN3 and ON3) and a hydrogen (PN4, MN4 and ON4) atom at C3. There were no clear or discernible patterns with respect to the shortening of the chain length to increase the antimalarial properties or cytotoxicity. Resulting in the antimalarial activities, PN3>PN4>PN2 (27.69>115.05>276.03 μM), ON2>ON4>ON3 (50>53.16>59.06 μM)($P < 0.05$). There was noticeable antimalarial activity observed when there was a substitution at position 7, or shortening of the chain, as with MN4>MN2>MN3 (56.21>113.47>260.4 μM). Against the human HEK293 cells, the intermediates of synthesis with nitro-substitutions also displayed no clear or apparent patterns in their toxicity. PN3 had an IC_{50} value of 18.59 μM, which was significantly toxic compared with PN2 and PN4 ($P < 0.0001$). While there was no significant difference between ON2, ON3 and ON4, as well as between MN 4 and MN2 ($P = 0.429$).

MN3 was the least toxic of the group with an IC_{50} value of 1495.43 µM. The lower the index, the greater the toxicity of the derivatives or less effect the derivative had on the viability of the malaria parasite (Table 4.3). The nitro 4-hydroxyquinolines and its intermediates were generally more toxic than the dialkylamino 4-hydroxquinolines.

In general, the addition of a HCl salt to the 6-, 7- and 8-substituted dialkylamino-4-hydroxyquinolines increased the antimalarial activities; where 6-substituted compounds (PN6S and 8S) possessed the most noticeable increase in antimalarial activity, while the 7-substituted compounds (MN6S-8S) displayed decreased antimalarial activity (Table 4.3). The addition of a HCl salt to the N,N-diethylamino-4-hydroxyquinolines in all three substitution positions decreased antimalarial activity. The same trend of increased toxicity could be observed across the board, with the only exception being the 6-substituted-N,N -diebutylamino-4-hydroxyquinolines which showed a sharp decrease in toxicity (Table 4.3).

There was no correlation between the calculated pKa (ionisation constant of acids or bases) and antimalarial activities of both dialkylamino 4 hydroxyquinolines and the 4-hydroxyquinoline intermediates of synthesis (van Dyk, 2001). Whilst, there was a poor correlation between the calculated log P (1-octanol-water partition coefficient which is an indicator of the lipophilicity of the compound) and the antimalarial activity for the dialkylamino 4-hydroxyquinolines (r^2 = 0.427) and similarly there was no correlation between the calculated log P and the antimalarial activity for the 4-hydroxyquinoline intermediates of synthesis (r^2 = 0.287) (van Dyk, 2001).

4.6.2.3 Dehydrogenase inhibition by 4-hydroxyquinoline derivatives

In order to elucidate a possible mechanism of action for 4-hydroxyquinoline derivatives, the structure-activity relationships were extensively studied using irreversible enzyme inhibitors against glutamate dehydrogenase, lactate dehydrogenase, malate dehydrogenase and glyceraldehyde phosphate dehydrogenase (Baker and Bramhall, 1972a; Baker and Bramhall, 1972b; Baker and Bramhall, 1972c; Baker and Bramhall, 1972d). Baker and Bramhall (1972b) demonstrated that increasing the hydrocarbon chain length would in general increase the inhibitory activities of dehydrogenases; while a chloro-substitution at C8 and increased hydrocarbon chain lengths would greatly increase the inhibition of dehydrogenase (Baker and Bramhall, 1972c). Increasing in the hydrocarbon aralkyl length increased the hydrophobicity of the derivatives, and hence increased their hydrophobic

bonding against the dehydrogenase enzymes tested (Baker and Bramhall, 1972b; Baker and Bramhall, 1972c). A phenylethyl series at C5 were synthesized with a chloro-substitution at C8 on the 4-hydroxyquinoline-3-carboxylic acid back bone by Baker and Bramhall (1972d). It was found that chloro- insertions into the phenylethyl chain increased activity against both glutamate dehydrogenase and malate dehydrogenase and the positions of the chloro-insertion also contributed to the inhibitory effect on the enzyme activities.

4.6.2.4 Anti-oxidant activities

The antimalarial activities of the 4-hydroxyquinoline derivatives may be linked to their anti-oxidant properties. The anti-oxidative and pro-oxidative effects of the 4-hydroxyquinoline derivatives were investigated by Liu *et al*. (2002), where in combination with α-tocopherol were able to inhibit 2,2'-azobis(2-amidinopropane hydrochloride) (APPH)-induced haemolysis. APPH generated free radicals that attacked the RBC membrane to induce lipid peroxidation resulting in haemolysis. It was found that the derivatives packaged in dipalmitoyl phosphatidylcholine (DPPC) played a pro-oxidative role due to the electron-attracting groups, such as the $COOC_2H_5$ and COOH at the *ortho* (7) position to the phenolic group, making the radicals unstable and function as pro-oxidants.

Neethling (2010) studied select 4-hydroxyquinolines (van Dyk, 2001) for their anti-oxidant properties as part of their neuroprotective effects. It was found that a position 6 substitution possessed better peroxyl radical scavenging capacity, whilst at position 7, the iron reducing properties were improved. An amino substitution had better activity than dibuthylamino- and nitro- substitutions at the same position. For superoxide anion scavenging, a nitro- substitution at position 7 was more active *in vitro* than dibuthylamino- and amino-substitutions. However, this latter activity was observed in *in vivo* studies for the MN4. Instead, the dibuthylamino-derivative (MN6) possessed better superoxide anion scavenging activities than MN4. The *in vivo* anti-oxidant activities of MN6 were independent of monoamine oxidase activity. The difference between the *in vitro* and *in vivo* effects were due to the increased lipophilicity of the dibuthylamino derivatives, which would allow these derivatives to readily cross the blood brain barrier to improve neurological function. For protection against lipid peroxidation, the 6-substituted hydroxyquinolines demonstrated more activity than the 7-substituted derivatives. Similarly, the dibuthylamino-substitution was more active than amino- and nitro-substitutions. MN6 was the most active in the *in vivo*

study inhibiting lipid peroxidation, due to its increased lipophilicity and ability to cross the blood brain barrier (Neethling, 2010).

In a study investigating 4-hydroxyl-3-methyl-2-alkylquinolones, it was found that its antibiotic actions against *Staphylococcus aureus* and *Candida albicans* could have been due to inhibition of the mitochondrial cytochrome *bc*1 complex, thereby affecting the electron transport chain and ultimately respiration (Kunz and Konstantinov, 1983; Curtis and Sperandio, 2001). Similarly to the antistaphylococcal actions of 2-heptyl-4-hydroxyquinoline-*N*-oxide, it was proposed that this 4-hydroxyquinoline could potentially target the four enzyme complexes located in the inner mitochondrial membranes in the *Plasmodium* species; namely, NADH:ubiquinone oxidoreductase (complex I), succinate:unbiquinone oxidoreductase (complex II or succinate dehydrogenase) ubiquinol:cytochrome *c* oxidoreductase (complex III or cytochrome bc_1) and cytochrome *c* oxidase (complex IV) (Mather *et al*., 2007).

4.6.2.5 5-Lipoxygenase inhibition by 4-hydroxyquinolines

An additional mechanism of action described for 4-hydroxyquinoline derivatives was that reported for 2-heptyl-4-hydroxyquinoline-*N*-oxide (isolated from *Pseudomonas methanica* KY4634) which was found to be a potent and selective inhibitor of 5-lipoxygenase (Kitamura *et al*., 1986). In addition, Machan *et al.* (1992) reported that the 2-heptyl-4-hydroxyquinoline-*N*-oxide isolated from *Pseudomonas aeruginosa*, was an antistaphylococcal agent. The alkyl hydroxyquinoline-*N*-oxides structurally resembled the quinolone antibiotics (ciprofloxacin and norfloxacin) which are known to inhibit DNA gyrase in both Gram-positive and Gram-negative bacteria (Hooper and Wolfson, 1991).

4.6.2.6 Cytotoxic and anticancer properties

The 4-hydroxyquinolines were found to possess variable cytotoxic activity to the human epithelial (HEK293) cells (IC_{50} range: 18.6 – 5695.7 µM) (van Dyk, 2001), with two compounds displaying highly favourable safety indexes of >100, namely ON6 (100.6) and PN8S (136.5) (Table 4.3). The structural differences between PN8S and OM8S/MN8S resulted in an eleven- and nine-fold difference in antimalarial and cytotoxic activity.

It has long been established that compounds of the thiosemicarbazones class exhibit strong antiproliferative activity (Yu *et al*., 2009; Lessa *et al.*, 2010). Their ability to chelate

metal ions depends on the presence of a N,N,S tridentate “soft donor” coordination system, which allows the thiosemicarbazone ligands to bind not only Fe, but also Cu, Zn, and other transition metals. Although their ability to chelate metal ions is known, the implication it has on the anticancer activity of these compounds is not clear; but could be related to their redox activity (Yu *et al*., 2002).

The anticancer potential of thiosemicarbazones came to the fore when 3-aminopyridine-2-carboxaldehyde thiosemicarbazone went into clinical trials, but during Phase I trials there were concerns over the toxicity of the compound where there was an unacceptably high incidence of grade 4 leukopenia (Yu *et al*., 2002).

In contrast, Mai *et al*. (2009) demonstrated that a series of 3-carboxylate-4-hydroxyquinolines and 4-hydroxy-3-quinolincarboxylic acids possessed selective inhibition towards the members of the p300/CBP family of histone acetyltransferases in the leukemic U937 cell line where induction of apoptosis and inhibition of granulocytic differentiation was noted.

2-Acetylpyridine thiosemicarbazones were reported to be highly cytotoxic against RT2 (IC_{50}: 1.4 - 24 nM) and T98 (IC_{50}: 1.0 - 50 nM) glioma cells; but presented with haemolytic activity with IC_{50} >10 mM, indicating a very good therapeutic index. The mechanism of action of α(N)-heterocyclic thiosemicarbazones was proposed to involve inhibition of ribonucleoside diphosphate reductase, a rate-limiting enzyme in DNA syntheses, which catalyzes the conversion of ribonucleotides into desoxiribonucleotides. Thiosemicarbazones have also been observed to activate apoptotic cell death pathways by mechanisms that were both dependent and independent of p53, and could probably recruit more than one pathway to trigger cell death (Lessa *et al.*, 2010).

Overall, the thiosemicarbazones show potential as antimalarial agents, however their chemical structures play a defining role between them being cytotoxic or safe for use. This base structure does warrant further investigation.

4.7 Summary

4.7.1 8-Hydroxyquinolines

- did not possess any β-haematin formation inhibition activity.
- possessed iron chelation properties as demonstrated by Albert *et al.* (1953) and Scheibel and Adler (1980).

- possessed low percentage haemolysis at 100 μM, however the toxic effects against human kidney epithelial cells could be due to the ion chelation properties and interaction with labile enzymes.

4.7.2 4-Hydroxyquinolines

- possessed negligible activities against β-haematin formation inhibition.
- PN8S displayed favourable activities for further study, namely promising antimalarial activity (IC_{50}: 2.92 μM), low cytotoxicity (IC_{50}: 398.3 μM) which resulted in the highest safety index of 136.5.
- PNS8S was the most active to inhibit β-haematin formation, but the primary mechanism of action is possibly related to its metal chelating abilities.

Chapter 5

Chalcones and Thiosemicarbazones

5.1 Introduction

5.1.1 Chalcones

The chalcone or 1,3-diphenyl-2-propen-1-one group of compounds are aromatic ketones which are the precursors for a variety of biological compounds, including one of the major classes of natural products of the flavonoid family. Chemically, chalcones consist of open-chain flavonoids in which the two aromatic rings are joined by a three-carbon α, β-unsaturated carbonyl system (Figure 5.1) (Nowakowska, 2007). Chalcones are small, non-chiral molecules with relative high lipophilicity (log *P* = 5 – 7) (Sisodia *et al*., 2012).

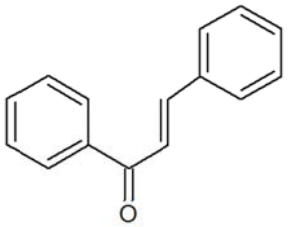


Figure 5.1 The chemical structure of chalcone (1,3-diphenyl-2-propen-1-one) (Nowakowska, 2007).

Chalcone derivatives have been found to possess many pharmacological properties, including anti-inflammatory (Hsieh *et al.,* 1998), immunomodulatory (Barfod *et al.* 2002), anticancer (Kumar *et al.,* 2003; Ducki *et al*., 1998), and antiviral activities (Nowakowska, 2007). The mechanisms of the anti-inflammatory activity of the chalcone derivatives were proposed to be due to the inhibitory or suppression effects on the activation of and/or degranulation of the mast cells and the neutrophils. It was also proposed to block the actions of histamine and 5-hydroxytryptamine, in a similar way to that of aspirin and indomethacin (Hsieh *et al.*, 1998). The immunomodulatory effects of licochalcone A, an oxygenated chalcone and its synthetic analogues were examined by Barfod *et al.* (2002) against pro- and anti-inflammatory cytokines from monocytes and T-cells. Both pro- and anti-inflammatory cytokines such as TNF-α, IL-1, IL-6 and IL-10 secretions were down regulated in a dose-dependent manner, in a similar manner to the antimalarial drug chloroquine (Karres *et al.,* 1998).

Kumar *et al*. (2003) demonstrated that a series of synthetic boronic-chalcone analogues, possessed selective effectiveness against breast cancer cells (MDA-MB-231, wtMCF7 and MDA-MB-435) compared to normal breast epithelial cell lines (MCF-10A and MCF-12A) as a consequence of p53-induced apoptosis. Against the K562 human chronic myelogenous leukaemia cell line, the (E)-1-(4"-hydroxyphenyl)but-1-en-3-one derivatives have an antimitotic activity by preventing the polymerisation of tubulin (Ducki *et al*., 1998).

Wang *et al.* (2004) demonstrated that xanthohumol, a prenylchalcone flavonoid purified from hops (*Humulus lupulus*) inhibited the human immunodeficiency virus (HIV-1) induced cytopathic effects and reverse transcriptase in C8166 lymphocytes and has also been shown to possess some inhibitory activity against ten other viruses including hepatitis B and *Herpes simplex* (type 1 and 2) (Buckwold *et al*., 2004). Licochalcones A and B and tetrahydroxy-methoxychalcone (3,3',4,4'-terahydroxy-2-methoxychalcone) were found to suppress 12-*o*-tetra-decanoyl phorbol-13-acetate-induced HIV promoter activity (Uchiumi *et al*., 2003). Thus selected chalcone-based structures could provide good templates for more effective novel anti-viral compounds.

There have been numerous chalcone derivatives, extracts, purified or synthesised compounds screened against the malaria parasite which warranted further study into additional novel chalcone derivatives. Table 5.1 summarises some of the research based on the chalcone chemical structure against different chloroquine-sensitive and chloroquine-resistant strains of the *P. falciparum* parasites.

Table 5.1 Antimalarial activities of chalcones.

Chalcones	***P. falciparum* strain(s) (IC_{50}: µM)**	**References**
2',3',4'-Trimethoxy, 2',4'-dimethoxy, 4'-methoxy, 4'-ethoxy, 2',4'-dihydroxy, and 4'-hydroxy on the B ring	K1 (2.1–600.0)	Lui *et al.* (2001)
5-Prenylbutein, licoagrochalcone A, homobutein	D6 (10.3–15.0); W2 (11.2–16.1)	Yenesew *et al.* (2004)
2,4-Dimethoxy-4'-butoxychalcone	3D7 (8.9); Dd2 (14.8)	Chen *et al.* (1997)
Suphonamide chalcones	W2 (1.0)	Domínguez *et al.* (2005a)
4'-*tert*-butylo-4-bromochalcone	HB3 (37); Dd2 (27)	Soulère *et al.* (2003)
Licochalcone A derivatives	3D7 *E*-isomer (2.2-15.1 µg/ml); *Z*-isomer (35 & >100 µg/ml)	Larsen *et al*. (2005)
Prenylated chalcone derivatives	poW (8.2-42.4) Dd2 (10.7-92.1)	Frölich *et al*. (2005)

5.1.2 Thiosemicarbazones

Semicarbazones, in organic chemistry, are usually synthesised by the condensation reaction between a ketone or aldehyde and semicarbazide. Thiosemicarbazone is an analog of a semicarbazone, which contains a sulphur atom in place of the oxygen atom (Figure 5.2).

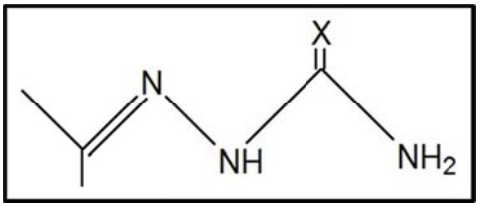


Figure 5.2 General structure of semicarbazones (X = O) and thiosemicarbazones (X = S).

Thiosemicarbazones possess many biological properties such as their therapeutic activities against viral infection (Boon, 1997; Shipman *et al.,* 1986; Beraldo and Gaminob, 2004), bacteria (Dobek *et al*, 1980; Dobek *et al.,* 1983; Beraldo and Gaminob, 2004), cancer, (Scovill *et al.,* 1982; Beraldo and Gaminob, 2004; Liberta and West, 1992), amoebiasis (Abid and Azam, 2005) and parasitic activities (Greenbaum *et al.,* 2004).

Thiosemicarbazones have also been exclusively studied *in vivo* and *in vitro*, in both chloroquine-sensitive and chloroquine-resistant strains of the *Plasmodium* parasites. Table 5.2 summerises some of the antimalarial activities of the thiosemicarbazone derivatives.

Based on the antimalarial activities of previously investigated thiosemicarbazone derivatives (Table 5.2), this study used thiosemicarbazone as the base structure for a set of novel derivatives, which were proposed to target the malaria parasites *in vitro*, as well as explore a preliminary mechanism of action of the derivatives.

5.2 Aims

The antimalarial activities of the chalcone derivatives (1-N-substituted thiocarbamoyl-3,5-diphenyl-2-pyrazolines and the palladium (II) complexes of 1-N-substituted thiocarbamoyl-3,5-diphenyl-2-pyrazolines) and the thiosemicarbazones derivatives (1-N-substituted cyclised pyrazoline analogues of thiosemicarbazones) were examined against the chloroquine-resistant strain (FCR-3) of the malaria parasite. The cytotoxicity activities of the derivatives were examined against the HEK293 and the activity of the derivatives against the formation of β-haematin formation was investigated as their possible mechanism of action.

Table 5.2 Antimalarial activities of thiosemicarbazones.

Thiosemicarbazones	*P. falciparum* strain(s) (IC_{50}: µM)	References
2-Acetylpyridine thiosemicarbazones	Smith strain* (1.7 – 37 ng/ml) Camp strain** (0.65 – 29 ng/ml)	Lambros *et al.* (1982)
Thiosemicarbazone cysteine protease inhibitors	W2-strain (0.03 – 9.9) Targeting falcipain-2 protease.	Greenbaum *et al*. (2004)
Thiosemicarbazone and ferroquine hybrid	3D7 (0.1 – 64.2) W2 (1.3 – 117.8) FCR-3 (0.2 – 74.0) Bre1 (0.3 – 46.0) Targeting falcipain-2 protease.	Biot *et al*. (2007)
Aroylhydrazone and thiosemicarbazone	3D7 (3 – 39) 7G8 (2.5 – 15) Acting as an iron chelators.	Walcourt *et al*. (2004)
Phenolic Mannich bases of benzaldehyde and (thio)semicarbazone	W2 (0.077 – 3.75) Targeting falcipain-2 protease.	Chipeleme *et al.* (2007)
Aminoquinoline thiosemicarbazone	D10 (0.79 – 1.37) K1 (0.054 – 0.71) W2 (0.051 – 1.23) Targeting falcipain-2 protease.	Chiyanzu *et al.* (2005)

*Smith strain is the multi-drug-resistant CQ IC_{50} = 60 ng/ml; **Camp strain is chloroquine-sensitive and pyrimethamine-resistant CQ IC_{50} = 7.6 ng/ml.

5.2.1 Objectives

- Evaluate the effectiveness of 1-N-substituted thiocarbamoyl-3,5-diphenyl-2-pyrazolines derivatives and their palladium (II) complexes and 1-N-substituted cyclised pyrazoline analogues of thiosemicarbazones in inhibiting *in vitro* β-haematin formation in comparison to chloroquine and quinine.
- Correlate the β-haematin inhibitory activity to their *in vitro* inhibitory effects against *P. falciparum*.
- Assess possible toxic properties against a human kidney epithelial cell line and human RBCs.

5.3 Methodology

5.3.1 Chalcone derivatives

The 1-N-substituted thiocarbamoyl-3,5-diphenyl-2-pyrazolines (Table 5.3) and the palladium (II) complexes of 1-N-substituted thiocarbamoyl-3,5-diphenyl-2-pyrazolines were synthesised and characterised by Professor Amir Azam (Jamia Millia Islamia, New Delhi, India, Budakoti *et al.*, 2006; Abid and Azam, 2005; Abid *et al.,* 2009). All the derivatives were dissolved in DMSO and stored at -20^{o}C until use (Section 2.7.2).

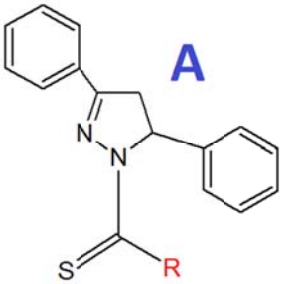
5.3.2 Thiosemicarbazone derivatives

The 1-N-substituted cyclised pyrazoline analogues of thiosemicarbazones (Table 5.4) were synthesized by Professor Amir Azam (Jamia Millia Islamia, New Delhi, India; Budakoti *et al.*, 2006; Abid and Azam, 2005 and Abid *et al.,* 2009). All the derivatives were dissolved in DMSO and stored at -20^{o}C until use (Section 2.7.2). The compounds have two side groups, namely $\mathbf{R_1}$ and $\mathbf{R_2}$. For the acetophenone A-series (designated "A"), $\mathbf{R_1}$ = H, and for the bromoacetophenone B-series (designated "B"), $\mathbf{R_1}$ = Br (Table 5.4).

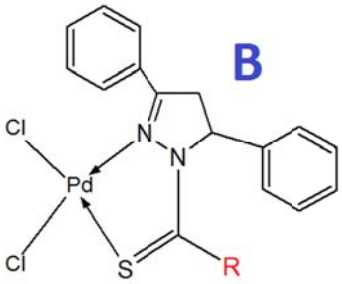
5.3.3 Pharmacological assays and analysis

Chloroquine and quinine were used as positive controls against the *in vitro* malaria parasites (Section 2.7). Chloroquine was the positive control in the β-haematin inhibition assay (section 2.4.3) and quinine was used as the positive control for the MTT cytotoxicity activity assay against the HEK293 cells (Section 2.9.6) and the selectivity index determined (Section 2.9.7). Each compound was tested in triplicate wells per experiment and at least three independent experiments were conducted to determine the final % activity or IC_{50} value. The Mann-Whitney U-test was performed to determine the statistical differences/similarities between the compounds and the positive controls, where a p value of ≤0.05 was considered significant (Section 2.12). Combination assays (Section 2.5) were performed for the most active thiosemicarbazone derivative in the tritiated hypoxanthine incorporation assay, combining with chloroquine and quinine to determine its combined effect against the whole parasites.

Table 5.3 The chalcone derivatives with their R-side groups and their chemical descriptions.



1-N-substituted thiocarbamoyl-3,5-diphenyl-2-pyrazolines base



Palladium complexes of the 1-N-substituted thiocarbamoyl-3,5-diphenyl-2-pyrazolines

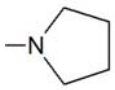
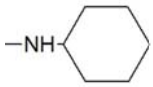
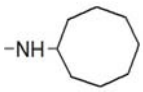
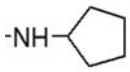
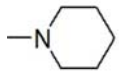
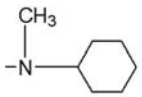
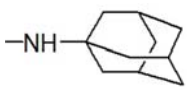
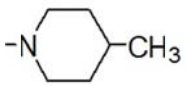
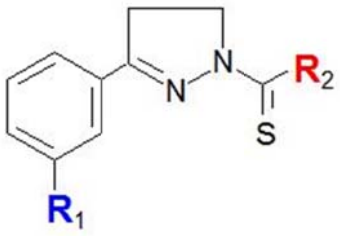
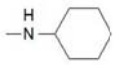
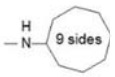
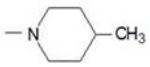
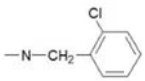
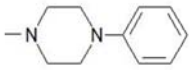
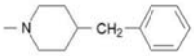
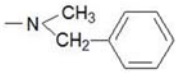
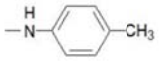
Derivative designation	Compound base	R-side group	Chemical description
CA-1	**A**		*1–(N-amino)thiocarbamoyl 3,5-diphenyl-2-pyrazoline*
M-1	**B**		*[Palladium{(1-N-amino)thiocarbamoyl–3,5-diphenyi–2-pyrazoline}chloride]*
CA-4	**A**		*1–(N-pyrrolidine)thiocarbamoyl 3,5-diphenyl-2-pyrazoline*
M-4	**B**		*[Palladium{(1-N-pyrrolidine)thiocarbamoyl–3,5-diphenyi–2-pyrazoline}chloride]*
CA-5	**A**		*1-(N-cyclohexyl)-thiocarbamoyl-3,5-diphenyl-2-pyrazoline*
M-5	**B**		*[Palladium{(1-N-cyclohexyl)-thiocarbamoyl-3,5-diphenyl-2-pyrazoline}chloride]*
CA-6	**A**		*1-(N-cyclooctyl)-thiocarbamoyl–3,5–diphenyl–2-pyrazoline*
M-6	**B**		*[Palladium(1-N-cyclooctyl)–thiocarbamoyl-3,5-diphenyl-2-pyrazoline)chloride]*
CA-7	**A**		*1-(N-cyclopentyl)-thiocarbamoyl-3,5-diphenyl-2-pyrazoline*
M-7	**B**		*[Palladium{(1-N-cyclopentyl)-thiocarbamoyl-3,5-diphenyl-2-pyrazoline}chloride]*
CA-8	**A**		*1-(N-adamantylamine)-thiocarbamoyl-3,5-diphenyl-2-pyrazoline*
M-8	**B**		*[Palladium{(1-N-piperidine)-thiocarbamoyl-3,5-diphenyl-2-pyrazoline}chloride]*
CA-9	**A**		*1-(N-hexamethylineimine)-1-thiocarbamoyl-3,5-diphenyl-2-pyrazolin*
M-9	**B**		*[Palladium{(1-N-hexamethylenimine)thiocarbamoyl-3,5-diphenyl-2-pyrazoline} chloride]*
CA-10	**A**		*1-(N-adamantylamine)-thiocarbamoyl-3,5-diphenyl-2-pyrazoline*
M-10	**B**		*[Palladium{(1-N-adamantylamine)thiocarbamoyl-3-5-diphenyl-2-pyrazoline} chloride]*
CA-13	**A**		*1-(N-methyl cyclohexyl)-1-thiocarbamoyl 3,5-diphenyl-2-pyrazoline*
M-13	**B**		*[Palladium{(1-N-methylcyclohexylamine) thiocarbamoyl-3,5-diphenyl–pyrazoline} chloride]*

Table 5.4 The 1-N-substituted thiocarbamoyl-3-phenyl-2-pyrazolines base structure with the various R-side groups and chemical descriptions.



R1: A= -H, B= -Br

Derivative designation		R_2-group	Chemical description
1	A		*N-cyclohexyl-3-phenyl-4,5-dihydro-1H-pyrazole-1-thiocarboxamide*
	B		*3-(3-Bromophenyl)-N-cyclohexyl-4,5-dihydro-1H-pyrazole-1-thiocarboxamide*
2	A		*N-cyclooctyl-3-phenyl-4,5-dihydro-1H-pyrazole-1-thiocarboxamide*
	B		*3-(3-Bromophenyl)-N-cyclooctyl-4,5-dihydro-1H-pyrazole-1-thiocarboxamide*
3	A		*N-cyclopentyl-3-phenyl-4,5-dihydro-1H-pyrazole-1-thiocarboxamide*
	B		*3-(3-Bromophenyl)-N-cyclopentyl-4,5-dihydro-1H-pyrazole-1-thiocarboxamide*
4	A		*4-Methyl-1-[(3-phenyl-4,5-dihydro-1H-pyrazol-1-yl)thiocarbamoyl]piperidine*
	B		*1-{[3-(3-Bromophenyl)-4,5-dihydro-1H-pyrazol-1-yl]thiocarbamoyl}-4-methyl piperidine*
5	A		*N-amino-4,5-dihydro-1H-pyrazole-1-thiocarboxamide*
	B		*N-amino-3-bromo-4,5-dihydro-1H-pyrazole-1-thiocarboxamide*
6	A		*N-[(2-chlorophenyl)methyl]-3-phenyl-4,5-dihydro-1H-pyrazole-1-thiocarboxamide*
	B		*3-(3-Bromophenyl)-N-[(2-chlorophenyl)methyl]-4,5-dihydro-1H-pyrazole-1-thiocarboxamide*
7	A		*4-Phenyl-1-[(3-phenyl-4,5-dihydro-1H-pyrazol-1-yl)thiocarbamoyl]piperazine*
	B		*1-{[3-(3-Bromophenyl)-4,5-dihydro-1H-pyrazol-1-yl]thiocarbamoyl}-4-phenyl piperazine*
8	A		*1-[(3-Phenyl-4,5-dihydro-1H-pyrazol-1-yl)thiocarbamoyl]-4-(phenylmethyl)- piperazine*
	B		*1-{[3-(3-Bromophenyl)-4,5-dihydro-1H-pyrazol-1-yl]thiocarbamoyl}-4-(phenyl methyl)piperazine*
9	A		*N-Benzyl-N-methyl-3-phenyl-4,5-dihydro-1H-pyrazole-1-carbothioamide*
	B		*N-Benzyl-3-(3-bromophenyl)-N-methyl-4,5-dihydro-1H-pyrazole-1-carbothioamide*
10	A		*3-Phenyl-N-p-tolyl-4,5-dihydro-1H-pyrazole-1-carbothioamide*
	B		*3-(3-Bromophenyl)-N-p-tolyl-4,5-dihydro-1H-pyrazole-1-carbothioamide*
11	A		*3-Phenyl-N-o-tolyl-4,5-dihydro-1Hpyrazole-1-carbothioamide*
	B		*3-(3-Bromophenyl)-N-o-tolyl-4,5-dihydro-1H-pyrazole-1-carbothioamide*

5.4 Results

5.4.1 Chalcone derivatives

5.4.1.1 Antimalarial, cytotoxic and β-haematin formation inhibitory properties

The results for the antimalarial, cytotoxic and β-haematin formation inhibition activities of the 1-N-substituted thiocarbamoyl-3,5-diphenyl-2-pyrazolines derivatives and their palladium (II) complexes are listed in Table 5.5. Palladium (II) alone was found to exhibit neither antimalarial activity at 100 µM (100.00 ± 5.50% parasite growth) nor cell toxicity at 50 µM (99.40 ± 5.50% cell viability). Palladium [IC_{50}: 0.21±0.01 µM] exhibited β-haematin formation inhibitory activity that was 9-fold less effective than chloroquine [IC_{50}: 23.03±8.33 µM].

Table 5.5 The pharmacological activities of the 1-N-substituted thiocarbamoyl-3,5-diphenyl-2-pyrazolines derivatives and their palladium (II) complexes.

Derivative designation	Antimalarial Activity IC_{50}±s.d. (µM)	Cytotoxicity IC_{50}±s.d. (µM) [% cell viability ± s.d. at 50 µM]	Safety index	Inhibition of β-haematin formation IC_{50}±s.d. (µM) [% inhibition ± s.d. at 1:1 ratio**]
CA-1	**5.46±1.18**	>50 µM [99.20±5.40]	**9.16***	[4.39±1.35]
CA-4	5.99±0.72	>50 µM [108.20±10.80]	8.35*	[14.50±2.77]
CA-5	10.02±1.35	>50 µM [175.10±4.40]	4.99*	[4.260±2.71]
CA-6	10.60±0.99	>50 µM [163.20±13.70]	4.72*	[2.61±1.67]
CA-7	14.21±0.94	>50 µM [187.90±7.90]	3.52*	[7.85±3.79]
CA-8	8.33±0.76	>50 µM [101.30±2.90]	6.01*	[2.01±1.01]
CA-9	6.16±0.44	>50 µM [135.10±7.30]	8.12*	[22.62±3.32]
CA-10	5.57±0.49	>50 µM [106.20±29.60]	8.98*	[26.23±9.20]
CA-13	10.36±0.87	>50 µM [123.40±26.20]	4.83*	[11.15±2.83]
M-1	32.67±5.20	43.99±1.86	1.35	[25.63±5.93]
M-4	21.98±0.57	54.02±3.08	2.46	[27.08±5.40]
M-5	6.32±0.74	18.02±1.09	2.85	**56.08±7.05**
M-6	69.56±8.51	>50 µM [107.80±14.50]	0.72*	186.53±23.36
M-7	**4.49±1.56**	**13.92±1.20**	3.10	313.52±99.90
M-8	14.69±2.07	>50 µM [111.40±5.90]	3.40*	[19.52±5.30]
M-9	6.85±0.70	>50 µM [95.70±4.80]	7.30*	[23.46±2.66]
M-10	15.48±1.08	>50 µM [76.40±11.10]	3.23*	[17.45±2.46]
M-13	6.05±7.62	>50 µM [99.20±6.30]	8.26*	514.76±58.19
Chloroquine	0.116±0.005	243.38±9.77	2098.10	23.03±8.33
Quinine	0.095±0.006	377.00±11.24	3950.13	44.76±4.28

*Safety index calculated using 50 µM as cytotoxicity IC_{50};
**1:1 ratio of Haemin = 191.73 µM.

Some of the Pd^{2+}-complexed M-series, specifically M-5, M-6, M7 and M-13, possessed the ability to inhibit β-haematin formation, where none of their uncomplexed derivatives inhibited β-haematin formation. However, the potency of these active derivatives ranged from 2.4 fold to 22.4 fold less effective when compared with chloroquine. M-5 possessed the best ability to inhibit β-haematin formation with IC_{50} value of 56.08 ± 7.05 µM. There was no correlation between the inhibitory effect on β-haematin formation and intra-erythrocytic growth (r^2 = 0.080, for those derivatives which generated IC_{50} values).

The CA-series derivatives (IC_{50} range: 5.46 – 14.21 µM; mean IC_{50}: 8.52 µM) were generally more effective against the malaria parasites than the M-series derivatives with the exceptions of M-5, M-7 and M-13 (IC_{50} range: 4.49 – 69.56 µM; mean IC_{50}: 19.79 µM) (Table 5.5). When the antimalarial activity of the uncomplexed derivatives was compared to that of the Pd^{2+}-complexed derivatives there was no correlation (r^2 = 0.0035; Figure 5.3); but when the outlying point of derivative CA-6/M-6 was excluded, the r^2 value increased to 0.47. However, all of the chalcone derivatives were 47 to 599 fold less effective than chloroquine and 57 to 732 fold less effective than quinine.

All the CA-series derivatives exhibited no toxicity towards the HEK293 cells (Table 5.5). While M-1, M-4, M-5 and M-7 inhibited cell viability with a potency range from 6 to 27-fold more toxic than quinine, with M-7 being the most toxic. The addition of the Pd^{2+} appears to have increased the toxicity properties of these four Pd^{2+} complexes. All of the derivatives had low safety indices with CA-1 the safest at 9.16 (Table 5.5).

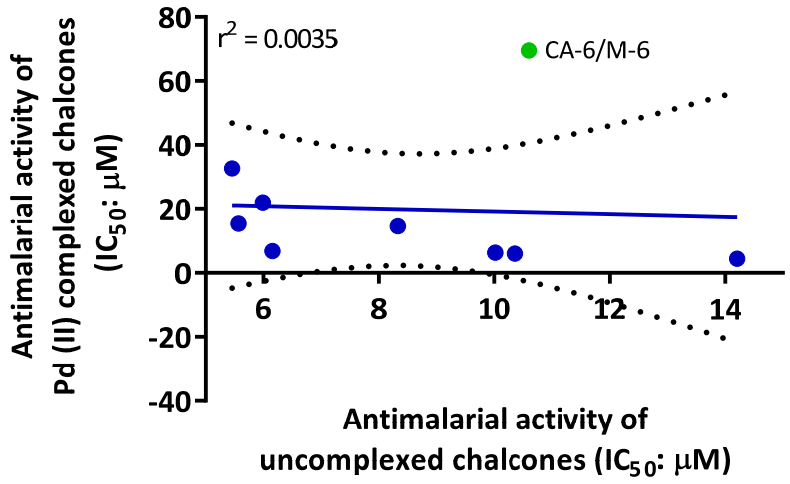


Figure 5.3 Correlation between the antimalarial activity of the uncomplexed derivatives compared to the Pd^{2+}-complexed derivatives.

5.4.1.2 Combination studies

Antimalarial combination studies were performed for quinine and a more active uncomplexed derivative, namely CA-9 and its Pd^{2+}-complex, M-9, which had more favourable safety indices than the most active derivatives. Additive relationships of both CA-9 and M-9 with quinine, CA-9 with the ∑FIC = 0.920 and M-9 with the ∑FIC = 0.985 was observed (Figure 5.4). The combination results indicated that the mechanism of action of the derivatives was not due to β-haematin formation inhibition, but another mechanism that complements the antiplasmodial action of quinine.

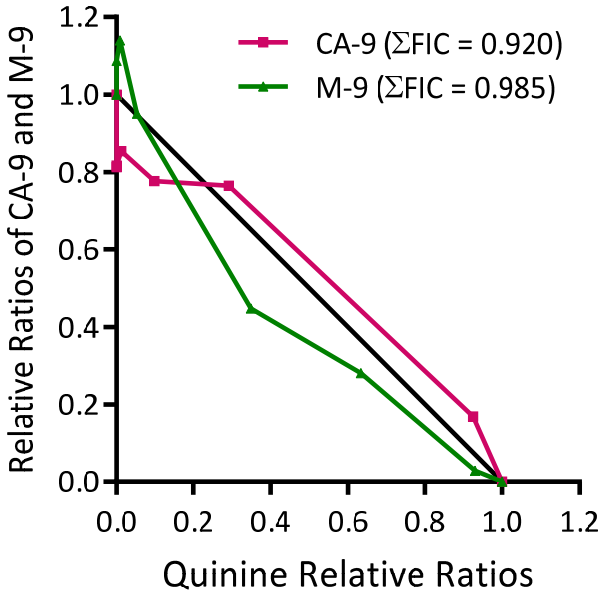


Figure 5.4 The isobologram of quinine in combination with CA-9 and M-9.

5.4.2 Thiosemicarbazone derivatives

5.4.2.1 Antimalarial, cytotoxic and β-haematin formation inhibitory properties

The β-haematin formation inhibitory and antimalarial activity of the 11 thiosemicarbazone derivatives resulted in variable results in micro- and millimolar concentration ranges, where the thiosemicarbazone derivatives possessed no cytotoxic effect on the HEK293 cells at 50 µM (Table 5.6).

The thiosemicarbazones possessed very little β-haematin formation inhibitory activity. The IC_{50} values were in the millimolar range (0.201 to 9.211 mM) which translated to 0.25 to 11.48% as effective as the positive control, chloroquine (IC_{50} 23.03 ± 8.33 µM), which

Table 5.6 The antimalarial activities and β-haematin formation inhibition activities of thiosemicarbazone derivatives.

Derivative designation		Antimalarial Activity IC_{50}±s.d. (μM) [% growth ± s.d. at 50 μM]	Inhibition of β-haematin formation IC_{50}±s.d. (mM) [% inhibition ± s.d. at 1:1 ratio*]	Toxicity profile IC_{50}±s.d. (μM) [% cell viability ± s.d. at 50 μM]	Safety index **
1	A	32.36±7.17	[25.86±5.39]	>50μM [95.81±18.64]	1.55
	B	>50 μM [56.86±8.58%]	[20.25±6.01]	>50μM [102.94±1010]	1.00
2	A	26.27±1.01	[23.75±2.54]	>50μM [102.43±7.04]	1.90
	B	30.39±4.64	1.09±0.24	>50μM [103.57±6.91]	1.65
3	A	>50 μM [56.16±9.00%]	7.41±0.89	>50μM [97.12±28.87]	1.00
	B	44.84±3.53	0.61±0.13	>50μM [110.16±15.54]	1.12
4	A	35.10±3.82	7.25±1.53	>50μM [97.66±20.02]	1.42
	B	27.94±1.02	2.60±0.16	>50μM [97.83±17.88]	1.79
5	A	34.83±0.81	3.30±0.51	>50μM [87.18±12.18]	1.44
	B	29.00±2.50	**0.52±0.05**	>50μM [96.65±12.11]	1.72
6	A	>50 μM [58.73±6.76%]	[21.96±4.27]	>50μM [102.27±16.83]	1.00
	B	**17.14±1.88**	0.52±0.07	>50μM [107.17±11.75]	**2.92**
7	A	46.73±5.46	[27.21±3.55]	>50μM [117.31±3.11]	1.07
	B	18.98±1.59	3.56±0.80	>50μM [107.12±3.62]	2.63
8	A	49.52±8.76	[38.82±4.37]	>50μM [103.64±10.13]	1.01
	B	29.68±0.85	3.71±0.60	>50μM [102.82±7.72]	1.68
9	A	48.55±2.38	[45.66±3.09]	>50μM [106.17±13.93]	1.03
	B	47.44±3.81	1.30±0.22	>50μM [99.11±2.24]	1.05
10	A	43.82±2.32	[33.16±3.03]	>50μM [104.01±19.86]	1.14
	B	>50 μM [60.06±4.74%]	1.67±0.20	>50μM [98.71±7.25]	1.00
11	A	37.48±5.25	[27.13±3.13]	>50μM [98.20±10.10]	1.33
	B	>50 μM [60.81±7.98%]	0.20±0.03	>50μM [112.15±7.65]	1.00
Chloroquine		0.116±0.005	0.023±0.008	243.38±9.77	2098.1
Quinine		0.095±0.006	0.045±0.004	377.00±11.24	3950.1

*1:1 ratio of β-haematin = 191.73 μM;

**Safety index calculated using 50 μM for cytotoxicity IC_{50}

indicated that the mechanism of action of the thiosemicarbazone derivatives did not involve inhibition of β-haematin/haemozoin formation in the malaria parasite. There was no correlation between the inhibitory effect on β-haematin formation and intra-erythrocytic growth (r^2 = 0.0009, for those compounds which generated IC_{50} values) (Figure 5.5).

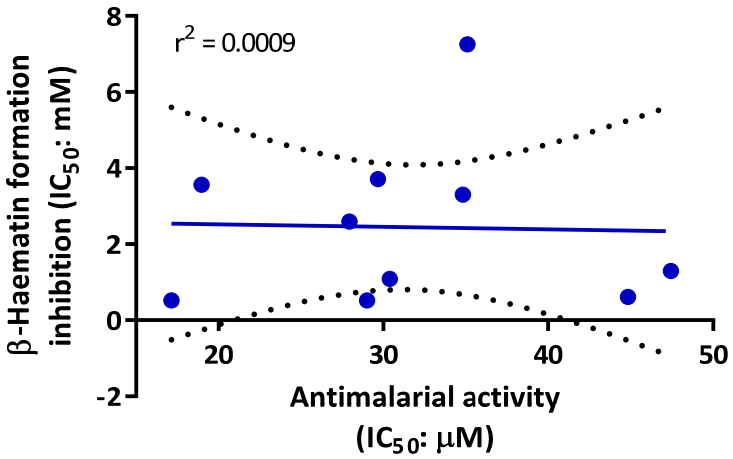


Figure 5.5 Correlation between the inhibitory effects of the thiosemicarbazones on β-haematin formation and antimalarial activity.

The acetophenones had antimalarial activity IC_{50} values within the range of 26.27 to 49.52 μM, while the IC_{50} values of the bromoacetophenones ranged between 17.14 to 47.44 μM. When the antimalarial activity of the acetophenones was compared to that of the bromoacetophenones there was no correlation (r^2 = 0.0035; Figure 5.3), indicating that the halogen did not contribute to the antimalarial property of these derivatives. In comparison to quinine, these two set of derivatives were between 180 to 521 fold less active (Table 5.6).

5.4.2.2 Combination studies

Antimalarial combination studies were performed for the most active of the bromoacetophenones, 6B and 7B with chloroquine and quinine. Additive relationships were observed between both chloroquine and quinine with 6B with ∑FIC of 0.971 and 0.908, respectively. Additive relationships were observed between both chloroquine and quinine with 7B with ∑FIC of 1.129 and 1.057, respectively (Figure 5.6).

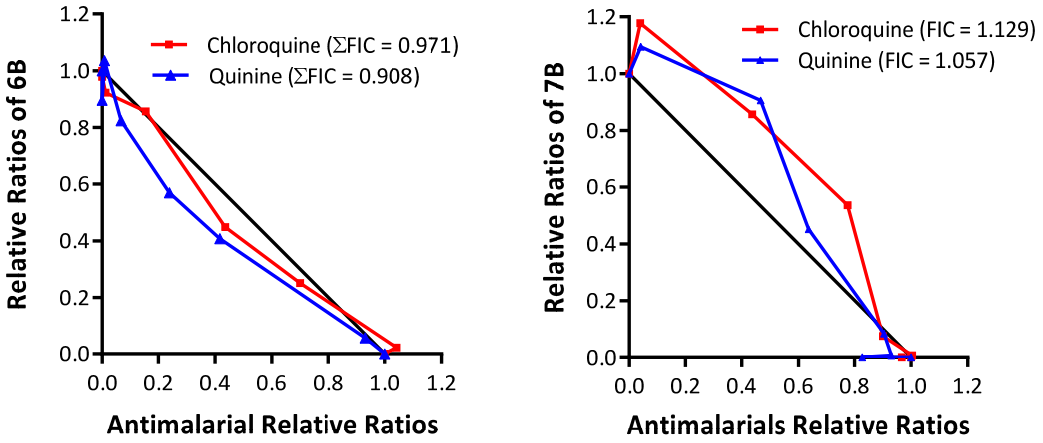


Figure 5.6 The isobolograms of chloroquine and quinine with 6B and 7B of the thiosemicarbazone derivatives.

5.5 Discussion

5.5.1 Chalcone derivatives

Overall, the tested 1-N-substituted thiocarbamoyl-3,5-diphenyl-2-pyrazolines derivatives and their palladium (II) complexes displayed moderate antimalarial activity; which was achieved by a mechanism of action other than inhibition of β-haematin/haemozoin formation (Table 5.5). Domínguez *et al.* (2005a) evaluated the *in vitro* effects of sulfonamide chalcone derivatives against the malaria parasite and β-haematin formation inhibition. The study had found that the aromatic ring of the chalcone moiety possessed minimal β-haematin inhibition activity; while derivatives which were strong basic in nature possessed strong β-haematin inhibition activity and correlated to the antimalarial activities reported. The basic nature of the derivatives enabled them to concentrate in the food vacuole to inhibit haemozoin formation, resembling the mechanism of action of chloroquine (Figure 3.9).

In a study by Guantai *et al.*, (2010), it was reported that there was no strain specificity for the novel triazole-linked chalcone and dienone hybrid derivatives that were evaluated against the chloroquine-sensitive (D10) and -resistant (Dd2) strains. As in this current study, the activities were reported to be in the low to sub micromolar range (IC_{50} values: 0.04 to 19.0 µM), although better activity was achieved with the triazole-linked chalcones (Table 5.5). These triazole-linked chalcones were able to inhibit β-haematin formation with

variable activity (range: 0.2 to 4.8 expressed as IC_{50} equivalents of the drug relative to haematin compared to chloroquine (1.91). The increased activity of these derivatives could also have been due to the azoles which have been reported to inhibit β-haematin formation (Mahlangu *et al*., 2014). Again as in this study there was no correlation between antimalarial activities and β-haematin inhibition activities (Figure 5.3).

A series of enone- and chalcone-chloroquinoline hydrid derivatives (Figure 5.7) were also found to inhibit chloroquine-sensitive (D10) and -resistant (Dd2, W2) strains with a similar potency (0.5 to 3.1 µM), with chloroquine still more active against the parasites (IC_{50} values: 0.017 to 0.097 µM) (Guantai *et al*., 2011). Again the derivatives inhibited β-haematin formation with IC_{50} equivalents between 0.2 and 0.6, which was more active than chloroquine (1.91). The accumulation of the derivatives within the parasite digestive vacuoles was proposed to be due to the presence of chloroquine in the derivative. The ability of the derivatives to inhibit haemozoin formation was proposed to also be due to the presence of the chloroquine molecule and not the chalcone. These enone- and chalcone-chloroquinoline hydrid derivatives were also reported to inhibit the cysteine protease, falcipain-2.

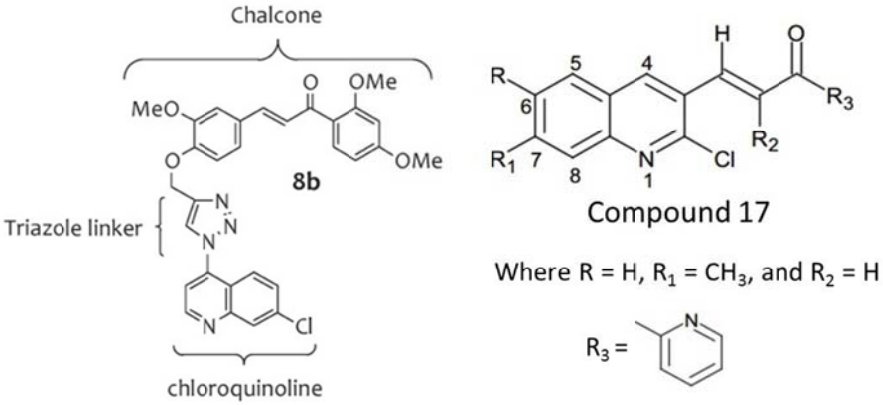


Figure 5.7 Comparative structures of the Guantai (8b) and Hayat chloroquine-chalcone derivatives (Compound 17) (Guantai *et al*., 2011; Hayat *et al*., 2011).

When evaluated against the chloroquine-sensitive 3D7 strain of the malaria parasites, another series of chloroquine-chalcone hybrids (Figure 5.7) synthesised by Hayat *et al*. (2011), were reported to possess antimalarial IC_{50} values between 31.31 to 74.84 µM. Again

the activity was not similar to that of the standard antimalarial, chloroquine (IC_{50} = 0.0065 µM). In contrast to the promising activity reported for the Gauntai-chloroquinoline-based chalcones, the Hayat-derivatives possessed no β-haematin formation inhibitory properties at 50 µM. This indicated that the antimalarial activity was also not via β-haematin formation inhibition as with the chalcone derivative in this study (Table 5.5).

There have been many proposed mechanism of actions for the chalcone derivatives against the malaria parasites, including inhibition of cysteine protease in the trophozoite stage (Li *et al*., 1995). Domínguez *et al.* (2005b) reported that phenylurenyl chalcone derivatives had some activity against the cysteine protease, falcipain-2 and that the inhibitory activity correlated with their antimalarial activities as determined by flow cytometry. Only one derivative had the ability to inhibit haemozoin formation, which was probably due to the aromatic pyridinyl group substitution that may have contributed to its accumulation in the digestive vacuoles of the malaria parasites. Arancibia *et al*. (2013) indicated that the low polarisation of the ketone carbonyl group (due to the positioning of the cyrhetrenyl group) in cyrhetrenyl organometalic chalcone derivatives, permitted the interaction between the derivatives and the amino acids of the catalytic centres of aspartate enzymes and cysteine proteases.

In addition to their inhibitory properties on the latter enzymes, Soulère *et al*. (2003) reported that chalcone-based derivatives inhibited *P. falciparum* superoxide-dismutase activity ranging from 25% to 100% inhibition at 50 µM. However, the three most potent derivatives possessing 100% superoxide-dismutase inhibition (BB29, F12 and SG5281) were inactive against the whole parasite *in vitro;* indicating that either they did not reach the site of action or the parasite was able to cope with increased superoxide radicals via another anti-oxidant pathway (Becker *et al*., 2004).

The World Health Organisation recommends that combination therapy be used when treating malaria parasites in attempts to delay or/and prevent the development of resistance (WHO, 2014). In accordance with this, the combination of quinine and a more active uncomplexed derivative, namely CA-9 and its Pd^{2+}-complex, M-9, were found to possess additive interactions (Figure 5.4). Ideally a synergistic interaction would be preferred, but a similar additive interaction was observed between quinine and the chloroquinoline-based chalcone derivative (Hayat *et al*. (2011). These additive interactions

could possibly have been due to the different, but complementary mechanism of actions of quinine and the test derivatives (other than inhibiting β-haematin formation).

The cytotoxicity of these uncomplexed derivatives were found to be relatively less than their palladium complexes; which were active in the micromolar range (IC_{50}: 13.92 to 54.02 μM) (Table 5.5). The inclusion of palladium increased the cytotoxicity of the uncomplexed derivative. A trend previously observed with the palladium-1-(2-dimethylaminoethyl)-1H-pyrazole derivatives, where the latter not only inhibited *P. falciparum* at micromolar concentrations (10.3 – 133.3 μM), and cancer cells at similar concentrations (16.2 – 38.5 μM) (Quirante *et al*., 2011). Thus indicating relatively no selectivity for the malaria parasite over the human cell, which would not be therapeutically beneficial. It has been reported that palladium compounds possess these antitumor effects due to their ability to bind DNA (Navarro *et al*., 2010), which could theoretically also be possible in the malaria parasite.

Overall the most active derivative, M-7 effectively inhibited the malaria parasite, but it also affected human cell viability with a safety index of only 3.10, which indicates relative non-selective toxicity. Similarly for M-5 which inhibited parasite growth possibly by inhibiting β-haematin formation, did so in a non-specific manner as it also inhibited human cell growth with a safety index of 2.85 (Table 5.5). With such low safety indices and moderate activity, these 1-N-substituted thiocarbamoyl-3,5-diphenyl-2-pyrazolines derivatives and their palladium (II) complexes do not warrant further investigation.

5.5.2 Thiosemicarbazone derivatives

Overall, the 1-N-substituted thiocarbamoyl-3,5-diphenyl-2-pyrazolines derivatives and their palladium (II) complexes were more active than the acetophenones and their bromide complexes (Table 5.5 and 5.6). More of the latter derivatives, especially the bromoacetophenones were able to inhibit β-haematin formation, but not as effectively as chloroquine. The bulkier groups at 1-*N* of the thiocarboxamide enhanced antimalarial activity compared to the other smaller molecules (Table 5.6).

The biological properties of the thiosemicarbazones are often related to metal ion coordination where lipophilicity, which controls the rate of the entry into the cell, is modified by coordination (Farrell, 2002). The metal complex can be more active than the free ligand and the mechanism of action can involve binding of a metal *in vivo* or the metal

complex can be a vehicle for activation of the ligand as the cytotoxic agent (Liberta and West, 1992; Zahra *et al*., 2005). Coordination may lead to significant reduction in drug-resistance (West *et al.,* 1991).

Thiosemicarbazone molecules exist predominantly in the amido form in the solid state, whereas due to the interaction of the solvent molecules, they can exhibit an amido-iminol tautomerism in solution state (Figure 5.8). The amido form acts as a neutral ligand and the iminol form can deprotonate and serve as anionic ligand in metal complexes. Therefore, thiosemicarbazones are versatile ligands in both neutral and anionic forms. Thiosemicarbazones usually react with metallic cations giving complexes in which the thiosemicarbazones behave as chelating ligands. Upon coordination to a metal centre, the delocalisation is further increased through the metal chelate rings. The coordination possibilities are further increased if the substituent has additional donor atoms (Casas *et al*., 2000).

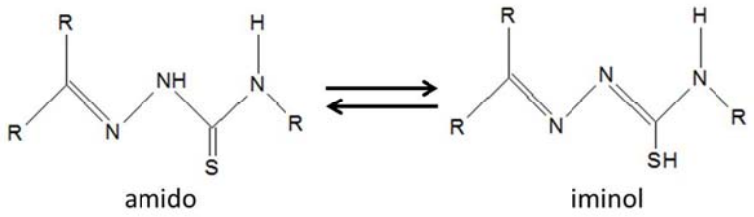


Figure 5.8 Amido-iminol tautomerism of thiosemicarbazone (Casas *et al*., 2000).

The thiosemicarbazones show a variety of coordination modes with transition metals and the coordination mode is influenced by the number and type of substituents as the active donor sites of the ligand vary depending upon the substituents. The thiosemicarbazones can form four possible metal complexes, such as in Figure 5.9 which illustrates the ONS tridentate coordination mode of the thiosemicarbazones (Sreekanth *et al*., 2004).

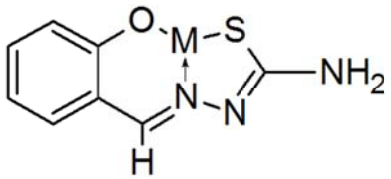


Figure 5.9 The O, N, S-tri-coordination of the thiosemicarbazones (Sreekanth *et al*., 2004).

The different coordination modes of the benzaldehyde thiosemicarbazone can be observed in Figure 5.10, where the C,N,S-tri-coodination and N,S-coordination forms a stable five member chelating ring, while a four-member chelate ring is formed with a N,S donor (Basuli *et al*., 1997).

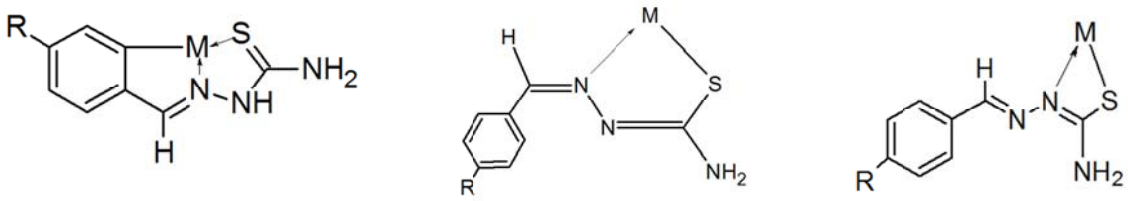


Figure 5.10 The C,N,S-tricoodination, N,S-coordination forming a five member chelating ring and N,S donor formed by a four-member chelating ring (Basuli *et al*., 1997).

Walcourt *et al*. (2004) used these chemical properties of the thiosemicarbazone structure to investigate aroylhydrazone iron chelators against *P. falciparum*. Two iron chelating agents, 2-hydroxy-1-naphthylaldehyde isonicotinoyl hydrazone and 2-hydroxy-1-naphthylaldehyde-4-phenyl-3-thiosemicarbazone where the most active against both chloroquine-sensitive (3D7) and -resistant (7G8) strains and were significantly more active than the ferric ion chelator, desferrioxamine. The high lipophilicity of these chelators was proposed to be critical in terms of the observed activity to ensure optimal entrance into the cell such as to access essential iron-containing intracellular targets, which is vital for inhibiting the growth of the malaria parasite. The target of the iron-chelating thiosemicarbazones was proposed to be the rate-limiting enzyme for DNA synthesis, namely ribonucleotide reductase (Rubin *et al.,* 1993).

Alternative mechanisms of actions for thiosemicarbazone derivatives have been proposed, such as the inhibition of *P. falciparum* cysteine protease falcipain-2 (Greenbaum *et al*., 2004; Chiyanzu *et al*., 2005; Chipeleme *et al*., 2007). However in three studies no conclusive or positive correlation could be found between the inhibition of falcipain-2 and antimalarial activities. Chiyanzu *et al*. (2005) reported that even though the 4-aminoquinoline isatin derivatives possessed antimalarial activities 5 to 6 times more than chloroquine, there was with little to no inhibition of falcipain-2 activity. Similarly, the thiosemicarbazone derivatives of Chipeleme *et al*. (2007) possessed some falcipain-2

inhibition activity, but possessed little to no antimalarial activity. However, with some more manipulation of the thiosemicarbazone structure, two analogues of a structural chimera of thiosemicarbazone and ferroquine analogues were found to exerted falcipain-2 inhibition with comparable antimalarial activities (Biot *et al*., 2007).

For thiosemicarbazones to be therapeutically viable the safety index should be ideally at least 100, if one considers that chloroquine and quinine was 3000 against the human kidney epithelial cells (Table 5.6). However, although there was no inhibition of cell growth at 50 μM, the highest safety index was at least 2.9, which indicated that these acetophenones and their bromide complexes required further structural alterations to improve their cytotoxicity profile. Two iron aroylhydrazone iron chelating agents, 2-hydroxy-1-naphthylaldehyde isonicotinoyl hydrazone and 2-hydroxy-1-naphthylaldehyde-4-phenyl-3-thiosemicarbazone showed high antiproliferative activity against SK-N-MC neuroepithelioma cells (IC_{50}: 0.5-1.5 μM). The antimalarial activity of these aroylhydrazone chelators correlated with the anti-proliferative activity against the neoplastic cells (Lovejoy and Richardson, 2002). As such, the thiosemicarbazones in Lovejoy and Richardson (2002) and Walcourt *et al*. (2004) did not undergo further investigation, and this appears to be the case for those in this study.

Chapter 6

Conclusion

With the prevalence of resistance to standard antimalarial chemotherapeutic agents, new drug targets are being researched as new antimalarial agents to be used in combination. The haemozoin formation pathway is not encoded and unexpressed in the parasite genome and as such is a viable and non-mutatable target for novel drug design (Hänscheid *et al*., 2007).

The first objective was to synthesise and characterise β-haematin, that were chemically and structurally identical to the parasite produced haemozoin (Egan *et al.,* 1994). The crystals were synthesised under acidic condition, similar to that of the digestive vacuoles in the malaria parasites. The synthesised crystals characterised via FTIR with two definitive spectra of 1661.96 and 1208.85 cm^{-1} (Figure 2.1), which were similar to the results produced by Egan *et al.* (1994), Basilico *et al*. (1997) and Slater *et al*. (1991). Scanning electron microscopy was also used to characterise the synthesised β-haematin crystals and compare them with the isolated haemozoin crystals from trophozoite-infected RBCs. Based on the protocol by Pretorius *et al*. (2006), SEM images of β-haematin, haemozoin and haemin crystals (Figure 2.2), revealed that the size, shape and appearance were similar those published by Egan *et al*. (2001) and Sullivan (2002).

Based on the modified methodology of Auparakkitanon *et al.* (2003), under acid conditions (Slater *et al.,* 1991; Egan *et al*., 1994), the β-haematin formation inhibition assay was conducted using microcentrifuge tubes. The β-haematin crystals were pelleted and dissolved in DMSO before being quantified spectrophotometrically at 405 nm. An IC_{50} value was obtained for the positive control, chloroquine (0.134 ± 0.004 mM), which was comparable with the published result of 0.125 mM (Auparakkitanon *et al.*, 2003).

The β-haematin inhibitory activity (BHIA) assay was established based on the modified methods of Parapini *et al*. (2000) and Deharo *et al.* (2002) for the high-throughput drug screening of compounds. Based on the standard curve of the assay (Figure 2.4) and the kinetics of the β-haematin formation (Figure 2.5), the percentage β-haematin recovery for the high-throughput BHIA assay was calculated. When compared with published methodologies, the use of a small starting amount of 0.5 mg/ml haemin in a low buffering-

capacity buffer (0.5 M acetate buffer), resulted in the recovery of 76% haematin from the starting material, as compared with 85% from Parapini *et al*. (2000), 54% recovered by Basilico *et al*. (1998) and 50% by Dorn *et al*. (1998). Once established that the high-throughput assay was viable, the $BHIA_{50}$ (concentration at which 50% of β-haematin formation was inhibited) was calculated for the test compounds from a log sigmoidal dose-response curve (Figure 2.6). The activity of the test compounds to inhibit β-haematin formation was compared to that of the positive control, chloroquine.

Porphyrin chemical structures have been reported to have β-haematin formation inhibition properties (Bascilio *et al.,* 1997), and therefore porphyrin thiosemicarbazide derivatives and corrins, which have similar chemical structures to porphyrins, were evaluated. The derivatives were found to possess varying β-haematin formation inhibitory properties. Of the six porphyrin thiosemicarbazides tested, only **P1** possessed potent β-haematin formation inhibitory activity and was 94% as active as chloroquine (Table 3.1). While all the other corrin derivatives (except for dicyanocobinamide) were able to inhibit β-haematin formation, with aquocobalamin, methylcobalamin and adenosylcobalamin being respectively, 43, 18 and 14 times more active than chloroquine and cyanocobalamin 92% as effectiveness as chloroquine (Figure 3.5). Adenosylcobalamin possessed a synergistic interaction (∑FIC = 0.522) when combined with chloroquine, thereby inhibiting β-haematin formation inhibition in a complementary manner. Whilst an additive interaction was observed when adenosylcobalamin was combined with quinine (∑FIC = 1.020) and mefloquine (∑FIC = 0.893) (Figure 3.7B).

The porphyrins and corrins inhibited the *in vitro* parasites in a micromolar IC_{50} range with P2 and adenosylcobalamin being the most active, with IC_{50} = 4.35 ± 0.08 μM and 2.65 ± 0.50 μM, respectively (Figures 3.4 and 3.5). It was proposed that due to the similarity of their structures with haemin, that they were incorporated into the developing haematin structure as false substrates, thereby destabilising the crystal structure. Adenosylcobalamin displayed additive interactions when combined with pyrimethamine, chloroquine, quinine, primaquine; but possessed an antagonistic interaction when combined with mefloquine (Figure 3.7A).

The 8- and 4-hydroxyquinoline derivatives possessed no ability to inhibit β-haematin formation, with the exception of PN8S which was 14.23% as active as chloroquine (Table 4.4). 8-Hydroquinoline derivatives were active against the *in vitro* malaria parasites with the

amino-substitution at C5 possessing the greatest antimalarial activity, IC_{50} = 0.12 ± 0.01 µM (Table 4.3). The low haemolysis activity combined with activities against the human kidney epithelial HEK293 cells, indicated that 8-hydroxyquinolines' possessed a different mechanism of action against the malarial parasites (Table 4.3). As such iron chelation and free radical scavenging activities were investigated and it was found that 5-amino-8-hydroquinoline was an effective iron chelator and free radical scavenger (Table 4.3 and Figure 4.4).

4-Hydroxyquinolines possessed poor antimalarial activities with PN8S being the most active, but was 29 and 28 times less active than quinine and chloroquine, respectively (van Dyk, 2001; Table 4.4). 4-Hydroxyquinoline derivatives with substitutions at C6 and C7 were investigated for their anti-oxidant properties which included iron reduction, superoxide scavenging and protection against lipid peroxidation (Neethling, 2010). Against the malaria parasite, the nitro-substituted derivatives were more active than the amino- and dibuthylamino-substitutions (Table 4.4). The increase in side-chain length in the dibuthylamino-derivatives increased the lipophilicity, as well as increased their anti-oxidant activity (Neethling, 2010). The exact mechanism of the pharmacological actions of the 4-hydroxyquinolines is still to be determined. However, by using a pharmacophore such as β-glucoside which uses the hexose transporters, this could be used as an effective drug delivery system to optimise the uptake and concentration of the drug in the parasite for treatment of multidrug-resistant malaria (Suzuki *et al*., 2007).

Chalcone derivatives, with and without palladium, possessed micromolar activity against the *in vitro* malaria parasites, and only select metal complexed chalcone derivatives possessed any β-haematin formation activity. The most active being M-5 which possessed 50% of chloroquine's activity against β-haematin formation (Table 5.5). The few metal-complexed chalcone derivatives were active against the HEK293 cells and were 7 to 27 times more toxic when compared with quinine and 4.5 to 17.5 times more toxic when compared with chloroquine (Table 5.5). Additive interactions between CA-9 and M-9 in combination with quinine ((∑FIC = 0.920 and 0.985, respectively) demonstrated that the chalcone derivatives possessed a different mechanism of action against the malaria parasites to that of quinine and did not compete with quinine to inhibit β-haematin formation (Figure 5.4). Chalcone derivatives have been reported to possess inhibitory effects on the cysteine protease falcipain-2 (Domínguez *et al.,* 2005b), while metal complexed chalcones were also

found to be active against cysteine proteases (Arancibia *et al*., 2013). The chalcone-chloroquinoline hybrids were active against both chloroquine-sensitive and –resistant strains of the malaria parasites, with more potent β-haematin formation inhibitory activities than chloroquine (Guantai *et al*., 2011). Future chalcone derivatives should ideally be synthesised as a hybrid compound with and without the metal-complexes to optimise their pharmacological potential.

The thiosemicarbazones derivatives, the acetophenone and the bromoacetophenone series were moderately active against the *in vitro* malaria parasites, and along with their inability to inhibit β-haematin formation, are not lead compounds for further investigations (Table 5.4 and 5.6). However, in combination, 6B and 7B both possessed additive relationships with chloroquine and quinine, meaning their antimalarial action is not competitive binding of the β-haematin subunit crystals or interference with the uptake of the of chloroquine and quinine into the digestive vacuoles. A metal-ion coordination of the thiosemicarbazones (Figures 5.9 and 5.10) would increase lipophilicity of the derivatives and therefore enhance the uptake of the derivative into the target cells (Farrel, 2002) and may also lead to reduction in drug-resistance (West *et al.,* 1991). Thiosemicarbazone derivatives have been tested as iron chelators in the malaria parasites (Walcourt *et al*., 2004), and against *P. falciparum* cysteine protease falcipain-2 (Greenbaum *et al*., 2004; Chiyanzu *et al*., 2005*;* Chipeleme *et al*., 2007). The current acetophenone and the bromoacetophenone series of thiosemicarbazones could form metal-ion complexes to increase its biological activities, as well as other substitutions instead of a bromine molecule should be explored.

Overall the most promising group of compounds to be taken forward are the corrin molecules due to their efficacy in inhibiting β-haematin formation. But their uptake into the malaria parasite needs optimising. This could be facilitated by linking them to a β-glucoside to facilitate the transport of the macromolecules via the hexose transporter system into the parasite. Alternatively they could be encapsulated into peptide-based nanostructures for optimal deliver to the target site within the malaria parasites.

References

Abid M and Azam A. Synthesis and antiamoebic activities of 1-N-substituted cyclised pyrazoline analogues of thiosemicarbazones. Bioorg Med Chem. 2005;13(6):2213-2220.

Abid M, Bhat AR, Athar F *et al*. Synthesis, spectral studies and antiamoebic activity of new 1-N-substituted thiocarbamoyl-3-phenyl-2-pyrazolines. Eur J Med Chem. 2009;44(1):417-425.

Akompong T, Kadekoppala M, Harrison T *et al*. Trans expression of a *Plasmodium falciparum* histidine-rich protein II (*HRPII*) reveals sorting of soluble proteins in the periphery of the host erythrocyte and disrupts transport to the malarial food vacuole. J Biol Chem. 2002;277(32):28923–28933.

Albert A, Gibson MI, Rubbo SD. The influence of chemical constitution on antibacterial activity. VI. The bactericidal action of 8-hydroxyquinoline (oxine). Br J Exp Pathol. 1953;34(2):119-130.

Albert A, Rubbo SD, Goldacre RJ *et al.* The influence of chemical constitution of antibacterial activity; a study of 8-hydroxyquinolin (oxine) and related compounds. Br J Exp Pathol. 1947;28(2):69-87.

Andersson MI and MacGowan AP. Development of the quinolones. J Antimicrob Chemother. 2003;51(S1):1-11.

Andriantsoanirina V, Ménard D, Rabearimanana S *et al*. Association of microsatellite variations of *Plasmodium falciparum* Na^+/H^+ exchanger (*Pfnhe-1*) gene with reduced *in vitro* susceptibility to quinine: lack of confirmation in clinical isolates from Africa. Am J Trop Med Hyg. 2010;82(5):782-787.

Arancibia R, Biot C, Delaney G *et al*. Cyrhetrenyl chalcones: Synthesis, characterization and antimalarial evaluation. J Organomet Chem. 2013;723:143-148.

Assefa H, Kamath S, Buolamwini JK. 3D-QSAR and docking studies on 4-anilinoquinazoline and 4-anilinoquinoline epidermal growth factor receptor (EGFR) tyrosine kinase inhibitors. J Comput Aided Mol Des. 2003;17(8):475–493.

Atamna H and Ginsburg H. Origin of reactive oxygen species in erythrocytes infected with *Plasmodium falciparum*. Mol Biochem Parasitol. 1993;61(2):231-241.

Atamna H and Ginsburg H. The malaria parasite supplies glutathione to its host cell--investigation of glutathione transport and metabolism in human erythrocytes infected with *Plasmodium falciparum*. Eur J Biochem. 1997;250(3):670-679.

Atamna H, Krugliak M, Shalmiev G *et al.* Mode of antimalarial effect of methylene blue and some of its analogues on *Plasmodium falciparum* in culture and their inhibition of *P.*

vinckei petteri and *P. yoelii nigeriensis in vivo*. Biochem Pharmacol. 1996;51(5):693-700.

Auparakkitanon S, Noonpakdee W, Ralph RK, *et al*. Antimalarial 9-anilinoacridine compounds directed at hematin. Antimicro Agents Chemother. 2003;47(12):3708-3712.

Baggish AL and Hill DR. Antiparasitic agent atovaquone. Antimicrob Agents Chemother. 2002;46(5):1163-1173.

Baker BR and Bramhall RR. Irreversible enzyme inhibitors. 189. Inhibition of some dehydrogenases by derivatives of 4-hydroxyquinoline-2and -3-carboxylic acids. J Med Chem. 1972a;15(3):230-233.

Baker BR and Bramhall RR. Irreversible enzyme inhibitors. 191. Hydrophobic bonding to some dehydrogenases by 6-, 7-, or 8-substituted-4-hydroxyquinoline-3-carboxylic acids. J Med Chem. 1972b;15(3):235-237.

Baker BR and Bramhall RR. Irreversible enzyme inhibitors. 192. Hydrophobic bonding to some dehydrogenases with 5-substituted-4-hydroxyquinoline-3-carboxylic acids. J Med Chem. 1972c;15(3):237-241.

Baker BR and Bramhall RR. Irreversible enzyme inhibitors. 194. Hydrophobic bonding to some dehydrogenases by substituted 5-phenylethyl-4-hydroxyquinoline-3-carboxylic acids. J Med Chem. 1972d;15(9):937-940.

Banerjee R and Ragsdale W. The many faces of vitamin B12: catalysis by cobalamin-dependent enzymes. Annu Rev Biochem. 2003;72:209-247.

Banerjee R, Liu J, Beatty W *et al*. Four plasmepsins are active in the *Plasmodium falciparum* food vacuole, including a protease with an active-site histidine. Proc Natl Acad Sci USA. 2002;99(2):990–995.

Banerjee RV and Matthews RG. Cobalamin-dependent methione synthase. FASEB J. 1990;4(5):1450-1459.

Barfod L, Kemp K, Hansen M *et al*. Chalcones from Chinese liquorice inhibit proliferation of T cells and production of cytokines. Int Immunopharmacol. 2002;2(4):545-555.

Basilico N, Monti D, Olliaro P *et al*. Non-iron porphyrins inhibit β-haematin (malaria pigment) polymerisation. FEBS Lett. 1997;409(2):297-299.

Basilico N, Pagani E, Monti D *et al*. A microtiter-based method for measuring the haem polymerization inhibitory activity (HPIA) of antimalarial drugs. J Antimicrob Chemother. 1998;42(1):55-60.

Basuli F, Peng S-M, Bhattacharya S. Steric Control of the Coordination Mode of the Salicylaldehyde Thiosemicarbazone Ligand. Syntheses, Structures, and Redox Properties of

Ruthenium and Osmium Complexes. Inorg Chem. 1997;36(24):5645-5647.

Batzinger RP, Ou SY, Bueding E. Antimutagenic effects of 2(3)-tert-butyl-4-hydroxyanisole and of antimicrobial agents. Cancer Res. 1978;38(12):4478-4485.

Becker K, Tilley L, Vennerstrom JL *et al*. Oxidative stress in malaria parasite-infected erythrocytes: host-parasite interactions. Int J Parasitol. 2004;34(2):163-189.

Begum K, Kim HS, Kumar V *et al*. *In vitro* antimalarial activity of metalloporphyrins against *Plasmodium falciparum*. Parasitol Res. 2003;90(3):221-224.

Bendrat K, Berger BJ, Cerami A. Haem polymerization in malaria. Nature. 1995;378(3553):138–139.

Bennett TL, Kosar AD, Ursos LM *et al*. Membrane Transport in the Malaria-Infected Erythrocyte. Mol Biochem Parasitol. 2004:133(1);99–114.

Beraldo H and Gambino D. The Wide Pharmacological Versatility of Semicarbazones, Thiosemicarbazones and Their Metal Complexes. Mini Rev Med Chem. 2004;4(1):31-39.

Berenbaum MC. A Method for Testing for Synergy with Any Number of Agents. J Infect Dis. 1978;137(2):122-130.

Bernotas RC, Singhaus RR, Kaufman DH *et al*. Biarylether amide quinolines as liver X receptors agonists. Bioorg Med Chem. 2009;17(4):1663-1670.

Bhat AR, Athar F, van Zyl RL *et al*. Synthesis and Biological Evaluation of Novel 4-Substituted 1-{[4-(10,15,20-Triphenylporphyrin-5-yl)phenyl]methylidene}-thiosemicarbazide as New Class of Potential Antiprotozoal Agents. Chem Biodivers. 2008;5(5):764-776.

Bhattacharjee AK. Assessment of cation–pi binding affinity of the aromatic ring in several chloroquine analogs and related antimalarials using the ab initio quantum chemical (6-31G∗∗) theory. J Mol Struct. (Theochem). 2001;549(1-2):27-37.

Biot C, Pradines B, Sergeant M-H *et al*. Design, synthesis, and antimalarial activity of structural chimeras of thiosemicarbazone and ferroquine analogues. Bioorg Med Chem Lett. 2007;17(23):6434-6438.

Biot C, Taramelli D, Forfar-Bares I *et al.* Insights into the mechanism of action of ferroquine. Relationship between physicochemical properties and antiplasmodial activity. Mol Pharm. 2005;2(3):185-193.

Bohle DS, Dinnebier RE, Madsen SK *et al*. Characterization of the products of the heme detoxification pathway in malarial late trophozoites by X-ray diffraction. J Biol Chem. 1997;272(2):713-716.

Boon R. Antiviral treatment: From concept to reality. Antivir Chem Chemother. 1997;8(6suppl):5-10.

Briolant S, Henry M, Oeuvray C *et al*. Absence of association between piperaquine *in vitro* responses and polymorphisms in the *pfcrt*, *pfmdr1*, *pfmrp*, and *pfnhe* genes in *Plasmodium falciparum*. Antimicrob Agents Chemother. 2010;54(9):3537-3544.

Brittenham, G. M. (2008). Disorders of iron metabolism: iron deficiency and overload. In R. Hoffman, E. J. Benz, S. J. Shattil *et al.* (Eds.), Hematology: Basic principles and practice (5th ed.) (Chapter 36). New York: Elsevier.

Brooks DR, Wang P, Read M *et al*. Sequence variation of the hydroxymethyldihydropterin pyrophosphokinase: dihydropteroate synthase gene in lines of the human malaria parasite, *Plasmodium falciparum*, with differing resistance to sulfadoxine. Eur J Biochem. 1994;224(2):397-405.

Brown KL, Zou X, Marques HM. NMR-restrained molecular modeling of cobalt corrinoids: cyanocobalamin (vitamin B12) and methylcobalt corrinoids. J Mol Struct (Theochem). 1998;453(1-3):209-224.

Buckwold VE, Wilson RJH, Nalca A *et al*. Antiviral activity of hop constituents against a series of DNA and RNA viruses. Antiviral Res. 2004;61(1):57-62.

Budakoti A, Abid M, Azam A. Synthesis and antiamoebic activity of new 1-N-substituted thiocarbamoyl-3,5-diphenyl-2-pyrazoline derivatives and their Pd(II) complexes. Eur J Med Chem. 2006;41(1):63-70.

Bush AI and Masters CL. Clioquinol's return. Science. 2001;292(5525):2251-2252.

Cai Z, Zhou W, Sun L *et al*. Synthesis and *HMG CoA* reductase inhibition of 4-thiophenyl quinolines as potential hypocholesterolemic agents. Bioorg Med Chem. 2007;15(24):7809-7829.

Caicedo O, Villamor E, Forero Y *et al*. Relation between vitamin B12 and folate status, and hemoglobin concentration and parasitemia during acute malaria infections in Colombia. Acta Trop. 2010;114(1):17-21.

Canfield CJ, Milhous WK, Ager AL *et al*. PS-15: a potent, orally active antimalarial from a new class of folic acid antagonists. Am J Trop Med Hyg. 1993;49(1):121-126.

Canfield CJ, Pudney M, Gutteridge WE. Interactions of atovaquone with other antimalarial drugs against *Plasmodium falciparum in vitro*. Exp Parasitol. 1995;80(3):373-381.

Casas JS, García-Tasende, MS, Sordo J. Main group metal complexes of semicarbazones and thiosemicarbazones. A structural review. Coord Chem Rev. 2000;209(1):176-261.

Cerqueira NM, Fernandes PA, Ramos MJ. Ribonucleotide reductase: a critical enzyme for cancer chemotherapy and antiviral agents. Recent Pat Anticancer Drug Discov. 2007;2(1):11-29.

Chemaly SM, Chen CT, van Zyl RL. Naturally occurring cobalamins have antimalarial activity. J Inorg Biochem. 2007;101(5):764-773.

Chen M, Brøgger Christensen S, Zhai L *et al*. The Novel Oxygenated Chalcone, 2,4-Dimethoxy-4'-Butoxychalcone, Exhibits Potent Activity against Human Malaria Parasite *Plasmodium falciparum In vitro* and Rodent Parasites *Plasmodium berghei* and *Plasmodium yoelii in vivo*. J Infect Dis. 1997;176(5):1327-1333.

Chen MM, Shi L, Sullivan DJ. *Haemoproteus* and *Schistosoma* synthesize heme polymers similar to *Plasmodium* hemozoin and β-hematin. Mol Biochem Parasitol. 2001;113(1):1–8.

Chen S, Chen R, He M *et al*. Design, synthesis, and biological evaluation of novel quinoline derivatives as HIV-1 Tat–TAR interaction inhibitors. Bioorg Med Chem. 2009;17(5):1948–1956.

Chen Y, Zhao Y, Lu C *et al*. Synthesis, cytotoxicity, and antiinflammatory evaluation of 2-(furan-2-yl)-4-(phenoxy)quinoline derivatives. Part 4. Bioorg Med Chem. 2006;14(13):4373–4378.

Chipelem A, Gut J, Rosenthal PJ *et al*. Synthesis and biological evaluation of phenolic Mannich bases of benzaldehyde and (thio)semicarbazone derivatives against the cysteine protease falcipain-2 and a chloroquine resistant strain of *Plasmodium falciparum*. Bioorg Med Chem. 2007;15(1):273-282.

Chiyanzu I, Clarkson C, Smith PJ *et al*. Design, synthesis and antiplasmodial evaluation *in vitro* of new 4-aminoquinline isatin derivatives. Bioorg Med Chem. 2005;13(9):3249-3461.

Chou TC. Drug Combination Studies and Their Synergy Quantification Using the Chou-Talalay Method. Cancer Res. 2010;70(2):440-446.

Clark IA and Cowden WB. Why is the pathology of *falciparum* worse than that of *vivax* malaria? Parasitol Today. 1999;15(11):458–461.

Clarkson C, Maharaj VJ, Crouch NR *et al*. *In vitro* antiplasmodial activity of medicinal plants native to or naturalised in South Africa. J Ethnopharmacol. 2004;92(2-3):177-191.

Cole KA, Ziegler J, Evans CA *et al*. Metalloporphyrins inhibit β-hematin (hemozoin) formation. J Inorg Biochem. 2000;78(2):109-115.

Coppens I and Vielemeyer O. Insights into unique physiological features of neutral lipids in Apicomplexa: from storage to potential mediation in parasite metabolic activities. Int J Parasitol. 2005;35(6):597–615.

Cowman AF, Galatis D, Thompson JK. Selection for mefloquine resistance in *Plasmodium falciparum* is linked to amplification of the *pfmdr1* gene and cross-resistance to halofantrine and quinine. Proc Natl Acad Sci USA. 1994;91(3):1143-1147.

Curtis MM and Sperandio V. A complex relationship: the interaction among symbiotic microbes, invading pathogens, and their mammalian host. Muscoal Immunol. 2001;4(2):133-138.

Dalal S and Klemba M. Roles for two aminopeptidases in vacuolar hemoglobin catabolism in *Plasmodium falciparum*. J Biol Chem. 2007;282(49):35978-35987.

Daniel KG, Chen D, Orlu S *et al*. Clioquinol and pyrrolidine dithiocarbamate complex with copper to form proteasome inhibitors and apoptosis inducers in human breast cancer cells. Breast Cancer Res. 2005;7(6):R897-R908.

De Villiers KA, Kaschula CH, Egan TJ *et al*. Speciation and structure of ferriprotoporphyrin IX in aqueous solution: spectroscopic and diffusion measurements demonstrate dimerization, but not μ-oxo dimer formation. J Biol Inorg Chem. 2007;12(1):101-117.

De Villiers KA, Marques HM, Egan TJ. The crystal structure of halofantrine-ferriprotoporphyrin IX and the mechanism of action of arylmethanol antimalarials. J Inorg Biochem. 2008;102(8):1660-1667.

Deharo E, García RN, Oporto P *et al*. A non-radiolabelled ferriprotoporphyrin IX biomineralization inhibition test for the high throughput screening of antimalarial compounds. Exp Parasitol. 2002;100(4):252-256.

Desjardins RE, Carfield CJ, Haynes JD *et al*. Quantitative Assessment of Antimalarial Activity *In vitro* by as Semiautomated Microdilution Technique. Antimicrob Agents Chemother. 1979;16(6):710-718.

Deutscher MP., 1990. General methods for handling proteins and enzymes, Buffers: principles and practice. In: Deutscher MP. (ed.), Methods in Enzymology. Guide to Protein Purification, vol 182. Academic Press, p. 32.

Dinis TCP, Madeira VMC, Almeida LM. Action of Phenolic Derivatives (Acetaminophen, Salicylate, and 5-Aminosalucylate) as Inhibitors of Membrane Lipid Peroxidation and Peroxyl Radical Scavengers. Arch Biochem Biophys. 1994;315(1):161-169.

Divo AA, Geary TG, Davis NL *et al*. Nutritional Requirements of *Plasmodium falciparum* in Culture. I. Exogenous Supplied Dialyzable Components Necessary for Continous Growth. J Protozool. 1985;32(1):59-64.

Dobek AS, Klayman DL, Dickson ET *et al*. Inhibition of clinically significant bacterial organisms *in vitro* by 2-acetylpyridine thiosemicarbazones. Antimicrob. Agents Chemother. 1980;18(1):27-36.

Dobek AS, Klayman DL, Dickson ET Jr *et al*. Thiosemicarbazones of 2-acetylpyridine, 2-acetylquinoline, 1- and 3-acetylisoquinoline and related compounds as inhibitors of clinically significant bacteria *in vitro*. Arzneimittelforschung. 1983;33(11):1583-1591.

Domínguez JN, León C, Rodrigues J *et al*. Synthesis and antimalarial activity of sulfonamide chalcone derivatives. Farmaco. 2005a;60(4):307-311.

Domínguez JN, León C, Rodrigues J *et al*. Synthesis and Evaluation of New Antimalarial Phenylurenyl Chalcone Derivatives. J Med Chem. 2005b;48(10):3654-3658.

Dorn A, Stoffel R, Matile H *et al*. Malarial haemozoin/beta-haematin supports haem polymerization in the absence of protein. Nature. 1995;374(6519):269–271.

Dorn A, Vippagunta SR, Matile H *et al*. A comparison and analysis of several ways to promote haematin (haem) polymerisation and an assessment of its initiation *in vitro*. Biochem Pharmacol. 1998;55(6):737-747.

Ducki S, Forrest R, Hadfield JA *et al*. Potent antimitotic and cell growth inhibitory properties of substituted chalcones. Bioorg Med Chem Lett. 1998;8(9):1051-1056.

Eboumbou Moukoko EC, Bogreau H, Briolant S *et al*. Molecular markers of *Plasmodium falciparum* drug resistance. Med Trop (Mars). 2009;69(6):606-612.

Egan TJ, Chen JY, de Villiers KA *et al*. Haemozoin (β-haematin) biomineralization occurs by self-assembly near the lipid/water interface. FEBS Lett. 2006;580(21):5105–5110.

Egan TJ, Combrinck JM, Egan J *et al*. Fate of haem iron in the malaria parasite *Plasmodium falciparum*. Biochem J. 2002;365(Pt2):343-347.

Egan TJ, Mavuso WW, Ncokazi KK. The mechanism of beta-hematin formation in acetate solution. Parallels between hemozoin formation and biomineralization processes. Biochemistry. 2001;40(1):204-213.

Egan TJ, Mavuso WW, Ross DC *et al*. Thermodynamic factors controlling the interaction of quinoline antimalarial drugs with ferriprotoporphyrin IX. J Inorg Biochem. 1997;68(2):137-145.

Egan TJ, Ross DC, Adams PA. Quinoline anti-malarial drugs inhibit spontaneous formation of beta-haematin (malaria pigment). FEBS Lett. 1994;352(1):54-57.

Egan TJ. Haemozoin (malaria pigment): a unique crystalline drug target. Targets. 2003;2(3):115-124.

Egan TJ. Haemozoin formation. Mol Biochem Parasitol. 2008;157(2):127-136.

Eggleson KK, Duffin KL, Goldberg DE. Identification and characterization of falcilysin, a metallopeptidase involved in haemoglobin catabolism within the malaria parasite

Plasmodium falciparum. J Biol Chem. 1999;274(45):32411–32417.

Fakhfakh MA, Fournet A, Prina E *et al*. Synthesis and biological evaluation of substituted quinolines: potential treatment of protozoal and retroviral co-infections. Bioorg Med Chem. 2003;11(23): 5013–5023.

Farrell N. Biomedical uses and applications of inorganic chemistry. An overview. Coord Chem Rev. 2002;232(1-2):1-4.

Fernández-Bachiller MI, Pérez C, González-Muñoz GC *et al*. Novel tacrine-8-hydroxyquinoline hybrids as multifunctional agents for the treatment of Alzheimer's disease, with neuroprotective, cholinergic, antioxidant, and copper-complexing properties. J Med Chem. 2010;53(13):4927-4937.

Fidock DA, Eastman RT, Ward SA *et al*. Recent highlights in antimalarial drug resistance and chemotherapy research. Trends Parasitol. 2008;24(12):537-544.

Fidock DA, Nomura T, Talley AK *et al*. Mutations in the P. *falciparum* digestive vacuole transmembrane protein *PfCRT* and evidence for their role in chloroquine resistance. Mol Cell. 2000;6(4):861-871.

Firth RA, Hill HAO, Pratt JM *et al*. The chemistry of vitamin B12. Part XI. Some further formation constants. J Chem Soc. (A). 1969:381-386.

Fitch CD and Kanjananggulpan P. The state of ferriprotoporphyrin IX in malaria pigment. J Biol Chem. 1987;262(32):15552-15555.

Fitch CD, Cai GZ, Chen Y-F *et al*. Involvement of lipids in ferriprotoporphyrin IX polymerization in malaria. Biochim Biophys Acta. 1999;1454(1):31–37.

Fournet A, Barrios AA, Munoz V *et al*. 2-Substituted quinoline alkaloids as potential antileishmanial drugs. Antimicrob Agents Chemother. 1993;37(4):859-863.

Franck X, Fournet A, Prina E *et al*. Biological evaluation of substituted quinolines. Bioorg Med Chem Lett. 2004;14(14):3635-3638.

Fraser RS and Creanor J. The mechanism of inhibition of ribonucleic acid synthesis by 8-hydroxyquinoline and the antibiotic Iomofungin. Biochem J. 1975;147(3):401-410.

Freese JA, Sharp BL, Ridl FC *et al*. *In vitro* cultivation of southern African strains of *Plasmodium falciparum* and gametogenesis. S Afr Med J. 1988;73(12):720-722.

Fry M and Pudney M. Site of action of the antimalarial hydroxynaphthoquinone, 2-[trans-4-(4'-chlorophenyl) cyclohexyl]-3-hydroxy-1,4-naphthoquinone (566C80). Biochem Pharmacol. 1992;43(7):1545-1553.

Frölich S, Schubert C, Bienzle U *et al*. *In vitro* antiplasmodial activity of prenylated

chaclone derivatives of hops (*Humulus lupulus*) and their interaction with haemin. J Antimicrob Chemother. 2005;55(6):883-887.

Fujioka H and Aikawa M. (1999) The Malaria Parasite and its Life-cycle (In Wahlgren M & Perlmann P. ed. Malaria. Molecular and Clinical Aspects. Harwood Academic Publishers. Amsteldijk 166, 1st Floor, 1079 LH Amsterdam, The Netherlands. p 19-55).

Gaeta A and Hider RC. The crucial role of metal ions in neurodegeneration: the basis for a promising therapeutic strategy. Br J Pharmacol. 2005;146(8):1041-059.

Gamboa de Domínguez ND and Rosenthal PJ. Cysteine proteinase inhibitors block early steps in haemoglobin degradation by cultured malaria parasites. Blood. 1996;87(10):4448-4454.

Gathirwa JW, Rukunga GM, Niagi EN *et al*. The *in vitro* anti-plasmodial and *in vivo* anti-malarial efficacy of combinations of some medicinal plants used traditionally for treatment of malaria by the Meru community in Kenya. J Ethnopharmacol. 2008;115(2):223-231.

Gershon H and Parmegiani R. Antimicrobial activity of 8-quinolinol, its saltsand salicyclic acid and 3-hydrox-2-naphthoic acid, and the respective copper (II) chelates in liquid culture. Appl Microbiol. 1963;11:62-65.

Gilbert AM, Bursavich MG, Lombardi S *et al*. N-((8-Hydroxy-5-substituted-quinolin-7-yl)(phenyl)methyl)-2-phenyloxy/amino-acetamide inhibitors of ADAMTS-5 (Aggrecanase-2). Bioorg Med Chem Lett. 2008;18(24):6454–6457.

Gilles HM. (2002) Historical Outline (In Warrell DA. & Gilles HM. ed. Essential Malariology. 4th ed. London. Arnold. p 1-3).

Goldberg DE. Hemoglobin degradation. Curr Top Microbiol Immunol. 2005:295;275-291.

Gomtsyan A, Bayburt EK, Schmidt RG *et al*. Novel transient receptor potential vanilloid 1 receptor antagonists for the treatment of pain: structure–activity relationships for ureas with quinoline, isoquinoline, quinazoline, phthalazine, quinoxaline, and cinnoline moieties. J Med Chem. 2005;48(3):744–752.

Goodyer ID, Pouvelle B, Schneider TG *et al*. Characterization of macromolecular transport pathways in malaria-infected erythrocytes. Mol Biochem Parasitol. 1997;87(1):13-28.

Greenbaum DC, Mackey Z, Hansell E *et al*. Synthesis and Structure-Activity Relationships of Parasiticidal Thiosemicarbazone Cysteine Protease Inhibitors against *Plasmodium falciparum*, *Trypanosoma brucei*, and *Trypanosoma cruzi*. J Med Chem. 2004;47(12):3212-3219.

Greenwood B and Mutabingwa T. Malaria in 2002 Nature. 2002;415(6872):670-672.

Guantai EM, Ncokazi K, Egan TJ *et al*. Design, synthesis and *in vitro* antimalarial evaluation of triazole-linked chalcone and dienone hybrid compounds. Bioorg Med Chem 2010;18(23):8243-8256.

Guantai EM, Ncokazi K, Egan TJ *et al*. Enone- and Chalcone-Chloroquinoline Hybrid Analogues: In Silico Guided Design, Synthesis, Antiplasmodial Activity, *in vitro* Metabolism, and Mechanistic Studies. J Med Chem. 2011;54(10):3637-3649.

Guidelines for the treatment of malaria in South Africa. Department of Health. 2011.

Gupta S, Thapar MM, Wernsdorfer WH *et al*. *In vitro* interaction of artemisinin with atovaquone quinine and mefloquine against *Plasmodium falciparum*. Antimicrob Agents Chemother. 2002;46(5):1510-1515.

Hänscheid T, Egan TJ, Grobusch MP. Haemozoin: from melatonin pigment to drug target, diagnostic tool, and immune modulator. Lancet Infect Dis. 2007;7(10):675-685.

Hawley SR, Bray PG, Mungthin M *et al*. Relationship between antimalarial drug activity, accumulation, and inhibition of heme polymerization in *Plasmodium falciparum in vitro*. Antimicrob Agents Chemother. 1998;42(3):682-686.

Hayat F, Moseley E, Salahuddin A *et al*. Antiprotozoal Activity of chloroquinoline based chalcones. Eur J Med Chem. 2011;46(5):1897-1905.

Hider RC and Hall AD. Clinically useful chelators of tripositive elements. Prog Med Chem. 1991;28:41-173

Hongmanee P, Rukseree K, Buabut B *et al*. *In vitro* Activities of Cloxyquin (5-Chloroquinolin-8-ol) against *Mycobacterium tuberculosis*. Antimicrob Agents Chemother. 2007;51(3):1105-1106.

Hooper DC and Wolfson JS. Fluoroquinolone antimicrobial agents. N Engl J Med. 1991;324(6):384-394.

Hsieh H-K, Lee T-H, Wang J-P *et al*. Synthesis and Anti-inflammatory Effect of Chalcones and Related Compounds. Pharm Res. 1998;15(1):39-46.

Hu B, Jetter J, Kaufman D. *et al*. Further modification on phenyl acetic acid based quinolines as liver receptor modulators. Bioorg Med Chem. 2007;15(10):3321-3333.

Huang D, Ou B, Prior RL. The chemistry behind antioxidant capacity assays. J Agri Food Chem. 2005;53(6):1841-1856.

Hunsaker DB and Schenk GH. The determination of thiols with diphenylpicrylhydrazyl as a spectrophotometric reagent. Talanta. 1983;30(7):475-80.

Hyde JE. The dihydrofolate reductase-thymidylate synthetase gene in the drug resistance of malaria parasites. Pharmacol Ther. 1990;48(1):45-59.

Jack DB and Riess W. Pharmacokinetics of iodochlorhydroxyquin in man. J Pharm Sci. 1973;62(12):1929-1932.

Jackson KE, Klonis N, Ferguson DJ *et al*. Food vacuole-associated lipid bodies and heterogeneous lipid environments in the malaria parasite, *Plasmodium falciparum*. Mol Microbiol. 2004;54(1):109–122.

James GT. Inactivation of the protease inhibitor phenylmethylsulfonyl fluoride in buffers. Anal Biochem. 1978;86(2):574-579.

Jensen JB and Trager W. *Plasmodium falciparum* in culture: Use of outdated Erythrocytes and Description of the Candle Jar Method. J Parasitol. 1977;63(5):883-886.

Karres I, Kremer JP, Dietl I, *et al*. Chloroquine inhibits proinflammatory cytokine release into human whole blood. Am J Physiol. 1998;274(4 Pt 2):R1058–1064.

Kirk K and Lehane AM. Membrane transport in the malaria parasite and its host erythrocyte. Biochem J. 2014;457(1):1-18.

Kirk K. Membrane transport in the malaria-infected erythrocyte. Physiol Rev. 2001;81(2):495-537.

Kitamura S, Hashizume K, Iida T *et al*. Studies on lipoxygenase inhibitors. II. KF8940 (2-n-heptyl-4-hydroxyquinoline-N-oxide), a potent and selective inhibitor of 5-lipoxygenase, produced by Pseudomonas methanica. J Antibiot (Tokyo). 1986;39(8):1160-1166.

Klayman DL, Scovill JP, Bartosevich JF *et al*. 2-Acetylpyridine thiosemicarbazones. 5. 1-[1-(2-Pyridyl)ethyl]-3-thiosemicarbazides as potential antimalarial agents. J Med Chem. 1983;26(1):35-39.

Klemba M, Gluzman I, Goldberg DE. A *Plasmodium falciparum* dipeptidyl aminopeptidase I participates in vacuolar haemoglobin degradation. J Biol Chem. 2004;279(41):43000-43007.

Krugliak M, Zhang F, Ginsburg H. Intraerythrocytic *Plasmodium falciparum* utilizes only a fraction of the amino acids derived from the digestion of host cell cytosol for the biosynthesis of its proteins. Mol Biochem Parasitol. 2002;119(2):249-56.

Krungkrai J. Webster HK, Yuthavong Y. Characterization of cobalamin-dependent methionine synthase purified from the human malarial parasite, *Plasmodium falciparum*. Parasitol Res. 1989;75(7):512-517.

Krungkrai J. Webster HK, Yuthavong Y. Folate and Cobalamin Metabolism in

Plasmodium falciparum. Parasitol Today. 1990;6(12):388-391.

Kumar S, Bawa S, Drabu S *et al*. Design and synthesis of 2-chloroquinoline derivatives as non-azoles antimycotic agents. Med Chem Res. 2011;20(8):1340-1348.

Kumar S, Bawa S, Gupta H. Biological Activities of Quinoline Derivatives. Mini Rev Med Chem. 2009;9(14):1648-1654.

Kumar SK, Hager E, Pettit C *et al*. Design, Synthesis, and Evaluation of Novel Boronic-Chalcone Derivatives as Antitumor Agents. J Med Chem. 2003;46(14):2813–2815.

Kunz WS and Konstantinov AA. Effect of *b-c1*-site inhibitors on the midpoint potentials of mitochondrial cytochromes b. FEBS Lett. 1983;155(2):237-240.

Lambros C and Vanderberg JP. Synchronization of *Plasmodium falciparum* Erythrocytic Stages in Culture. J Parasitol. 1979;65(3):418-420.

Lambros C, Childs GE, Notsch JD *et al*. *In vitro* Assessment of 2-Acetylpyridine Thiosemicarbazones Against Chloroquine-Resistant *Plasmodium falciparum*. Antimicrob Agents Chemother. 1982;22(6):981-984.

Landfear SM. Nutrient transport and pathogenesis in selected parasitic protozoa. Eukaryot Cell. 2011;10(4):483-493.

Larsen M, Kromann H, Kharazmi A *et al*. Conformationally restricted anti-plasmodial chalcones. Bioorg Med Chem Lett. 2005;15(21):4858-4861.

Leirião P, Rodriques CS, Albuquerque SS *et al*. Survival of protozoan intracellular parasites in host cells. EMBO Rep. 2004;5(12):1142-1147.

Lessa JA, Mendes IC, da Silva PR *et al*. 2-Acetlpyridine thiosemicarbazones: cytotoxic activity in nanomolar doses against malignant gliomas. Eur J Med Chem. 2010;45(12):5671-5677.

Li R, Kenyon GL, Cohen FE *et al*. *In vitro* Antimalarial Activity of Chalcones and Their Derivatives. J Med Chem. 1995;38(26):5031-5037.

Liberta AE and West DX. Antifungal and antitumor activity of heterocyclic thiosemicarbazones and their metal complexes: current status. Biometals. 1992;5(2):121-126.

Liu M, Wilairat P, Go ML. Antimalarial alkoxylated and hydroxylated chalcones: structure-activity relationship analysis. J Med Chem. 2001;44(25):4443-4452.

Liu ZD and Hider RC. Design of clinically useful iron(III)-selective chelators. Med Res Rev. 2002;22(1):26-64.

Liu ZQ, Han K, Lin YJ *et al*. Antioxidative or prooxidative effect of 4-hydroxyquinoline derivatives on free-radical-initiated hemolysis oferythrocytes is due to its distributive status. Biochim Biophys Acta. 2002;1570(2):97-103.

Lloyd J, Ryono DE, Bird JE *et al*. Quinoline-4 carboxylic acids as angiotensin II receptor antagonists. Bioorg Med Chem Lett. 1994;4(1):195-200.

Lovejoy DB and Richardson DR. Novel "hybrid" iron chelators derived from aroylhydrazones and thiosemicarbazones demonstrate selective antiproliferative activity against tumor cells. Blood. 2002;100(2):666-676.

Ma L, Liu Z, Zhou B, *et al*. Inhibition of free radical induced oxidative hemolysis of red blood cells by green tea polyphenols. Chin Sci Bull. 2000;45(22):2052–2056.

Ma X, Zhou W, Brun R. Synthesis, *in vitro* antitrypanosomal and antibacterial activity of phenoxy, phenylthio or benzyloxy substituted quinolones. Bioorg Med Chem Lett. 2009;19(3):986–989.

Mabeza GF, Loyevsky M, Gordeuk VR *et al*. Iron Chelation Therapy for Malaria: A Review. Pharmacol Ther. 1999;81(1):53-75.

Machan ZA, Taylor GW, Pitt TL *et al.* 2-Heptyl-4-hydroxyquinoline N-oxide, an antistaphylococcal agent produced by *Pseudomonas aeruginosa*. J Antimicrob Chemother. 1992;30(5):615-623.

Mahlangu TJ, Chen CT, van Zyl RL. Clotrimazole and its interaction with synthetic β-haematin formation. Basic & Clinical Pharmacology & Toxicology. 2014;115(S1):106.

Mai A, Rotili D, Tarantino D *et al*. Identification of 4-hydroxyquinolines inhibitors of *p300*/*CBP* histone acetyltransferases. Bioorg Med Chem Lett. 2009;19(4);1132–1135.

Manera C, Cascio, MG, Benetti V *et al*. New 1,8-naphthyridine and quinoline derivatives as *CB2* selective agonists. Bioorg Med Chem Lett. 2007;17(23):6505–6510.

Martin RE, Ginsburg H, Kirk K. Membrane transport proteins of the malaria parasite. Mol Micorbiol. 2009;74(3):519-528.

Mather MW, Henry KW and Vaidya AB. Mitochondrial drug targets in apicomplexan parasites. Curr Drug Targets. 2007;8(1):49-60.

Mckintosh CL, Beeson JG, Marsh K. Clinical features and pathogenesis of severe malaria. Trends Parasitol. 2004;20(12):597-603.

Meshnick SR. Artemisinin: mechanisms of action, resistance and toxicity. Int J Parasitol. 2002;32(13):1655-1660.

Milhouse WK, Weatherly NF, Bowdre JH *et al*. *In vitro* activities of and mechanisms of

resistance to antifol antimalarial drugs. Antimicrob Agents Chemother. 1985;27(4):525-530.

Miller LH, Baruch DI, Marsh K *et al*. The pathogenic basis of malaria. Nature. 2002;415(6872):673-679.

Miller LM, Mayer SC, Berger DM *et al*. Lead identification to generate 3-cyanoquinoline inhibitors of insulin-like growth factor receptor (*IGF-1R*) for potential use in cancer treatment. Bioorg Med Chem Lett. 2009;19(1):62-66.

Mishra A, Panda JJ, Basu A *et al*. Nanovesicles Based on Self-Assembly of Conformationally Constrained Aromatic Residue Containing Amphiphilic Dipeptides. Langmuir. 2008;24(9):4571-4576.

Mookherjee S, Howard V, Nzila-Mouanda A *et al*. Identification and analysis of dihydrofolate reductase alleles from *Plasmodium falciparum* present at low frequency in polyclonal patient samples. Am J Trop Med Hyg. 1999;61(1):131-140.

Mossman T. Rapid colorimetric assay for cellular growth and survival: Application to proliferation and cytotoxicity assays. J Immunol Methods. 1983;65(1-2):55-63.

Mungthin M, Bray PG, Ridley RG *et al*. Central role of hemoglobin degradation in mechanisms of action of 4-aminoquinolines, quinoline methanols, and phenanthrene methanols. Antimicrobial Agents Chemother. 1998;42(11):2973-2977.

Nakashima RA and Garlid KD. Quinine inhibition of Na^+ and K^+ transport provides evidence for two cation/H^+ exchangers in rat liver mitochondria. J Biol Chem. 1982;257(16):9252-9254.

Navarro M, Gabbiani C, Messori L *et al*. Metal-based drugs for malaria, trypanosomiasis and leishmaniasis: recent achievements and perspectives. Drug Discov Today. 2010;15(23-24):1070-1078.

Ncokazi KK and Egan TJ. A colorimetric high-throughput beta-hematin inhibition screening assay for use in the search for antimalarial compounds. Anal Biochem. 2005;338(2):306-319.

Ndiaye D, Daily JP, Sarr O *et al*. Mutations in *Plasmodium falciparum* dihydrofolate reductase and dihydropteroate synthase genes in Senegal. Trop Med Int Health. 2005;10(11):1176-1179.

Neethling SE. Antioxidant properties of 4-hydroxyquinolines. Potchefstroom: PU for CHE (Dissertation-MSc) 2010.

Nowakowska Z. A review of anti-infective and anti-inflammatory chalcones. Eur J Med Chem. 2007;42(2):125-137.

Nune-Alves C. Parasite physiology: Propelling artemisinin resistance. Nat Rev Microbiol. 2015;13(2):66-67.

Oakley GP Jr. The neurotoxicity of the halogenated hydroxyquinolines. A commentary. JAMA. 1973;225(4):395-397.

Oh RC and Brown DL. Vitamin B12 Deficiency. Am Fam Physician. 2003;67(5):979-986.

Oliphant CM and Green GM. Quinoliones: A Comprehensive Review. Am Fam Physician. 2002;65(3):455-464.

Oliveira MF, d'Avila JC and Torres CR *et al*. Haemozoin in Schistosoma mansoni. Mol Biochem Parasitol. 2000;111(1):217–221.

Oliveira MF, Silva JR, Dansa-Petretski M *et al*. Haem detoxification by an insect. Nature 1999;400(6744):517–518.

Olliaro PL and Goldberg DE. The *Plasmodium* digestive Vacuole: Metabolic Headquarters and Choice Drug Target. Parasitol Today. 1995:11(8);294–297.

Olliaro PL and Milhous WK. The Antimalarial Drug Portfolio and Research Pipeline. Antimalarial Chemother Infect Dis. 2001:219-232.

Orjih AU, Banyal HS, Chevli R *et al*. Heme lyses malaria parasite. Science. 1981;214(4521):667-669.

Orjih AU. Saponin haemolysis for increasing concentration of *Plasmodium falciparum* infected erythrocytes. Lancet. 1994;343(8892):295.

Pagola S, Stephens PW, Bohle DS *et al*. The structure of malaria pigment (β-haematin). Nature. 2000;404(6775):307–310.

Papalexis V, Siomos MA, Campanale N *et al*. Histidine-rich protein 2 of the malaria parasite, *Plasmodium falciparum*, is involved in detoxification of the by-products of haemoglobin degradation. Mol Biochem Parasitol. 2001;115(1):77–86.

Parapini S, Basilico N, Pasini E *et al*. Standardization of the Physiochemical parameters to Assess *in vitro* the β-Hematin Inhibitory Activity of Antimalarial Drugs. Exp Parasitol. 2000;96(4):249-256.

Paraskevopoulos JK. An Investigation into the Antimalarial Activity of Metal Chelators. UKZN (Dissertation-MSc) 2008.

Phillips JP. The Reactions of 8-Quinolinol. Chem Rev. 1956;56(2):271–297.

Pink R, Hudson A, Mouriès MA *et al*. Opportunities and challenges in antiparasitic drug discovery. Nat Rev Drug Discov. 2005;4(9):727-40.

Pirahmadi S, Zkeri S, Afsharpad M *et al*. Mutation analysis in *pfmdr1* and *pfmrp1* as potential candidate genes for artemisinin resistance in *Plasmodium falciparum* clinical isolates 4 years after implementation of artemisinin combination therapy in Iran. Infect Genet Evol. 2013;14:327-334.

Pisciotta JM, Coppens I, Tripathi AK *et al*. The role of neutral lipid nanospheres in *Plasmodium falciparum* heme crystallization. Biochem J. 2007;402(1):197–204.

Pisciotta JM, Ponder EL, Fried B *et al*. Hemozoin formation in Echinostoma trivolvis rediae. Int J Parasitol. 2005;35(10):1037–1042.

Pouvelle B and Gysin J. Presence of the parasitophorus duct in *Plasmodium falciparum* and *P.vivax* parasitized Saimiri monkey red blood cells. Parasitol Today. 1997;13(9):357-361.

Prachayasittikul V, Prachayasittikul S, Ruchirawat S *et al*. 8-Hydroxyquinolines: a review of their metal chelating properties and medicinal applications. Drug Des Devel Ther. 2013;7:1157-1178.

Prentice AM, Ghattas H, Doherty C *et al*. Iron metabolism and malaria. Food Nutr Bull. 2007;28(4):S524-S539.

Pretorius E, Bornman MS, Marx J *et al*. Ultrastructural effects of low dosage endocrine disrupter chemicals on neural cells of the chicken embryo model. Horm Metab Res. 2006;38(10):639-649.

Price RN, Uhlemann AC, Brockman A *et al*. Mefloquine resistance in *Plasmodium falciparum* and increased *pfmdr1* gene copy number. Lancet 2004;364(9432):438-447.

Quirante J, Ruiz D, Gonzalez A *et al*. Platinum(II) and palladium(II) complexes with (N,N') and (C,N,N')- ligands derived from pyrazole as anticancer and antimalarial agents: synthesis, characterization and *in vitro* activities. J Inorg Biochem. 2011;105(12):1720-1728.

Ramos AIM, Mecom JS, Kiesow TJ *et al*. Tetrahydro-4-quinolinamines identified as novel *P2Y1* receptor antagonists. Bioorg Med Chem Lett. 2008;18(23):6222-6226.

Rano TA, McMaster ES, Pelton PD *et al*. Design and synthesis of potent inhibitors of cholesteryl ester transfer protein (CETP) exploiting a 1,2,3,4-tetrahydroquinoline platform. Bioorg Med Chem Lett. 2009;19(9):2456–2460.

Reed MB, Saliba KJ, Caruana SR *et al*. *Pgh1* modulates sensitivity and resistance to multiple antimalarials in *Plasmodium falciparum*. Nature 2000;403(6772):906-909.

Rosenthal PJ, Sijwali PS, Singh A *et al*. Cysteine proteases of malaria parasites: targets for chemotherapy. Curr Pharm Des 2002;8(18):1659–1672.

Rubbo SD, Albert A, Gibson MI. The influence of chemical constitution on antibacterial activity. V. The antibacterial action of 8-hydroxyquinoline (oxine). BrJ Exp Pathol. 1950;31(3):425-441.

Rubin H, Salem JS, Li LS *et al*. Cloning, sequence determination, and regulation of the ribonucleotide reductase subunits from *Plasmodium falciparum*: a target for antimalarial therapy. Proc Natl Acad Sci USA. 1993;90(2):9280-9284.

Sachs J and Malaney P. The economic and social burden of malaria. Nature. 2002;415(6872):680-685.

SAMF 11th Ed (2014) Rossiter D ed.

Scheibel LW and Adler A. Antimalarial Activity of Selected Aromatic Chelators. Mol Pharmacol. 1980;18(2):320-325.

Scheibel LW and Stanton GG. Antimalarial activity of selected aromatic chelators. IV. Cation uptake by *Plasmodium falciparum* in the presence of oxines and siderochromes. Mol Pharmacol. 1986;30(4):364-369.

Schuster FL. Cultivation of *Plasmodium spp*. Clin Microbiol Rev. 2002;15(3):355-364.

Scott DA, Balliet CL, Cook DJ *et al*. Identification of 3-amido-4-anilinoquinolines as potent and selective inhibitors of *CSF-1R* kinase. Bioorg Med Chem Lett. 2009;19(3):697–700.

Scovill JP, Klayman DL, Franchino CF. 2-Acetylpyridine Thiosemicarbazones. 4. Complexes with Transition Metals as Antimalarial and Antileukemic Agents. J Med Chem. 1982;25:1261-1264.

Shachar DB, Kahana N, Kampel V *et al*. Neuroprotection by a novel brain permeable iron chelator, VK-28, against 6-hydroxydopamine lession in rats. Neuropharmacology. 2004;46(2):254-263.

Shen AY, Wu SN, Chiu CT. Synthesis and cytotoxicity evaluation of some 8-hydroxyquinoline derivatives. J Pharm Pharmacol. 1999;51(5):543-548.

Shipman C Jr, Smith SH, Drach JC *et al*. Thiosemicarbazones of 2-acetylpyridine, 2-acetylquinoline, 1-acetylisoquinoline, and related compounds as inhibitors of herpes simplex virus *in vitro* and in a cutaneous herpes guinea pig model. Antiviral Res. 1986;6(4):197-222.

Siakallis G, Spandidos DA, Sourvinos G. Herpesviridae and novel inhibitors. Antiviral Ther. 2009;14:1051-1064.

Sidhu AB, Uhlemann AC, Valderramos SG *et al*. Decreasing *pfmdr1* copy number in

Plasmodium falciparum malaria heightens susceptibility to mefloquine, lumefantrine, halofantrine, quinine, and artemisinin. J Infect Dis. 2006;194(4):528-535.

Sinden RE and Gilles HM. (2002) The malaria parasites (*In* Warrell DA. & Gilles HM. *ed.* Essential Malariology. 4th ed. London. Arnold. p 8-29).

Sisodia BS, Negi AS, Darokar MP *et al*. Antiplasmodial activity of steroidal chalcones: evaluation of their effect on hemozoin synthesis and the new permeation pathway of *Plasmodium falciparum*-infected erythrocyte membrane. Chem Biol Drug Des. 2012;79(4):610-615.

Slater AF, Swiggard WJ, Orton BR *et al*. An iron-carboxylate bond links the heme units of malaria pigment. Proc Natl Acad Sci USA. 1991;88(2):325-329.

Slater AF. Chloroquine: mechanism of drug action and resistance in *Plasmodium falciparum*. Pharmacol Ther. 1993;57(2-3):203-235.

Slater AFG and Cerami A. Inhibition by chloroquine of a novel haem polymerase enzyme activity in malaria trophozoites. Nature. 1992;355(6356):167–169.

Slavic K, Straschil U, Reininger L *et al*. Life cycle studies of the hexose transporter of *Plasmodium* species and genetic validation of their essentiality. Mol Microbiol. 2010;75(6):1402-1413.

Snow RW and Gilles HM. (2002) The epidemiology of malaria (In Warrell DA. & Gilles HM. ed. Essential Malariology. 4th ed. London. Arnold. p 85-85).

Solomonov I, Osipova M, Feldman Y, *et al*. Crystal nucleation, growth, and morphology of the synthetic malaria pigment β-hematin and the effect thereon by quinoline additives: the malaria pigment as a target of various antimalarial drugs. J Am Chem Soc. 2007:129(9);2615–2627.

Soulère L, Delplace P, Davioud-Charvet E *et al*. Screening of *Plasmodium falciparum* Iron Superoxide Dismutase Inhibitors and Accuracy of the SOD-Assays. Bioorg Med Chem. 2003;11(23):4941-4944.

Sreekanth A, Kala UL, Nayar CR *et al.*Cobalt(III) complexes of 2-hydroxyacetophenone N(4)-phenyl semicarbazone containing heterocyclic coligands: syntheses, structure and spectral studies. Polyhedron. 2004;23(1):41-47.

Srimal Rc, Gulati K, Nityanand S *et al*. Pharmacological studies on 2-(2-(4-(3-methylphenyl)-1-piperazinyl)ethyl) quinoline (centhaquin). I. Hypotensive activity. Pharmacol Res. 1990;22(2):319–329.

Srivastava IK, Morrisey JM, Darrouzet E *et al*.Resistance mutations reveal the atovaquone-binding domain of cytochrome b in malaria parasites. Mol Microbiol. 1999;33(4):704-711.

Stack CM, Lowther J, Cunningham E *et al*. Characterization of the *Plasmodium falciparum* M17 leucyl aminopeptidase. J Biol Chem. 2006;282(3):2069–2080.

Sullivan DJ, Gluzman IY, Goldberg DE. *Plasmodium* hemozoin formation mediated by histidine-rich proteins. Science. 1996;271(5246):219–222.

Sullivan DJ. Theories on malarial pigment formation and quinoline action (Invited review). Int J Parasitol. 2002;32(13):1645-1653.

Suzuki H, Aly NS, Watasy Y. Preparation of quinoline hexose analogs as novel chloroquine-resistant malaria treatments (1). Synthesis of 4-hydroxyquinoline-beta-glucosides. Chem Pharm Bull. (Tokyo). 2007;55(5):821-824.

Thunell S. Porphyrins, porphyrins metabolism and porphyrias. I. Update. Scand J Clinc Lab Invest. 2000;60(7):509-540.

Trager W and Jensen JB. Human malaria parasites in continuous culture. Science. 1976;193(4254):673-675.

Triglia T and Cowman AF. Primary structure and expression of the dihydropteroate synthetase gene of *Plasmodium falciparum*. Proc Natl Acad Sci USA. 1994;91(15):149-153.

Tsubaki T, Honma Y, Hoshi M. Neurological syndrome associated with clioquinol. Lancet. 1971;1(7701):696-697.

Uchiumi F, Hatano T, Ito H *et al*. Transcriptional suppression of the HIV promoter by natural compounds. Antiviral Res. 2003;58(1):89-98.

Vaidya AB, Lashgari MS, Pologe LG *et al*. Structural features of *Plasmodium* cytochrome b that may underlie susceptibility to 8-aminoquinolines and hydroxynaphthoquinones. Mol Biochem Parasitol. 1993;58(1):33-42.

Van Dyk S. Synthesis and biological activity of selected 4-hydroxyquinolines. Potchefstroom: PU for CHE (Thesis-Ph.D.) 2001.

Van Zyl RL, Seatlholo St, Viljoen AM. Pharmacological interactions of essential oil constituents on the *in vitro* growth of *Plasmodium falciparum*. South African Journal of Botany. 2010;76(4):662-667.

Vennerstrom JL, Nuzum EO, Miller RE *et al.* 8-Aminoquinolines active against blood stage *Plasmodium falciparum in vitro* inhibit hematin polymerization. Antimicrob Agents Chemother. 1999;43(3):598-602.

Voet D and Voet JG. Biochemistry (4th ed.), John Wiley & Sons Inc.: Hoboken, NJ (2011).

von Castel-Dunwoody KM, Kauwell GP, Shelnutt KP *et al*. Transcobalamin 776C->G polymorphism negatively affects vitamin B-12 metabolism. Am J Clin Nutr. 2005;81(6):1436-1441.

Walcourt A, Loyevsky M, Lovejoy DB *et al*. Novel aroylhydrazone and thiosemicarbazone iron chelators with anti-malarial activity against chloroquine resistant and –sensitive parasites. Int J Biochem Cell Biol. 2004;36(3):401-407.

Waller KL, Cooke BM, Nunomura W, *et al*.Mapping the binding domains involved in the interaction between the *Plasmodium falciparum* knob-associated histidine-rich protein (*KAHRP*) and the cytoadherence ligand *P. falciparum* erythrocyte membrane protein 1 (*PfEMP1*). J Biol Chem. 1999;274(34):23808–23813.

Wang Q, Ding Z-H, Liu J-K *et al*. Xanthohumol, a novel anti-HIV-1 agent purified from Hops *Humulus lupulus*. Antiviral Res. 2004;64(3):189–194.

Wang Y, Ai J, Wang Y *et al*. Synthesis and c-Met kinase inhibition of 3,5-disubstituted and 3,5,7-trisubstituted quinolines: identification of 3-(4 acetylpiperazin-1-yl)-5-(3-nitrobenzylamino)-7 (trifluoromethyl)quinoline as a novel anticancer agent. J Med Chem. 2011;54(7):2127–2142.

Warhurst DC, Craig JC, Adagu IS *et al*. Activity of piperaquine and other 4-aminoquinoline antiplasmodial drugs against chloroquine-sensitive and resistant blood-stages of *Plasmodium falciparum*. Role of beta-haematin inhibition and drug concentration in vacuolar water- and lipid-phases. Biochem Pharmacol. 2007;73(12):1910-1926.

Warhurst DC. A molecular marker for chloroquine-resistant *falciparum* malaria. N Engl J Med. 2000;344(4):299-302.

Warshawsky B, Youdim MBH, Ben-Shacar D. harmaceutical compositions compromising iron chelators for the treatment of neurodegenerative disorders and some novel iron chelators. International Publication number WO 00/74664A2. 2000.

West DX, Padhye SB, Sonawane PB. Structural and physical correlations in the biological properties of transition metal heterocyclic thiosemicarbazone and *S*-alkyldithiocarbazate complexes. Struct Bonding (Berlin). 1991;76:1-50.

Wilson CM, Volkman SK, Thaithong S *et al*. Amplification of pfmdr 1 associated with mefloquine and halofantrine resistance in *Plasmodium falciparum* from Thailand. Mol Biochem Parasitol. 1993;57(1):151-160.

Winstanley PA, Mberu EK, Szwandt IS *et al*. *In vitro* activities of novel antifolate drug combinations against *Plasmodium falciparum* and human granulocyte CFUs. Antimicrob Agents Chemother. 1995;39(4):948-952.

Winter RW, Kelly JX, Smilkstein MJ *et al*. Evaluation and lead optimization of anti-

malarial acridones. Exp Parasitol. 2006;114(1):47-56.

Winzeler EA. Malaria research in the post-genomic era. Nature. 2008:455(7214);751-756.

World Health Organisation (WHO) World Malaria Report 2014.

Yenesew A, Induli, M, Derese S *et al*. Anti-plasmodial flavonoids from the stem bark of Erythrina absysinica. Phytochemistry. 2004;65(22):3029-3032.

Yu Y, Kalinowski DS, Kovacevic Z *et al*. Thiosemicarbazones from the old to new: iron chelators that are more than just ribonucleotide reductase inhibitors. J Med Chem. 2009;52(17):5271-5294.

Zahra JA, Abu Thaher BA, El-Abadelah MM *et al*. 3-Mercaptopropionic acid-nitrile imine adducts. An unprecedented cyclization into 1,3,4-thiadiazol-2(3H)-ones and -2(3H)-thiones. Org Biomol Chem. 2005;3(14):2599-2603.

Zhang F, Krugliak M, Ginsburg H. The fate of ferriprotoporphyrin IX in malaria infected erythrocytes in conjunction with the mode of action of antimalarial drugs. Mol Biochem Parasitol. 1999;99(1):129–141.

Zheng H, Weiner LM, Bar-Am O *et al*. Design, synthesis and evaluation of noval bifunctional iron-chelators as potential agents for neuroprotection in Alzheimer's, Parkinson's, and other neurodegenerative diseases. Bioorg Med Chem. 2005;13(3):773-783.

Research Office

INSTITUTIONAL BIOSAFETY COMMITTEE
(R 14/16)

CLEARANCE CERTIFICATE - RENEWAL **PROTOCOL NUMBER: 20090503**

BRIEF DESCRIPTION OF APPLICATION:

Chemotherapeutic properties of novel synthetic and natural compounds

APPLICANT: Dr R van Zyl

SCHOOL/DEPARTMENT : Pharmacy/Pharmacology

DATE CONSIDERED: 20090528 and 20140327

DECISION OF COMMITTEE:

Approved unconditionally

1. This clearance certificate expires on 20190402 and may be renewed on application
2. An annual report must be provided on the anniversary date of this certificate, for as long as the project continues
3. Notification of any proposed modifications must be submitted on the attached form

DATE: 20140403 **CHAIRPERSON** _____
(Professor A Capovilla)

DECLARATION BY APPLICANT:

To be completed in duplicate and **one copy** returned to the Secretary, Room 10004, 10th floor, Senate House, University.

1. I have read, understood and accepted the approval conditions above
2. I agree to submit a yearly progress report to the Committee and to submit an interim report on the form provided, in the event of any significant unforeseen event, *e.g.* suspension of a drug trial, temporary closure or relocation of my laboratory, etc
3. I note that the University Safety Officer, or his/her representative, may at any reasonable time inspect my laboratory or trial site to ensure compliance with current Health and Safety legislation. I undertake to offer my full co-operation in any such inspection.
4. I have read, understood and will comply with the *recommended standard operating procedures for the handling of biohazardous materials* posted at http://web.wits.ac.za/Academic/Research/Biosafety.htm
5. I declare (delete as appropriate) that:
    a. I have all the approvals required by statute or regulation and by the funding agencies supporting this work, or
    b. that I will not begin work until such approvals are obtained

Signed: _____ **Date:** _____

MSWorks2000/Iain0015/IBCClearRenew.wps

PLEASE QUOTE THE PROTOCOL NUMBER IN ALL ENQUIRIES

Research Office

Institutional Biosafety Committee (IBC)

Proposed modification to approved protocol

Name of person in whose name the original approval was granted (usually the principal Investigator):

_____

Name of person making this request, if different:

_____

School/Department:

_____

Contact details:

E mail: _____ **Telephone No.:** _____

IBC Protocol No:

_____

Full project title:

_____

_____

_____

Details of proposed modification

(a) data:

Please be sure to include the original specifications, any previously agreed modifications and details of what is now being proposed, eg in patient numbers, sites to be used, dosage frequency, alterations to drug specifications, duration of the study, etc.

(b) rationale:

Why do you wish to do this and what outcomes are anticipated? In addition to any other points, please comment specifically on any implications for the risk and containment levels, as described in Section 6 of the original application. Please include key dates.

(c) are any other approvals required and have these been obtained, or applied for?

eg Medicines Control Council, Dept of Agriculture, Human Research Ethics Committee, Hospital Administration, Trial Sponsors, etc.

(d) explain any proposed changes to key personnel:

(e) any other relevant information:

Human Research Ethics Committee (Medical)

Research Office Secretariat: Senate House Room SH 10005, 10th floor. Tel +27 (0)11-717-1252
Medical School Secretariat: Medical School Room 10M07, 10th Floor. Tel +27 (0)11-717-2700
Private Bag 3, Wits 2050, www.wits.ac.za. Fax +27 (0)11-717-1265

Ref: W-CJ-131030-1 30/10/2013

TO WHOM IT MAY CONCERN:

Waiver: This certifies that the following research does not require clearance from the Human Research Ethics Committee (Medical).

Investigator: Prof R van Zyl.

Project title: The chemotherapeutic properties of novel synthetics and natural compounds.

Reason: This is a laboratory study in which human blood and plasma for the in vitro maintenance of *Plasmodium falciparum* for experimental purposes such as drug sensitivity and toxicity studies. There are no human participants.

UNIVERSITY OF THE WITWATERSRAND
PROF PE CLEATON-JONES
HREC (MEDICAL)
2013 -10- 30
JOHANNESBURG

Professor Peter Cleaton-Jones

Chair: Human Research Ethics Committee (Medical)

Copy - HREC(Medical) Secretariat: Anisa Keshav, Zanele Ndlovu.

R14/49 Dr Robyn L van Zyl

HUMAN RESEARCH ETHICS COMMITTEE (MEDICAL)

CLEARANCE CERTIFICATE NO. M140669

NAME: (Principal Investigator) Dr Robyn L van Zyl

DEPARTMENT: Pharmacy & Pharmacology
Medical School

PROJECT TITLE: The Chemotherapeutic Properties of Novel Synthetic and Natural Compounds (Renewal previously M090532)

DATE CONSIDERED: 29/05/2009 (Initial Approval) 26/06/2014 (Renewal)

DECISION: Approved unconditionally

CONDITIONS:

SUPERVISOR:

APPROVED BY: Professor PE Cleaton-Jones, Chairperson, HREC (Medical)

DATE OF APPROVAL: 26/06/2014

This clearance certificate is valid for 5 years from date of approval. Extension may be applied for.

DECLARATION OF INVESTIGATORS

To be completed in duplicate and **ONE COPY** returned to the Secretary in Room 10004, 10th floor, Senate House, University.

I/we fully understand the conditions under which I am/we are authorized to carry out the above-mentioned research and I/we undertake to ensure compliance with these conditions. Should any departure be contemplated, from the research protocol as approved, I/we undertake to resubmit the application to the Committee. **I agree to submit a yearly progress report**.

Principal Investigator Signature

21-07-2014
Date

PLEASE QUOTE THE PROTOCOL NUMBER IN ALL ENQUIRIES

Human Research Ethics Committee (Medical)

Research Office Secretariat: Senate House Room SH10005, 10th floor. Tel +27 (0)11-717-1252
Medical School Secretariat: Tobias Health Sciences Building, 2rd floor Tel +27 (0)11-717-2700
Private Bag 3, Wits 2050, www.wits.ac.za. Fax +27 (0)11-717-1265

Ref: W-CJ-150330-1 30/03/2015

TO WHOM IT MAY CONCERN:

Waiver: This certifies that the following research does not require clearance from the Human Research Ethics Committee (Medical).

Investigator: **Prof R L van Zyl, Mr C-T Chen (student no. 9902245A).**

Project title: **The effect of novel compounds on the growth of *Plasmodium falciparum,* human cells and haemozoin formation.**

Reason: This is a laboratory study using a commercial cell line – Graham. There are no human participants

UNIVERSITY OF THE WITWATERSRAND
PROF PE CLEATON-JONES
HREC (MEDICAL)
2015 -03- 30
JOHANNESBURG

Professor Peter Cleaton-Jones

Chair: Human Research Ethics Committee (Medical)

Copy – HREC (Medical) Secretariat: Zanele Ndlovu, Langutani Masingi.